Chemical Engineering Journal 510 (2025) 161574

Contents lists available at ScienceDirect

Chemical Engineering Journal

journal homepage: www.elsevier.com/locate/cej

Review

Industrial sulfur separation and purification: Paving the way to energy applications

Aitolkyn Uali [a,b,1], Aizhan Kazymbetova [a,1], Ayaulym Belgibayeva [a,c], Arailym Nurpeissova [a,c,*], Zhumabay Bakenov [a,c,d,*], Aliya Mukanova [a,c,*]

[a] National Laboratory Astana PI, Nazarbayev University, Kabanbay Batyr Ave. 53, Astana 010000, Kazakhstan
[b] Department of Chemistry, L.N. Gumilyov Eurasian National University, Kazhymukan Street 13, Astana 010000, Kazakhstan
[c] Institute of Batteries LLC, Kabanbay Batyr Ave. 53, Astana 010000, Kazakhstan
[d] Department of Chemical and Materials Engineering, School of Engineering and Digital Sciences, Nazarbayev University, Kabanbay Batyr Ave. 53, Astana 010000, Kazakhstan

ARTICLE INFO

Keywords:
Sulfur
Purification
High purity
Metal-sulfur batteries
Energy storage

ABSTRACT

Sulfur, a by-product of industrial processes, presents a unique opportunity for advancing sustainable energy storage systems, particularly in metal-sulfur batteries (MSBs) and thermal energy storage (TES) applications. Both MSBs and TES technologies benefit from sulfur's abundance, cost-effectiveness, and high energy storage potential. However, the effective utilisation of sulfur in these systems relies on its purification to meet stringent quality standards, as impurities can significantly impact performance. This review examines sulfur's role as an industrial by-product, detailing conventional and alternative purification methods from sources such as petroleum and coal. Techniques such as hydrodesulfurisation (HDS), adsorptive desulfurisation (ADS), oxidative desulfurisation (ODS), and biodesulfurisation (BDS) as well as extraction and flotation are evaluated for their efficiency, scalability, and environmental impact. Sulfur's dual application in MSBs and TES positions it as a critical material for sustainable, large-scale energy storage solutions, underscoring this research's significance and impact implications. The review emphasises the need for continued innovation in sulfur purification methods and integrating green chemistry principles to enhance sustainability. The insights provided here pave the way for broader sulfur utilisation, offering sustainable pathways for its application in industrial processes and energy storage technologies.

1. Introduction

Sulfur is the tenth most abundant element in the universe and the fourteenth most abundant element in the Earth's crust [1]. The total sulfur content in the Earth's crust is approximately 0.026 %, and as an anion-forming element, sulfur ranks second after oxygen [2]. On the other hand, a proportion of the native sulfur is reported to be relatively small. Sulfur's main content in Nature is accounted for sulfide compounds (sulfur pyrite, copper pyrite, zinc blende, lead lustre, etc.) and sulfate (gypsum anhydrate, gypsum, mirabilite, etc.). In addition, sulfur is presented in various forms in coal, oil, natural gas, bituminous sandstones, *etc.* [3–6].

Today's sulfur industry is unique compared to other mining industries in that it is produced primarily as a by-product. Moreover, there has been an oversupply of sulfur on the market since the supply and demand for sulfur have not been balanced over the past many years. It has been estimated that about seven million tons of excess sulfur are generated annually, and a further continuous increase in production is expected [5]. Among potential sulfur sources of industrial value, coal, petroleum hydrocarbons, and metallurgical products have dominated the market (Fig. 1) [4].

According to Wagenfeld et al. [5], most sulfur is extracted in reduced form and subsequently oxidised; sulfur often passes from the sulfide to the sulfate form. However, the exception is petrochemical products, in which sulfur is present as elemental sulfur or is utilised as hydrogen sulfide (or mercaptans). Nevertheless, this does not detract from the value of sulfur, as it is considered an essential chemical for the global economy. In addition, as a significant precursor to sulfuric acid, sulfur

* Corresponding authors at: National Laboratory Astana PI, Nazarbayev University, Kabanbay Batyr Ave. 53, Astana 010000, Kazakhstan.
E-mail addresses: arailym.nurpeissova@nu.edu.kz (A. Nurpeissova), zbakenov@nu.edu.kz (Z. Bakenov), aliya.mukanova@nu.edu.kz (A. Mukanova).
[1] These authors contributed equally.

https://doi.org/10.1016/j.cej.2025.161574
Received 25 October 2024; Received in revised form 20 February 2025; Accepted 13 March 2025
Available online 16 March 2025

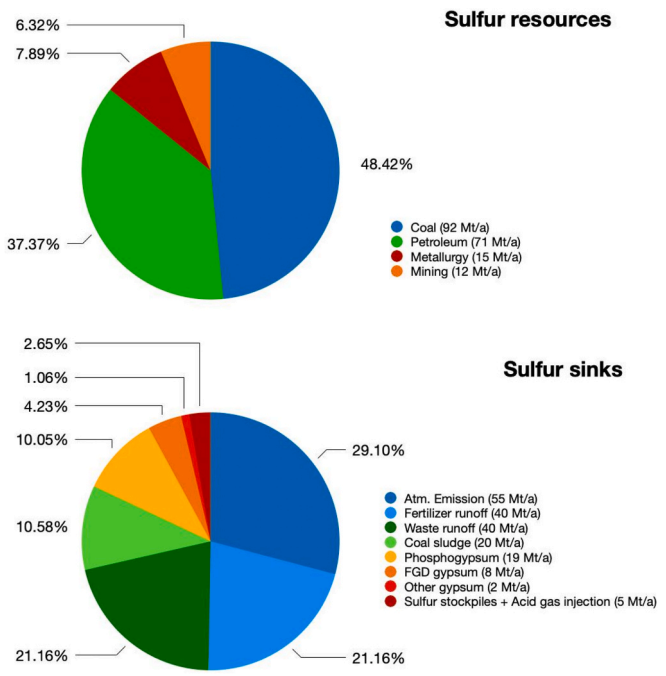

Fig. 1. Distribution of global sulfur sources (petroleum, coal, minerals) and sinks (energy storage, industrial processes) with estimated production/consumption rates (million tons/year −Mt/a). The top pie chart represents the primary sources of sulfur, including coal (48.42%, 92 Mt/a), petroleum (37.37%, 71 Mt/a), metallurgy (7.89%, 15 Mt/a), and mining (6.32%, 12 Mt/a). The bottom pie chart illustrates the major sinks of sulfur, such as atmospheric emissions (29.10%, 55 Mt/a), fertilizer runoff (21.16%, 40 Mt/a), waste runoff (21.16%, 40 Mt/a), coal sludge (10.58%, 20 Mt/a), phosphogypsum (10.05%, 19 Mt/a), and smaller contributions from flue gas desulfurization (FGD) gypsum, other gypsum, and sulfur stockpiles. These figures highlight the sulfur cycle, emphasizing its distribution in industrial activities and environmental impacts. The data used to build this chart were adapted from [4]

can serve as the basis for more sustainable technologies, including polymer production [6,7], thermal energy storage systems [8,9], and battery manufacturing [10,11].

Developing new and more advanced energy storage systems is important in solving the problem of the unsustainability of renewable energy production and the transformation of the entire energy system (ES). Scientific assistance in developing energy storage systems is one of the critical tasks in successfully solving this challenge and transforming ES. Sulfur has a high potential for energy storage and conversion, being an electrochemically active material which can accept up to two electrons per atom at ~2.1 V vs Li/Li^+ [12]. This makes sulfur cathode materials possess a high theoretical capacity of up to 1675 mAh g^{-1}, and the predicted theoretical energy density of the Li/S batteries is around ~2600 Wh kg^{-1} [12]. To compare, the theoretical energy density of the Na/S batteries is up to ~1245 Wh kg^{-1} [13]. Moreover, using sulfur in the battery industry and developing electrochemical energy storage systems could potentially solve the utilisation problem of medium/high-sulfur petroleum and petroleum products. The K/S batteries from high-sulfur petroleum coke demonstrated long-term cycle stability [14]. Similarly, the Li/S electrodes of petroleum coke demonstrated highly effective performance, increased cycling time, and reduced net cost [15,16]. All this leads to the hypothesis that employing industrial sulfur for rechargeable battery systems is a promising step in developing ways forward to sustainable energy storage. However, although sulfur-focused review papers with all prospects and challenges have been published today, they are still narrowed by one particular topic. For instance, the first group is about the presence of sulfur, its chemical forms found in matrices of various natures, and its properties [17,18], while another group of articles is focused on individual desulfurisation methods of these S-containing systems [17–22]. The third category of works reflects only the prospects for using sulfur in energy storage systems [11,23]. From this perspective, a comprehensive review that would cover all aspects together, bringing the gap between academic research of separation/purification and application of industrial by-product sulfur for energy purposes, is of great importance. This review examines industrial sources of sulfur and its chemical forms, the methods of separation/extraction/(deep) purification, and highlights the necessity for ongoing innovation in sulfur purification techniques to widen the sulfur horizons for sustainable electrochemical purposes. The review focuses on sulfur's features, its forms and characteristics in hydrocarbons and metallurgical raw materials and products/wastes, and the extraction and purification methods in world practice. This makes it possible to balance the supply and demand for sulfur more accurately and widen the areas of its use for sustainable electrochemical purposes.

2. Sulfur from petroleum/petroleum products and its removal/purification ways

2.1. Sulfur in crude oil and light/heavy hydrocarbons

All crude oils contain significant amounts of sulfur and its compounds. According to Orr et al. [24], the sulfur content of crude oil and natural bitumen varies from 0.05 to 14 wt%, depending on the place of origin; however, for few commercially produced ones, it rarely exceeds 4 wt%. Fahim et al. stated that these values vary from less than 0.05 to more than 10 wt% but generally fall in the range of 1–4 wt% [25]. Thus, crude oils can be divided into two classes, depending on their sulfur content: crude oil with less than 1 wt% sulfur is considered low sulfur or "sweet", while oil with more than 1 wt% sulfur is regarded as high sulfur or "sour" [25]. However, another study defines crude oil as "sour" when it contains more than 0.5 wt% sulfur [26]. The World Oil Outlook forecasted that sulfur content would fall from 1.28 % in 2022 to 1.24 % by 2029–2030 [27] due to the increased supply of sweet crude from the US, Latin America, and Kazakhstan [28]. However, the forecast [27] also predicts that after this initial decline, the global average S content will increase up to 1.37 % in 2045.

The high-sulfur oils (≈3.5 % S), derived from carbonate or carbonate-evaporite rock sequences, are cheaper than the low-sulfur oils (≈0.5 % S), mainly derived from clay-rich clastic sequences [24]. According to the ESMAP technical report, each one per cent of sulfur lowers the price by 0.056 USD per dollar of Brent brand as an example [29]. This might be explained by the fact that higher sulfur crude oil requires costly treatment, and hence, sour crude oils are generally sold at a significant discount compared to sweet crude oils. For instance, the Primer on the cost of marine fuel compliant with the IMO 2020 Rule (technical report) stated that a price differential between low- and high-sulfur oil peaked in the first days of 2020 at 240–320 USD per ton and dropped precipitously (along with price levels) in the spring of 2020 stabilising at 50–60 USD per ton in the second half of the year [30].

2.2. Sulfur distribution and molecular characterisation of sulfur compounds in oils

Sulfur-containing compounds (SCCs) are generally the most abundant heteroatom-containing components in oils [5,17,31–33]. According to Han et al., six types of SCCs can be differentiated based on their functional groups (Fig. 2) [17].

Elemental sulfur and hydrogen sulfide are soluble inorganic compounds due to the thermochemical transformations of sulfur organics, bacteria sulfate reduction, and incorporation of inorganic sulfur. The elemental sulfur, hydrogen sulfide, mercaptans (thiols) and sulfides (acyclic and cyclic) are reactive and corrosive; because of these activities, the exploration and/or production of high-sulfur reservoirs can lead to fatal incidents. To compare, polysulfides, in which sulfur is surrounded or contained within the molecule, are known to be stable

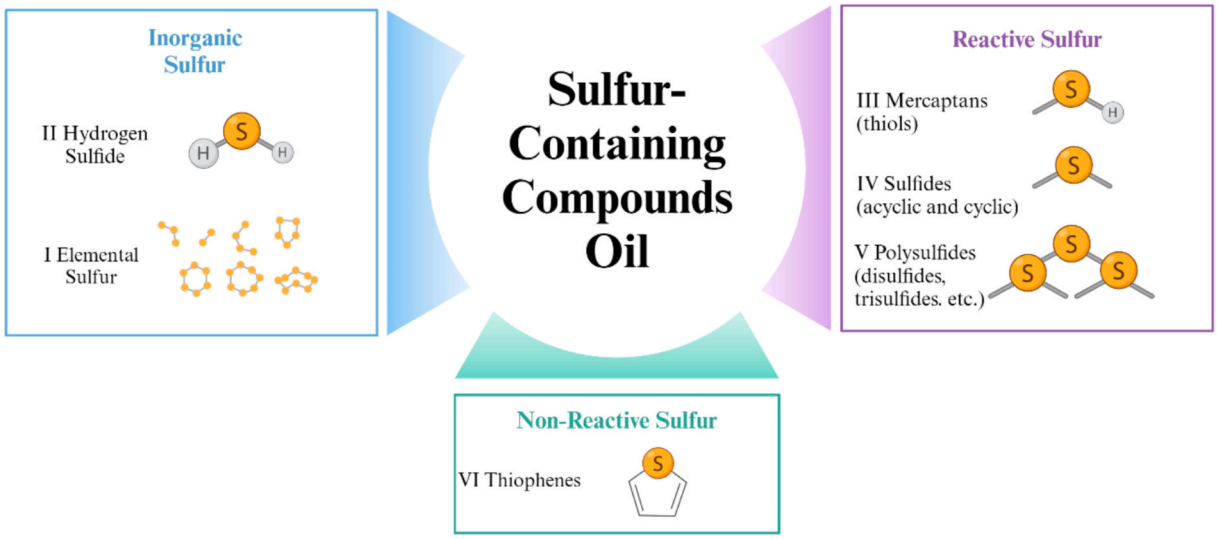

Fig. 2. The diversity of sulfur-containing compounds in oils. This diagram categorizes sulfur-containing compounds (SCCs) in crude oil into six main types based on their functional groups: elemental sulfur, hydrogen sulfide, mercaptans (thiols), sulfides (acyclic and cyclic), polysulfides, and thiophenics. The figure highlights the chemical reactivity and stability of these compounds, which are crucial for understanding their behaviour during desulfurization processes.

and less reactive. As for thiophenics, they are the most prevalent organosulfur compounds in petroleum; their common content there is up to 2/3 of the total sulfur. Despite being non-corrosive, thiophenic sulfur requires hydrodesulfurisation treatment at more severe conditions so that to meet standards for transportation fuels [34].

The diversity and concentration of SCCs vary across distillation fractions based on boiling point (Fig. 3) [19]. Higher boiling points correlate with increased sulfur content, leading to greater SCCs saturation in the heaviest fraction.

According to Singh et al. [35], the type of sulfur compounds depends on the fraction's boiling range and the source of the crude oil. If thiols and alkylthiophenes predominate in light naphthalene fraction, the main sulfur compounds are thiophenes in the case of heavy naphthalene fraction.

The chemical nature of sulfur directly affects its removal. The reason is that with increasing the b.p. of sulfur compounds, they become more refractory. For instance, the b.p. of 1-ethanethiol (ethyl mercaptan), 1-propanethiol (propyl mercaptan), and dimethyl disulfide are 35 °C, 67 °C and 109.7 °C, respectively [19,36]. To compare, the b.p. of benzothiophene and dibenzothiophene are known respectively as 221 °C and 332 °C [19,36]. This raises the question of which removal method is needed since desulfurising SCCs with aliphatic sulfur (thiols and sulfides) is easier than SCCs with aromatic sulfur (thiophenes). The examples of different crudes (Fig. 4) have demonstrated that sulfur is more concentrated in kerosene and gas oil fractions with higher b.p., not depending on the crude origin [35].

In kerosene fraction, major SCCs are presented as substituted thiophenes (C2TH, here and further C is a carbon number) and

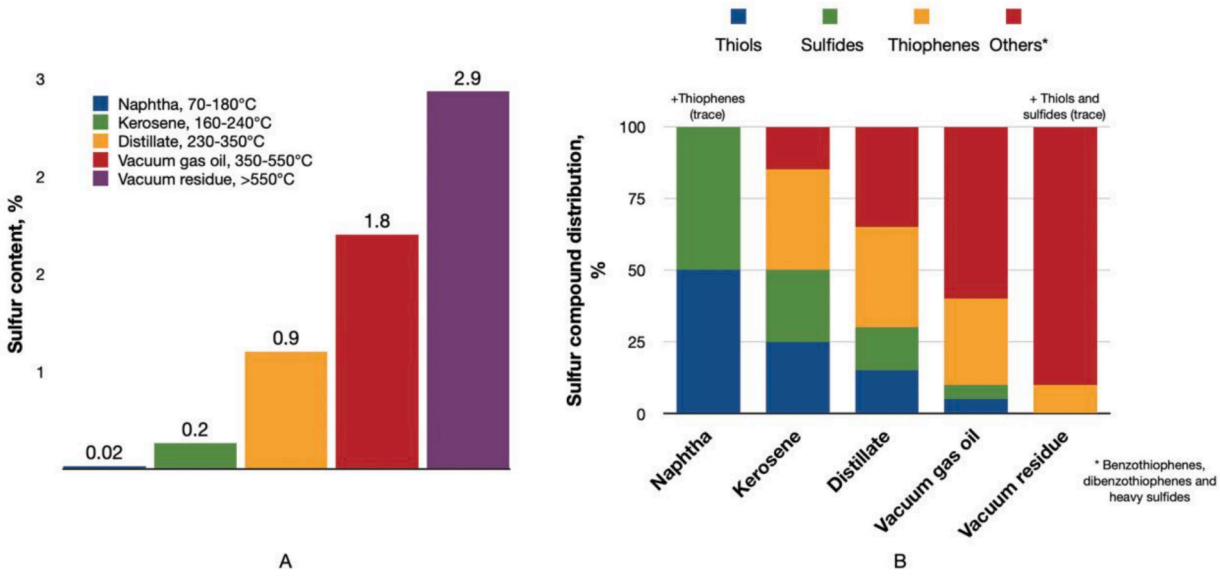

Fig. 3. Distribution of sulfur compounds over the distillation range of crude oil with a total sulfur content: (A) sulfur contents and (B) sulfur compounds distribution in different fractions. Panel (A) shows the sulfur content in different distillation fractions, while panel (B) illustrates the distribution of sulfur compounds across these fractions. The figure demonstrates that sulfur concentration increases with higher boiling points, with the heaviest fractions (e.g., gas oil) containing the most refractory sulfur compounds, such as dibenzothiophenes. This information is critical for selecting appropriate desulfurization methods for different petroleum fractions. The data used to build these histograms were adapted from [19]

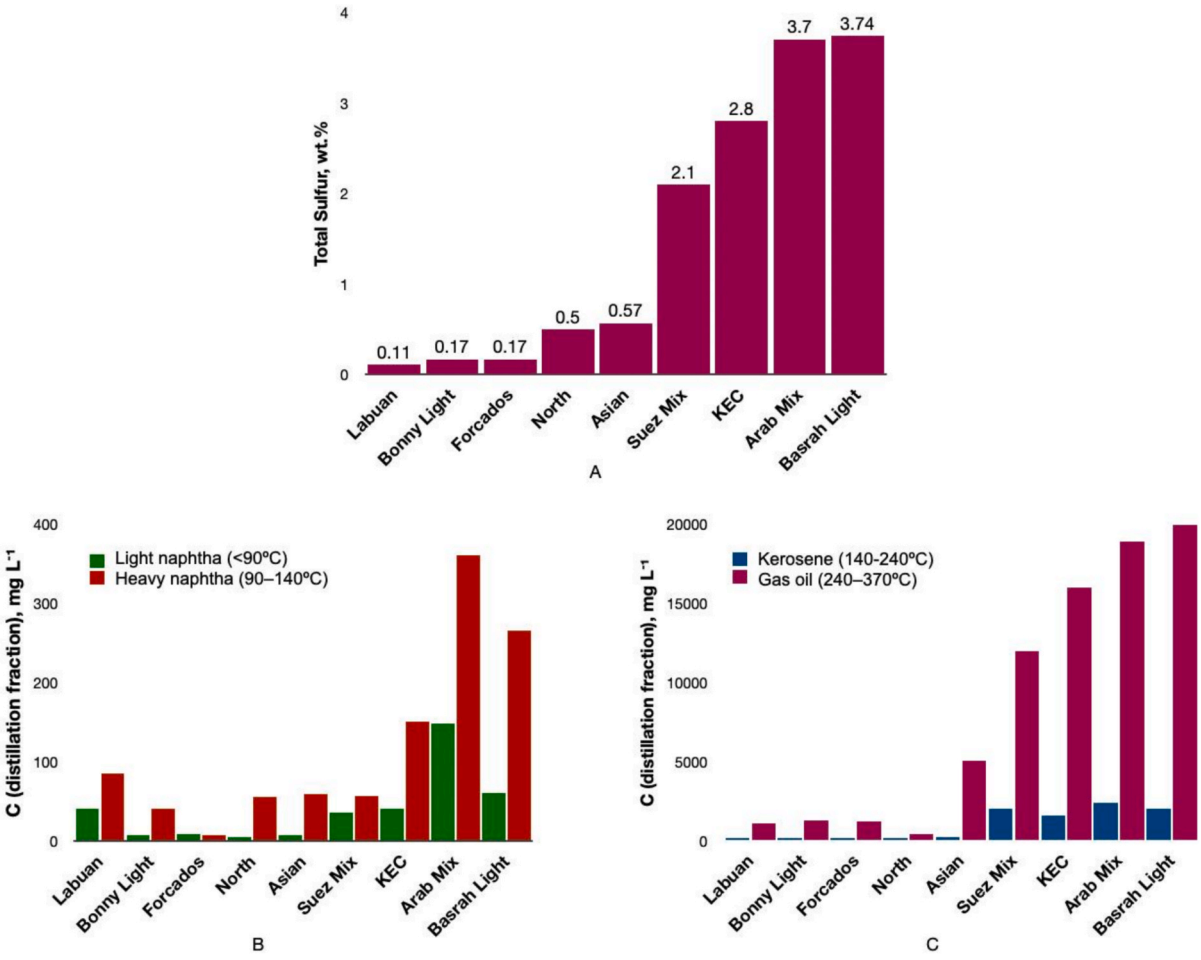

Fig. 4. The sulfur content in nine crude oils and their fractions: (A) the total sulfur content, (B) the content of light and heavy naphtha fractions, (C) the content of kerosene and gas oil fractions. Panel (A) displays the total sulfur content in each crude oil, while panels (B) and (C) break down the sulfur content in light/heavy naphtha and kerosene/gas oil fractions, respectively. The figure reveals that sulfur is more concentrated in the heavier fractions (kerosene and gas oil), regardless of the crude oil's origin. This distribution is essential for optimizing desulfurization strategies in petroleum refining. The data used to build these histograms were adapted from [35]

benzothiophene (C2BT), while gas oils fraction is made up of substituted benzothiophene (C2BT) and substituted dibenzothiophene (C3 + DBT) [35]. The desulfurisation efficiency of kerosene oils is nearly 100 % [37]; however, for gas oil fraction, achieving high efficiency is a significant problem because of dibenzothiophenes with low reactivity.

From the chemical reactivity point of view of aliphatic and aromatic sulfur in oils (Fig. 2), thiophene sulfur is non-reactive; it does not cause corrosion and also requires hydrosulfurisation conducted under more severe conditions [34]. As for aliphatic classes, sulfides, disulfides, and thiols are easily hydroconvertible, but corrosive in refinery pipe still operations. For this reason, these SCCs are known as "reactive". Since sulfur and SCCs in crude oil and other hydrocarbons cause corrosion challenges, air pollution, catalyst deactivation, etc., one of the essential tasks in the petroleum refining industry is removing sulfur from petrochemicals.

2.3. Desulfurisation of petroleum and petroleum products

Several techniques, such as hydrodesulfurisation (HDS), adsorptive desulfurisation (ADS), extractive desulfurisation (EDS), oxidative desulfurisation (ODS) and biodesulfurisation (BDS) have been applied to remove sulfur-containing compounds from petroleum and petrochemicals [38,39].

HDS is a well-known chemical process consisting of the action of hydrogen in the presence of catalysts on heavy oil fractions to reduce the sulfur content (to remove aliphatic and acyclic SCCs) by converting them into H_2S (Fig. 5) [40]. Preheating of the feed oil occurs via a heat exchanger (A) downstream of the reactor, exchanging heat with the reactor effluent. Further heating is achieved through a furnace (B) to reach the desired operating temperature. The heated oil undergoes hydro-processing over a series of catalyst beds inside a fixed bed reactor (C). Effluent temperature is then reduced using a cooling tower (D). Products undergo further separation in a fractionation column based on b.p. (E). Treated hydrogen gas is recycled back into the reactor.

HDS is usually conducted under high temperatures up to 400 °C and pressure up to 100 atm [19,20]. The most used catalysts in practice are based on transition metals such as Ni, Co, and Mo, but many more types are available [41]. For instance, MoS_2-based HDS catalysts are most prevalent in the refining sector. Ding et al. suggest adding Co/Ni by increasing the concentration of corner sites, which might boost the efficiency of HDS and overall catalytic performance [40,42]. In addition, Liang et al. examined the novel Waugh Co-Mo polyoxometalate (POM) cluster as a precursor for Co_4Mo_9 and $CoMo_9$ catalysts [43]. The result indicated that catalysts from this POM displayed notably more efficient dibenzothiophene (DBT) conversion than traditional precursors, making a 20 % improvement in DBT conversion due to an increase in the Co/Mo ratio. POM-containing media converts DBT into Co_4Mo_9-CAT (95 %) and $CoMo_9$-CAT (77 %), while conventional POM-free media forms Co_4Mo_9-FC (75 %) and $CoMo_9$-FC (60 %) [43]. The work conducted by Valles et al. [44] examined the efficacy of iridium catalysts on zirconium-

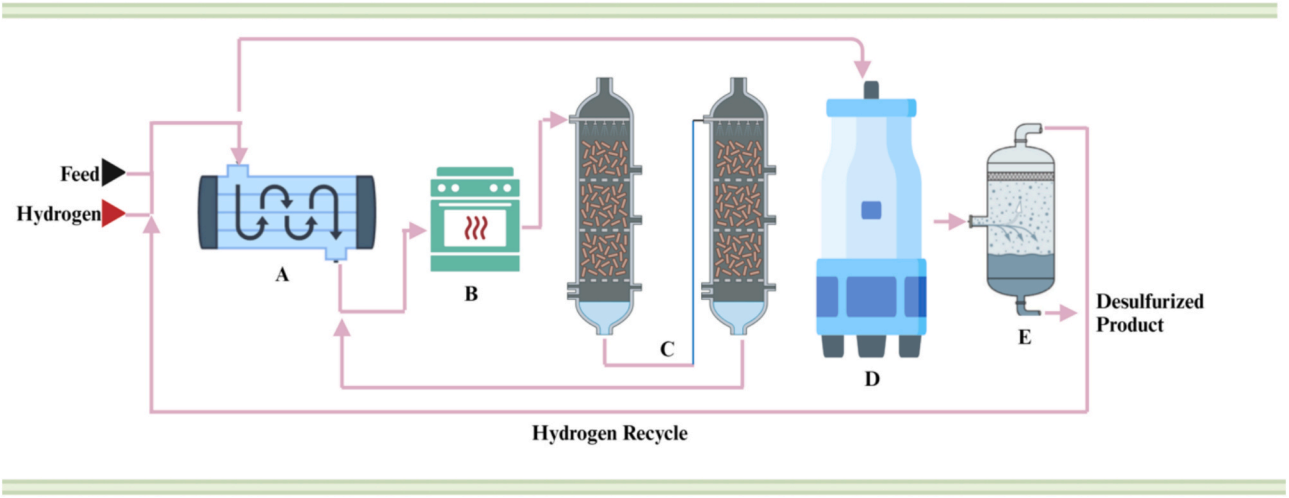

Fig. 5. Schematic representation of a hydrodesulfurization (HDS) unit. Key components include a heat exchanger (A), furnace (B), fixed-bed reactors (C), cooling tower (D), and phase separator (E). Typical operating conditions (350–400 °C, 6 MPa) are noted. The process efficiently removes sulfur from petroleum fractions by converting it into hydrogen sulfide, which is further processed in downstream units. The data used to build this scheme were adapted from [40].

modified SBA-15. The catalyst had a notable impact on its catalytic characteristics, enhancing the dispersion and reducibility of the active iridium species. The work [45] details the effective production of a highly efficient three-dimensional Zirconium (Zr)-modified TUD-1 mesoporous material. This was achieved using triethylamine (TEA) as a template and tetraethylammonium hydroxide (TEAOH) as an auxiliary template via the sol–gel process. The NiMo/Al_2O_3-ZrT-100 catalyst demonstrates exceptional efficiency in the HDS process, with an astonishing 99.3 %. The operational parameters require a temperature range of 350–360 °C, a pressure of 6 MPa, and a hydrogen-to-oil ratio of 600 ml ml^{-1}. A study [46] investigated the catalytic performance of $XMo_6(S)/\gamma$-Al_2O_3 and Ni-$XMo_6(S)/\gamma$-Al_2O_3 catalysts developed from Anderson hetero-polycompounds (HPCs), where X represents various elements like Al, Ga, In, Fe, Co, and Ni. The effectiveness of In and Ni catalysts in sulfur removal achieves 98.0 wt% at 380 °C, promoting the production of cleaner and eco-friendly fuels.

The higher the content of refractory SCCs, those with fully conjugated aromatic rings attached with fewer and longer side chains, the higher the temperature and pressure of HDS; thus, the more costly the process is. Previous studies indicated [47] that HDS efficiently removes aliphatic sulfur compounds, thiol, sulfides, and disulfides characterised by simple structures in the desulfurisation process. Thiophene (T), benzothiophene (BT), dibenzothiophene (DBT), and their derivatives are difficult to remove due to the aromatic structures and steric hindrances (Fig. 6).

A recent study demonstrated the effectiveness of the methylation/demethylation separation method in separating sulfur compounds in HDS-derived types of diesels into thiophene and sulfide fractions [48]. According to a new selective separation of thiophenic and sulfidic compounds from petroleum (Fig. 7) [48], these compounds can be methylated to sulfonium salts using $AgBF_4$ and CH_3I, followed by the precipitation of the latter from a petroleum matrix.

After this, thiophene and sulfidic sulfonium salts, via demethylation with 7-azaindole and 4-dimethylamino pyridine, can be converted to highly purified thiophenic and sulfidic compounds, respectively. Although there have been improvements, challenges still exist in the desulfurization of diesel fuel, requiring higher temperatures, more pressure, and numerous procedural steps. The constraints of the multi-stage HDS process are apparent in the inconsistent temperature and time criteria needed to attain specified sulfur reduction goals. With the increasing stringency of environmental requirements, more than relying on the classic HDS approach is required.

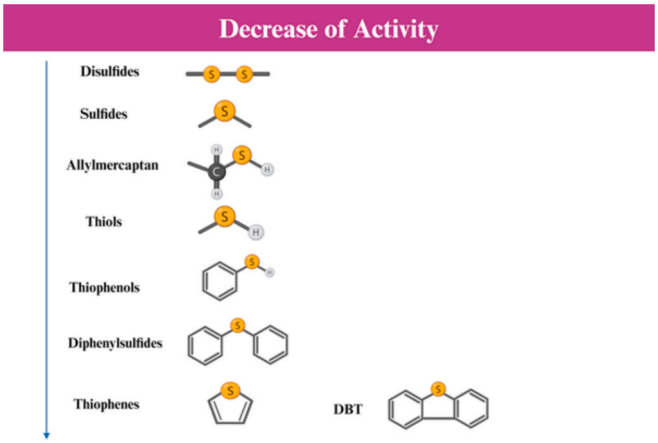

Fig. 6. Reactivity hierarchy of sulfur compounds in HDS processes present in crude oil. This figure ranks sulfur species based on their ease of removal, with thiols and sulfides being more reactive and easier to eliminate, while thiophenes, benzothiophenes, and dibenzothiophenes require more severe reaction conditions due to steric hindrance and electronic stabilization.

The most common HDS substitute, ADS, is frequently used to achieve ultra-deep fuel desulfurisation, even below the required limit. ADS operates predominantly through chemisorption or physisorption mechanisms, leveraging Van der Waals forces, chemical affinities, and electrostatic attractions for adsorption. Notably, ADS operates effectively at moderate temperatures (typically from room temperature to approximately 100 °C) and does not necessitate hydrogen [49], as shown in Fig. 8 [49]. Moreover, its reusable nature enhances economic viability as a diesel fuel sulfur removal technique.

ADS is based on physicochemical adsorption using a selective adsorbent to remove sulfur compounds. Therein, carbon and its modified varieties, metal–organic frameworks (MOF), clays, zeolites, silica-based, and supported metal(s) have acted effectively as sorbents [21]. It is reported that the adsorption efficiency is controlled by the properties of the adsorbent, such as surface area, pore volume, and the chemical nature of the adsorption surface area [41]. SCCs can be removed due to π-complexation, acid-base, metal-sulfur and van der Waals forces depending on the chemical composition of the adsorbent surface.

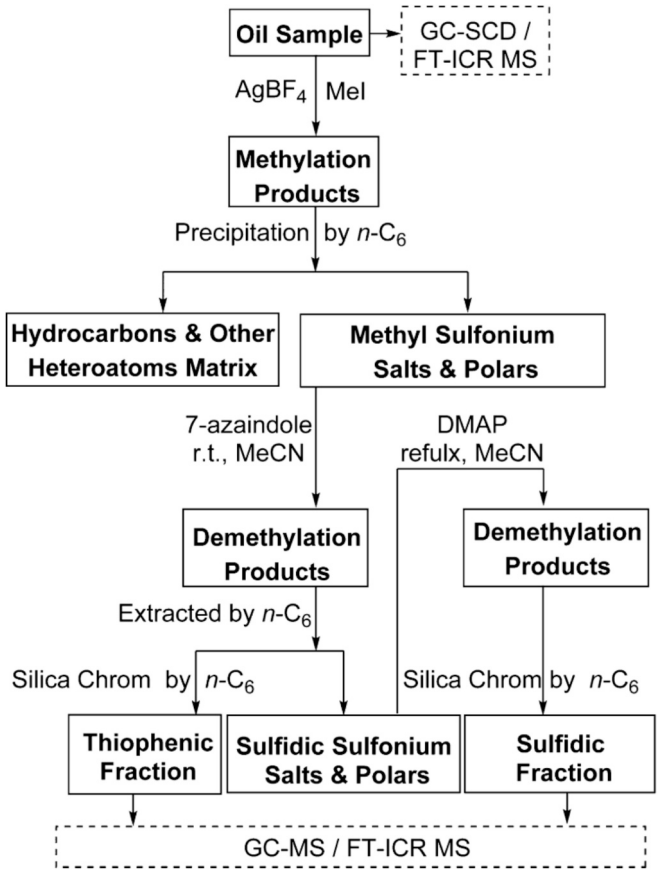

Fig. 7. Reaction-analytical scheme for selective separation of thiophenic and sulfidic compounds from petroleum. The figure outlines a novel method for separating thiophenic and sulfidic sulfur compounds using methylation/demethylation reactions. The process involves converting these compounds into sulfonium salts, followed by precipitation and purification. This approach offers a promising alternative to traditional desulfurization methods. Reprinted with permission from M. Wang, S. Zhao, K.H. Chung, C. Xu, Q. Shi, Approach for selective separation of thiophenic and sulfidic sulfur compounds from petroleum by methylation/demethylation, Anal Chem 87 (2015) 1083–1088 [48]. Copyright © 2014 American Chemical Society.

There has been a recent advancement in the field of ADS, which includes metals into the existing adsorbent materials that enhance selectivity, stability, and reusability [21]. Natural zeolites, such as clinoptilolite [50], are effective for initial efficiency in sulfur removal but need modifications. Modified clinoptilolite, especially those treated with Cu^{+} and Ni^{+}, shows substantial effectiveness in sulfur removal. Generally, when zeolites are exchanged with cationic metals, the reaction of their electropositive character with sulfur atoms bounds to their basic structure, leading to an increase in adsorption capacity. For example, the adsorption capacity of the optimal modified Cu^{+} meso clinoptilolite achieved 28.12 g DBT kg^{-1} adsorbent [51,52].

Synthetic zeolites, specifically those within the faujasite framework (FAU) [53], have some advantages, including pore structures and surface acidity. Their adsorption capacity can be improved through modifications with metals such as Ce and Cu, which enable high sulfur adsorption even with aromatics. Desulfurisation performance can be significantly modified if rendered hierarchical or doped with Ce or Cu. Moreover, these modifications enable access to the adsorbent's active sites, thus improving the adsorbent ability. Zhang et al. synthesised Ag-Y (II) and CuZn-Y(I) with a potential reduction of DBT and 4,6-DMDBT at 97 % and 99 %, respectively [54].

Among basolite-type MOFs, C300 ($Cu_3(C_9H_3O_6)_2$) Cu-BTC (55 gDBT kg^{-1}) and A100 ($C_8H_5AlO_5$) MIL-53(Al) (40 gDBT kg^{-1}) exhibit higher adsorption capacities for DBT than F300 ($C_9H_3FeO_6$) Fe-BTC (25 gDBT kg^{-1}) and traditional zeolite-Y (7 gDBT kg^{-1}). Interestingly, $CuCl_2$-loaded MIL-47 (vanadium-benzenedicarboxylate) has the best adsorption capacity, which is 215 g kg^{-1} at 25 °C for DBT and 0.37–0.39 g kg^{-1} for BT adsorption [55,56]. Additionally, the adsorption capacity of MOFs with flexible structures, explored under the influence of diethyl ether and water, was 0.373 mmol g^{-1} under certain conditions and had MIL-53 topology [57]. Including ionic liquids into MIL-101 (Cr) enhanced sulfur removal efficiency by promoting acid-base interaction. Further improvements were achieved by incorporating Cu-cations on MIL-100 (Fe), demonstrating 100 gBT kg^{-1} adsorption capacity. The findings of the model gasoline feed study on HKUST-1 and CPO-27-Ni showed that specific interactions between adsorbate and adsorbent are necessary for the high selectivity of thiophene and toluene [58].

An impactful study on the synthesis and design of magnetic nanoadsorbents for model and commercial fuel ADS was reported by Ali et al. [59]. These nanoadsorbents, which had wire, rod and flower-like structures, were made of Fe_3O_4@MnO_2–coated palm kernel shell-activated carbon prepared by hydrothermal method. Optimised ADS conditions for model fuel included an adsorption temperature of 25–35 °C, 0.4 g adsorbent dose, 530 ppm DBT concentration, and 100 min contact time, resulting in up to 99 % DBT removal. For commercial kerosene and diesel fuels, sulfur removal efficiencies ranged from 73 % to 97.6 % under optimised conditions. In general, improving adsorbents towards sulfur elimination calls for proper knowledge of the compositions of materials used, their surface chemistry, as well as modification methods applied.

EDS is a method that uses alternative, environmentally friendly, and cheap solvents for effective fuel desulfurisation. The peculiarity of this method is that desulfurisation is carried out under mild conditions (low temperature and pressure), and there is no need to use hydrogen and a catalyst [19,60,61]. Crucially, EDS selectively removes sulfur compounds from the fuel oil without destroying other compounds in it. The extracted compounds can then be reused as raw materials. This becomes possible due to the difference in the distribution of sulfur compounds between the oil phase and the extractant phase. Accordingly, the critical point is the choice of extraction solvent. For this reason, both traditional molecular solvents and a new class of sustainable solvents named deep eutectic solvents and ionic liquids are employed for EDS [62–64].

Ionic liquids (ILs) have been included in the list of potential candidates for EDS because of their green characteristics, non-volatile, thermally stable, and highly adjustable nature. Jiang et al. [65] carried out a study on the verification and mechanism analysis of 16 different ILs through quantum chemistry calculations and molecular dynamic simulations, indicating that $[C_2COOCH_3ImC_6H_{13}][NTF_2]$ showed considerable capabilities in extracting DBT of over 60 % purity. Moreover, $[C_2COOCH_3ImC_6H_{13}][NTF_2]$ effectively eliminated sulfur at room temperature. Similarly to this, after comparing 800 IL combinations [66], it was demonstrated that $[P66614]_2[CuCl_4]$ is reported as the best performer, achieving an impressive 85.07 % conversion rate of H_2S to elemental sulfur.

Yu et al. [67] examined the potential of desulfurisation for porous liquid (PL) MIL-53 (Al) in sulfur elimination of T, BT, and DBT from fuel oil with the efficiency of 67.67 %, 85.50 %, and 84.34 %, respectively, within 30 min at 25 °C with 5000 ppm initial concentration of sulfur. Therefore, deep eutectic solvent (DES) from imidazole and tetrabutylammonium bromide salt showed 70 % DBT and 47 % T recovery during one-step extraction [68]. Further studies conducted by Makoś et al. [63] revealed that the most optimal conditions for desulfurisation were obtained using ChCl:Ph solvent with a 1:4 M ratio, an extraction period of 40 min, and a temperature of 40 °C. Under these circumstances, a one-step cycle extracted T, BT, and DBT at 91.5 %, 95.4 %, and 99.2 %, respectively. Additionally, the efficiency was up to 99.99 % after three cycles. The effectiveness of EDS could be boosted by adjusting the proper extraction period, solvent constitution and temperature.

ODS is a promising deep desulfurisation method consisting of two

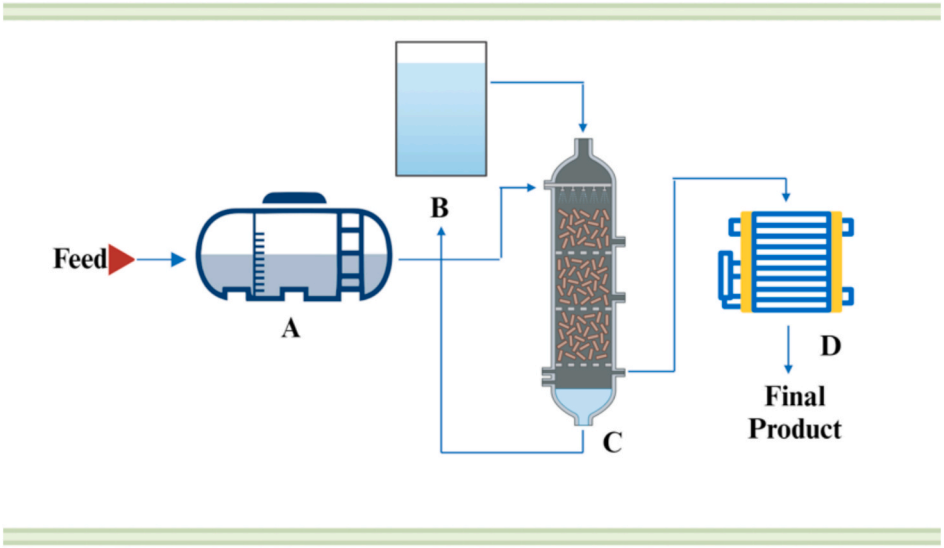

Fig. 8. Fixed-bed adsorptive desulfurization (ADS) system. The setup consists of a fuel reservoir (A), water tank (B), reactor (C) packed with an adsorbent material, and condenser (D) for collecting treated fuel. ADS operates under mild conditions and selectively removes sulfur species through physical and chemical adsorption interactions. Adapted with permission [49]. Copyright © 2023 Azeez et al. Published by Elsevier. Licensed under CC-BY-NC-ND 4.0.

stages: (i) oxidation and (ii) separation operations [19,22,69]. In the first stage, divalent sulfur is oxidised to the corresponding hexavalent sulfone in the presence of an oxidising agent. This occurs due to adding two oxygen atoms to the sulfur without breaking the carbon–sulfur bonds; the intermediate is a sulfoxide. If an excess of oxidising agent is used, sulfones are formed. In the second, purification stage, oxidised sulfur compounds are separated from oil and petroleum products due to the difference in polarity and boiling points from the original sulfur compounds.

Hydrogen peroxide is a good oxidising agent for ODS because it is cheap, available, and eco-friendly. Other oxidants used include oxygen, nitric acid, nitrogen oxides, and organic hydroperoxides (such as *tert*-butyl hydroperoxide). The oxidation capabilities are enhanced by combining hydrogen peroxide with various catalysts such as acetic acid, formic acid and polyoxomolybdates. Furthermore, solid catalysts such as alumina-supported polymolybdates (V_2O_5/Al_2O_3, Co-Mo/Al_2O_3, and V_2O_5/TiO_2) showed successful modifications for ODS process [70–72].

The catalytic ODS of sulfur from BT, DBT, and 4,6-DMBT has proven effectiveness. Mamaghani et al. [73] studied ODS using HCOOH as a catalyst and H_2O_2 as the oxidising agent, achieving 100 % sulfur elimination under optimised conditions.

POM-based catalysts in desulfurisation DBT have been an essential advancement in the ODS process. The development of highly polar catalysts like TiO_2/MWCNTs-NH_2-HPW exhibited superior oxidation adsorption desulfurisation (OADS) performance, achieving a 99 % DBT removal rate within 30 min at 60 °C; similarly, polar PW-H_3N^+-SBA-15 catalyst demonstrated a 100 % desulfurisation rate of DBT in 120 min [74]. The catalysts like $(NH_4)^{3-}HPMo_{11}VO_{40}$ and SiW_{12}@C@SiO_2 can be used to oxidise DBT, achieving 100 % sulfur removal within 90 min at 130 °C [75] and at 60 °C in 20 min [76].

Regarding MOFs as ODS catalysts, most pure MOFs have exhibited poor catalytic ODS performance due to the limited availability of active sites. However, they can be improved significantly by the insertion of defect sites. For example, Zr and Ti-ions increased DBT efficiency to 100 % within 2 h [77].

Furthermore, the study of aerobic ODS addressed global energy challenges and promoted clean and sustainable fuel conversion. It involves using molecular oxygen from the air as an oxidant, which is also preferred because it is available, non-polluting, and low-cost. The results showed the maximum sulfur conversion of 95 % under mild conditions, minimising the impact on fuel octane ratings [78].

Electrochemical ODS (EODS) has gained considerable attention recently due to its mild operating conditions, minimal pollution, high efficiency, and versatility [79]. Sulfur compounds are converted into soluble sulfates or gaseous sulfides, which can be separated using solid–liquid or gas–liquid techniques. During electro-reduction, sulfur is reduced to H_2S or S^{2-} by the reducing medium generated at the cathode. This process enhances the hydrophobicity of minerals by reducing oxygen-containing functional groups on the mineral surface. The reducing agents, such as H_2 or $NaBH_4$, are crucial in lowering inorganic sulfides and hydro-desulfurizing organic sulfur compounds.

The next processing method, BDS, uses microorganisms to metabolise SCCs at low temperatures and pressures. Compared to HDS, this method reduces all capital and operating costs by 2 % and 15 %, respectively [80].

Several microorganisms, such *as Rhodococcus, Gordonia*, and *Pseudomonas*, perform BDS by oxidising sulfur via two main pathways: the Kodama pathway and the sulfur-specific pathway. These pathways break down sulfur compounds while maintaining the carbon structure. The efficiency of BDS with *Rhodococcus* species displays high desulfurisation efficiency but decreases with an increase in sulfur concentration [81–83]. The results obtained by Davoodi-Dehaghani et al. [84] demonstrate that *Rhodococcus* strains can achieve BDS efficiencies ranging from 100 % to 80 %, depending on the sulfur concentration in the process. For instance, at 1842 ppm and 16100 ppm sulfur concentrations, the BDS efficiencies were only 36 % and 11.9 %, respectively. In contrast, other bacterial species like *Gordonia, Arthrobacter*, and *Desulfubacterium* exhibit high BDS efficiency, ranging from 99.4 % to 77 %, across sulfur concentrations of 167.7 ppm to 37 ppm, respectively. However, some bacterial species, including the bacteria of *Achrobacter* and *Spingomonas*, yield less than 70 % BDS efficiencies when the sulfur concentration exceeds 280 ppm. Similarly, *Pseudomonas* and *Bacillus* species demonstrate lower BDS efficiency, particularly at higher sulfur concentrations. For example, *Pseudomonas* sp. achieved a BDS efficiency of 47.03 % with a sulfur concentration of 591 ppm, while *Bacillus* sp. exhibited an efficiency of 31 % at a sulfur concentration of 1842 ppm [85].

Recent advancements supplemented BDS technology with catalytic processes utilising enzymes or catalytic agents. The development of heterogeneous bio-nanocatalysts, such as lignin nanoparticles functionalised with concanavalin A, has substantially improved the performance of BDS, enhancing its efficiency and efficacy in sulfur removal

from fuels. Derikvand et al. [86] employed the Taguchi method to optimise the BDS of *Rhodococcus erythropolis* R1 using calcium alginate beads and γ-Al_2O_3 nanoparticles. BDS rates increased by 80 % using a bioreactor with immobilised *Rhodococcus rhodochrous* cells in a silica catalytic bed.

Biphasic systems have also shown promise. Nassar et al. [87] reported 94 % BDS of 100 mg DBT L^{-1} by *Paenibacillus glucanolyticus* HN_4 in an oil/water enrichment medium. *Rhodococcus erythropolis* SHT87 achieved complete DBT degradation within 10 h in a biphasic system, while *Rhodococcus erythropolis* exhibited 95.5 % BDS in a batch reactor using n-dodecane (v/v) [84,88].

Abo-State et al. [89] conducted comparative media optimisation studies with different carbon sources for BDS strains *Rhodococcus erythropolis* and *Brevibacillus invocatus* C19. Both showed maximum activity with glucose or glycerol. Moreover, researchers compared *Rhodococcus erythropolis* with *Gordonia alkanivorans*, favouring the latter. Several bacterial species, including thermophiles and genetically modified organisms, have demonstrated high BDS activity, with some achieving efficiencies up to 99 %.

While BDS has shown potential, some challenges still need to be addressed, such as slow reaction kinetics and poor performance in a high sulfur level. Moreover, combining BDS with other desulfurisation methods holds promise for industrial implementation.

Based on the comparative analysis provided above, the benefits and drawbacks of different desulfurisation methods were summarised in Fig. 9 [21,74,86,87,90,91]. HDS is known for its efficiency but faces challenges related to energy intensity, high operating conditions, and environmental concerns associated with hydrogen sulfide formation. ADS operates at mild conditions without the need for hydrogen, although this may demand large amounts of sorbents while also lacking selectivity for certain sulfur compounds. EDS seems attractive because of its simplicity and integration potential with existing refinery methods, although solvent selection and sulfur extraction efficiency pose significant considerations. ODS offers an opportunity for lower operating costs and moderate reaction conditions, but still challenges exist associated with optimising oxidising agents and addressing potential by-product formation.

Engineering efforts have improved the efficiency of green BDS alternatives, but the need for sanitisation, transportation, storage, and use of microorganisms in refinery environments limits the method's commercial use.

During pyrolysis, metal oxides are added to the petroleum coke, which is rich in sulfur, to facilitate desulfurisation by reducing the energy barrier of the pyrolysis process. Specifically, iron promotes the formation of FeS. It prevents these S radicals from combining with other free radicals to create more stable sulfides due to Fe's strong affinity for S radicals formed during pyrolysis [92]. Shen F et al. [93] have developed the chemical looping desulfurisation method for high-sulfur petroleum coke. This method employs a Fe_2O_3/Al_2O_3 composite as an oxygen carrier and effectively oxidises the organic sulfur, specifically the thiophene, representing the key difficulty in desulfurisation. It achieves a removal efficiency of 63 %. Similarly, in [94], reduced iron powder catalytic roasting has effectively worked on desulfurisation and modification of high-sulfur petroleum coke. The desulfurisation rate of high-sulfur petroleum coke reaches 87.93 %, reducing the sulfur content to 0.91 wt%.

Along with conventional chemical ways, sulfur might be removed using wave technologies based on electric pulse effects, cavitation, hydrowave, magnetic and electromagnetic effects, and combined wave technologies [95]. In these ways, the penetration degree can be

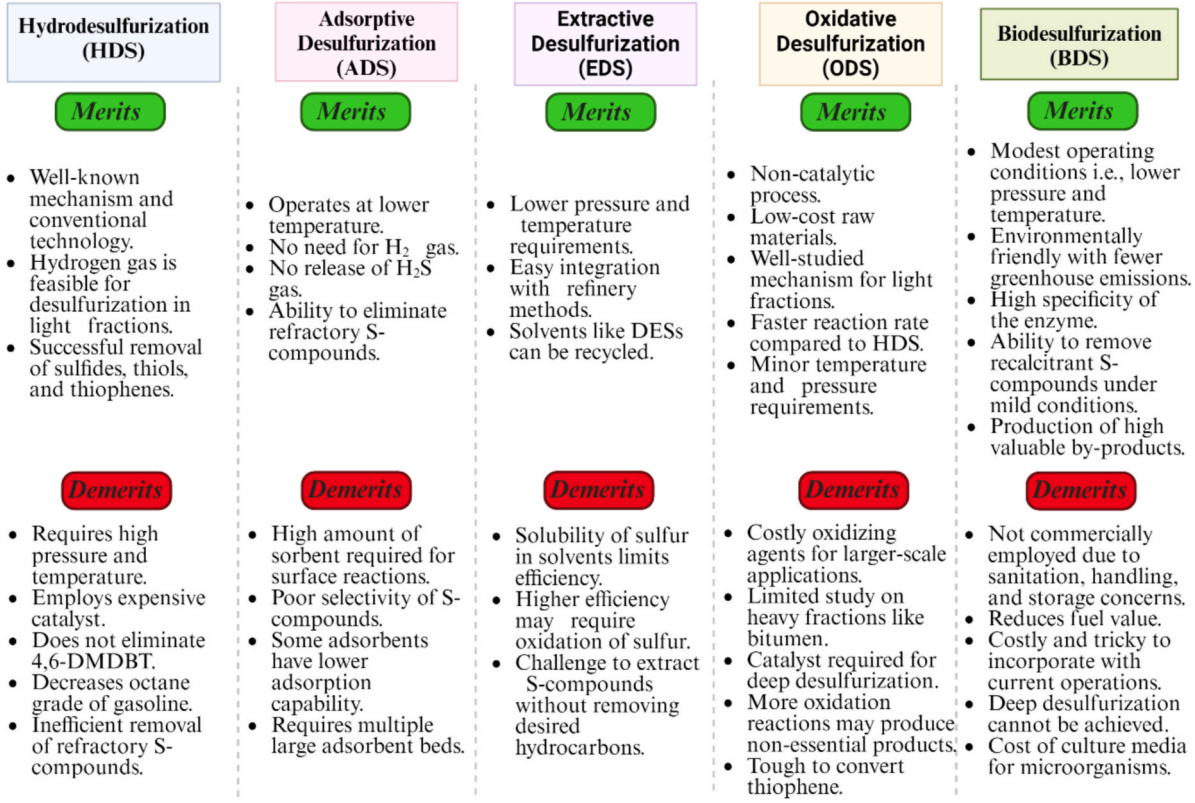

Fig. 9. Comparative analysis of desulfurization methods (HDS, ADS, ODS, BDS). The figure highlights the efficiency (%), energy requirements, scalability, and environmental impact of various desulfurization techniques. Hydrodesulfurization (HDS) is highly efficient but energy-intensive, while adsorptive desulfurization (ADS) operates under milder conditions. Oxidative desulfurization (ODS) and biodesulfurization (BDS) offer environmentally friendly alternatives but face challenges in scalability and reaction kinetics. The data used to build this figure were adapted from [21,74,86,87,90,91].

controlled by changing wave frequencies (wavelengths) and predetermining their energies. Consequently, it leads to radical transformations in chemical and physical processes. To confirm this, the irreversible direct desulfurisation reaction of tetraceneothiophene was carried out in an electric field by cleavage of two carbon–sulfur bonds of thiophene and exergonic detachment of the sulfur atom [96]. Another study revealed that electropulsed fields separated 96.3 %, 98.8 % and 99.1 % of sulfur from fuel oil, diesel fraction and gasoline fraction, respectively [95].

2.4. Elemental sulfur separated from petroleum and petrochemical products and its purification

2.4.1. Sulfur from gaseous petrochemical products

One of the typical sulfur-containing petrochemical by-products is a gas, hydrogen sulfide (H_2S). There are various ways to desulfurise fuel gases with sulfur recovery. For example, one part is based on liquid redox processes known as the Stretford process, the Unisulf process, the Sulfolin process, etc., and another part is based on gaseous redox processes with recovery of elemental sulfur [97]. The hydrogen sulfide formed at HDS can be oxidised to elemental sulfur by the Claus process in the presence of a specific Claus catalyst [98]. The conventional Claus process recovers 92–95 % sulfur from H_2S concentration [97].

The gas conversion operates in two stages: thermal oxidation and catalytic conversion. In the thermal oxidation stage, H_2S reacts with oxygen (O_2) to produce elemental sulfur (S) and water (H_2O) through several reaction pathways (Eqs. (1) and (2)). The overall conversion of H_2S into sulfur is achieved through intermediate reactions involving the formation of sulfur dioxide (SO_2) and sulfur (Eqs. (3) and (4)).

Thermal Stage:

$$2H_2S + 3O_2 \rightarrow 2SO_2 + 2H_2O \quad (1)$$

$$2H_2S + SO_2 \rightarrow 3S + 2H_2O \quad (2)$$

Catalytic Stage:

$$2H_2S + SO_2 \rightarrow 3/nS_n + 2H_2O \quad (3)$$

$$2H_2S + SO_2 \rightarrow 3/8S_8 + 2H_2O \quad (4)$$

The first stage consists of high-temperature combustion of H_2S at temperatures ranging from 1000 to 1300 °C (depending on the H_2S concentration and the presence of hydrocarbons, ammonia, and other impurities). The second stage operates at 200 to 300 °C [99,100]. Fig. 10 shows a schematic diagram of the Claus process [100].

The performance of the Claus process may be detracted from the thermal reduction of sulfur, temperature, pressure, catalyst type, and residence time. The partially redesigned Claus process shows relatively low operational temperatures and high H_2S conversion efficiency while reducing sulfur compound emissions and mitigating air pollution. Still, major challenges include sulfur dioxide emissions and complex sulfur recovery systems. Some of the current research areas include modifying the structure of the reactors to increase efficiency and sustainability, designing catalysts that can increase the rates of recovery and reduce power consumption, and optimising the operational processes to enhance the efficiency of the system [101,102].

Ghahraloud et al. [103] proposed a modified way to recover Claus sulfur using isothermal reactors to decrease sulfur contaminant emission. This resulted in increased H_2S conversion, 1.87 % and 1.78 % higher than the conventional Claus process. Besides, the proposed case provided higher sulfur recovery and lower sulfur contaminant emissions such as COS and CS_2. Another study revealed that it is better to first convert the H_2S into elemental sulfur with the modified Claus process and employ the Claus tail-gas treatment to increase overall recovery to $>$ 99.5 % [104].

Huang et al. reported a novel process alternative to the high-temperature Claus process [105]. It allowed the conversion of H_2S from gasified synthesis gas and SO_2 in fuel gas into sulfur powder through three-stage acid washing technology. The recovered sulfur is of high purity, similar to sulfur from the Claus process.

The next group of desulfurisation methods is dedicated to bacterial conversion of hydrogen sulfide and separation of elemental sulfur. Mol et al. showed polysulfides' role in forming and growing elemental sulfur from the bacterial conversion of hydrogen sulfide (Fig. 11) [106]. In Fig. 11, for the design without compartment B, the liquid from absorber A was introduced at reactor C. Liquid flows are indicated with solid lines and gas flows with dashed lines. In compartments A and B, polysulfide formation was the primary reaction of interest to sulfur crystallisation. In compartment C, the main reaction of interest to sulfur crystallisation was (poly)sulfide bio-oxidation.

Noted that the key element is the nucleophilic dissolution of S by sulfide (HS^-) to polysulfides (S_x^{2-}), which is enhanced by an oxygen-free reactor with a high sulfide content. It has been experimentally established that an increased concentration of polysulfides S_x^{2-} leads to crystalline agglomerates of elemental sulfur of uniform size (14.7 ± 3.1 μm). As hypothesised, the crystallisation product (agglomerate) is controlled by the balance between dissolution and elemental sulfur formation, which could potentially prevent poor S precipitation in BDS. To confirm this, Chen et al. [107] revealed polysulfides that enhance the

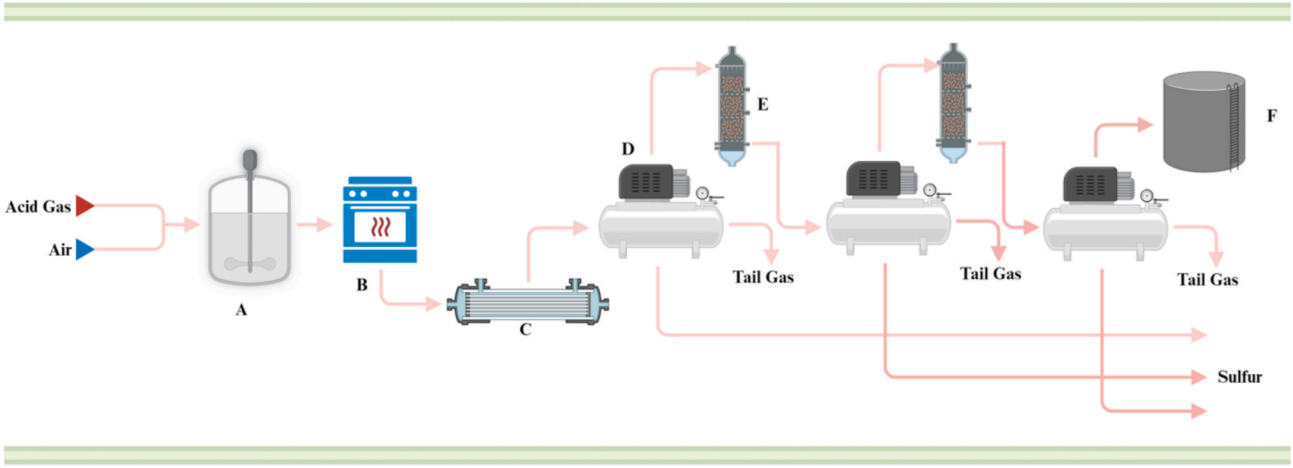

Fig. 10. Three-stage Claus process for converting hydrogen sulfide into elemental sulfur. The system comprises a thermal oxidation unit (A–C), catalytic reactors (D–E), and a tail-gas treatment unit (F). The Claus process is widely used in industrial applications to recover sulfur from refinery gases, reducing sulfur dioxide emissions and maximizing sulfur yield. Adapted with permission [100]. Copyright © 1997 Kohl et al.

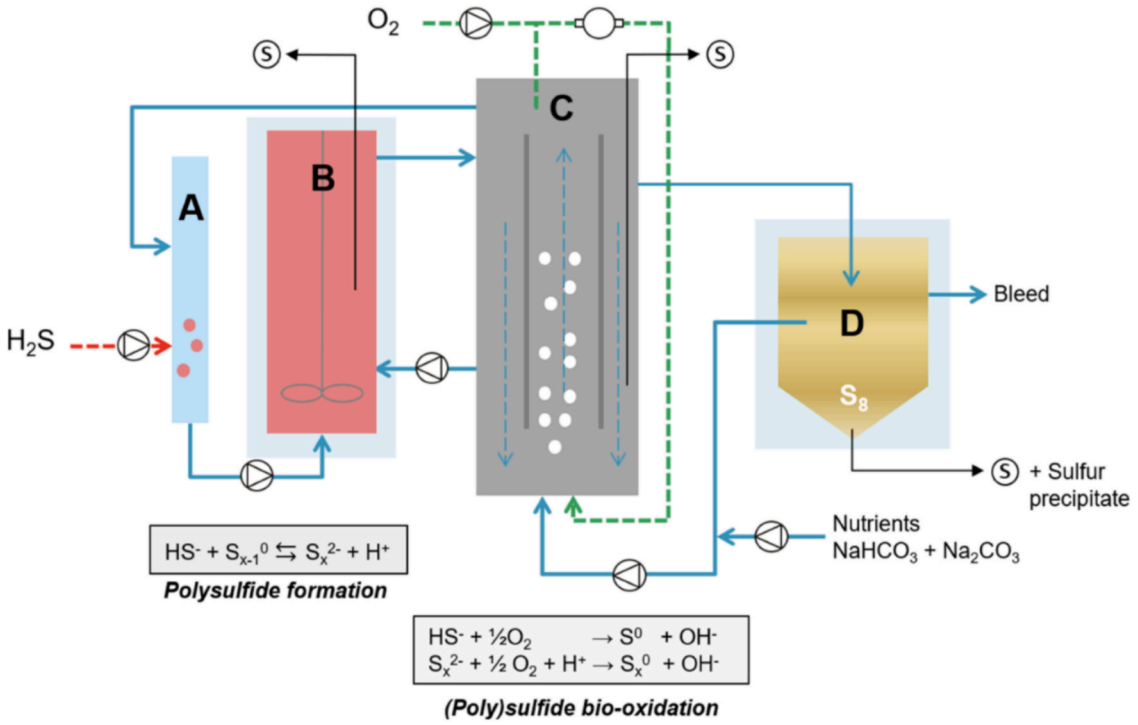

Fig. 11. Biodesulfurization reactor system: (A) absorber, (B) anoxic reactor, (C) gas-lift reactor, (D) settler, and (S) sampling ports. The system uses microorganisms to convert sulfur compounds into elemental sulfur, offering a sustainable alternative to chemical desulfurization methods [106]. Reproduced with permission. Copyright © 2021 Mol et al. Published by American Chemical Society. Licensed under CC-BY-NC-ND 4.0.

agglomeration of elemental biosulfur in gas biodesulfurisation systems.

2.4.2. *Sulfur from liquid petrochemicals*

Another source of elemental sulfur is hydrocarbons but in a liquid phase. In this case, there are also different ways to separate sulfur. For example, a patent describing how to separate elemental sulfur from refined petroleum fuel stated that petroleum-based liquids must be treated with an aqueous solution containing caustic, sulfide and elemental sulfur [108]. It produces an aqueous layer containing metal polysulfides separated from a liquid layer with a reduced level of elemental sulfur. In addition, as predicted, adding organo-mercaptans to the liquid can speed up the removal of elemental sulfur.

Membrane technologies may also be employed to extract elemental sulfur from crude oil. According to Al-Zahrani et al. [109], a porous hollow fibre membrane filled with triphenylphosphine was used to extract simultaneously and derivatise elemental sulfur in Arabian crude samples. As reported, relative recoveries ranged between 98.2 % and 101.2 %.

There are traditional and alternative methods for purifying elemental sulfur from impurities. Conventional methods are based on thermal treatment and distillation. Thermal treatment leads to the decomposition of higher hydrocarbons into carbon and lower hydrocarbons, which then react with sulfur. For instance, it can be performed by long-term (up to a few days) boiling of sulfur. This is known as the Bacon-Fanelli method [99], in which sulfur is boiled with magnesium oxide and decanted. After boiling, the sulfur fraction must be filtrated through glass wool to remove the black residue that has formed. The following known method is the Wartenberg method [110], which introduces a quartz rod heated to 750—800 °C into molten sulfur. This allows for a decrease in the carbonaceous impurities to 10^{-6}%.

Another method of purifying elemental sulfur is passing sulfur vapour through a high-temperature zone (up to 800–1000 °C) multiple times [110]. Similarly, Adamchik et al. conducted purification thermochemically by placing sulfur in a distilling still heated in a quartz reactor packed with powdered quartz glass [111]. As a result, the content of aliphatic hydrocarbons in sulfur decreased to $2{\cdot}10^{-5}$ wt%. To compare, Susman et al. reported that dynamic pyrolysis could be employed for obtaining elemental sulfur with carbon, oxygen and hydrogen in a total content of < 10 μg g^{-1} [112]. According to Churbanov et al., extra pure sulfur might be obtained by vacuum extraction of sulfur from gaseous hydrocarbons [113]. Sukhanov et al. reported an ultra-purification method of elemental sulfur, allowing it to achieve a high purity of 99 % [114]. This method includes the thermochemical treatment of sulfur vapour on silica, followed by melting with aluminium and distilling. To compare, Altayi et al. proposed the process of catalytic purification of sulfur from bituminous impurities (Fig. 12) [115], leading to a decrease in impurity content from 1.35 wt% to $\leq$ 0.015 wt%.

As an alternative to the traditional distillation method, plasma-chemical technology has been proposed by Logunov et al. [116] and Mochalov et al. [117]. Using plasma (40 MHz)-chemical distillation at low pressure (0.1 Torr) under dynamic vacuum conditions makes obtaining elemental sulfur for IR-optical purposes possible. A potential mechanism underlying the plasma charge effect on sulfur agglomerate S_8, which is most thermodynamically stable in a system under treatment, is shown as follows (Eqs. (5)–(13)) [117]:

$$e^- + Ar \rightarrow e^- + Ar^* \quad (5)$$

$$e^- + S_8 \rightarrow 4S_2 + e^- \quad (6)$$

$$Ar^* + S_8 \rightarrow 4S_2 + Ar \quad (7)$$

$$e^- + S_2 \rightarrow e^- + 2S \quad (8)$$

$$e^- + S_2 \rightarrow S^- + S \quad (9)$$

$$e^- + S_2 \rightarrow S^* + S + e^- \quad (10)$$

$$Ar^* + S_2 \rightarrow 2S + Ar \quad (11)$$

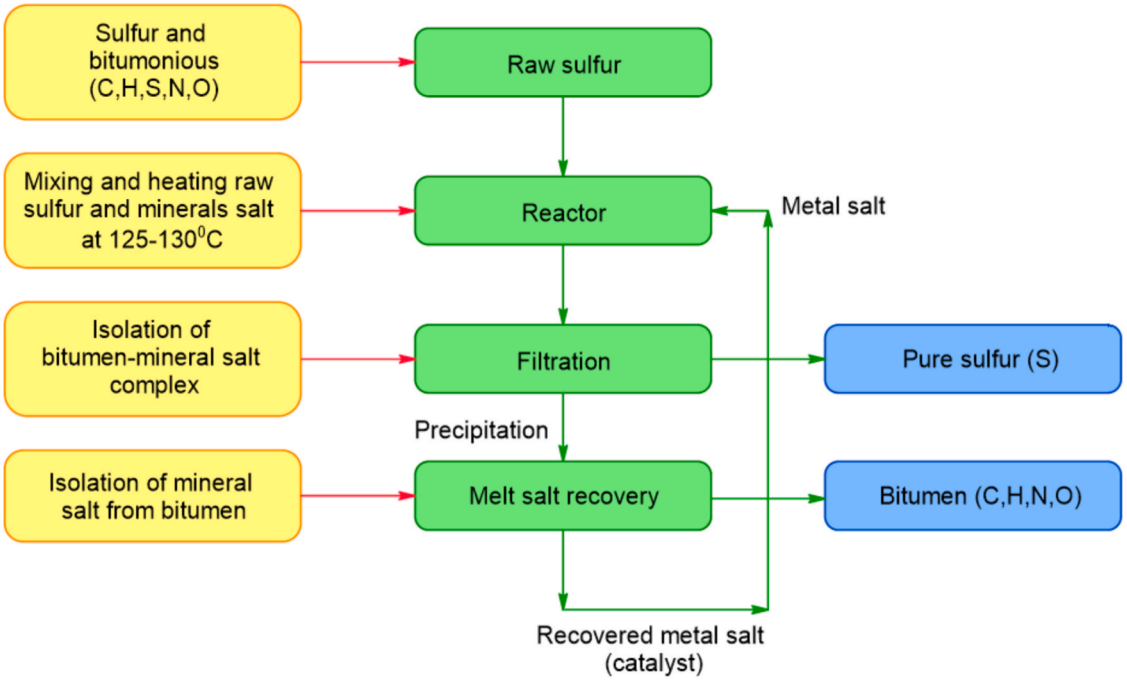

Fig. 12. A flow diagram of the proposed process for purifying sulfur from bituminous impurities. The figure outlines a catalytic purification process that reduces impurity content from 1.35 wt% to ≤ 0.015 wt%. The method involves treating sulfur with a catalyst to remove bituminous impurities, resulting in high-purity sulfur suitable for industrial applications [115]. Transformed with permission. Copyright © 2024 Pakistan Journal of Analytical & Environmental Chemistry. Licensed under CC-BY-NC-SA 4.0.

$$e^- + S \rightarrow 2e^- + S^+ \quad (12)$$

$$Ar^* + S^* \rightarrow e^- + S^+ + Ar \quad (13)$$

Gunaratna et al. [118] compared traditional and laboratory methods of sulfur processing. The former was based on the '*gandhaka shodhana*' process, which uses cow's milk, ghee or occasionally plant extracts to purify elemental sulfur. In comparison, recrystallisation of the crude sulfur was chosen as the laboratory method. According to this method, crude powdered sulfur was heated with xylene under continuous stirring. Once sulfur was completely dissolved, the mixture was then filtered through a clean cotton cloth and cooled slowly to room temperature, allowing the formation of crystals. It was reported that the laboratory purification method separates sulfur from chemical impurities, the '*gandhaka shodhana*' process transforms sulfur into a state with increased porosity and brittleness for pharmaceutical purposes.

3. Sulfur from coal and its removal/purification ways

3.1. Sulfur in coals: Distribution and chemical forms

Coal is the most significant fossil fuel source worldwide, and its demand is still growing in some countries [119]. Moreover, coal can be considered a chemical source for numerous compounds and substances. Its complex chemical structure makes it one of the most complicated geological materials, containing all the elements of nature. The primary components of coal are organic and mineral matter, with the latter containing more than 200 minerals, poorly crystalline mineraloids, and elements associated with non-mineral inorganics [120,121].

The most important parameter determining the quality of the coal is its sulfur content. The sulfur content of coals is highly variable but generally in the range of 0.5 % to 5 % overall sulfur. Coals with a sulfur content below < 1 %, 1-–3 % and > 3 % are defined as low-sulfur, medium-sulfur, and high-sulfur coals, respectively [122]. For instance, Xiao and Liu reported that most Chinese coals are low in sulfur (sulfur contents in Chinese coals average 0.9–1.0 %) [123]. To compare, Indian coals are characterised by a total sulfur content that varies from 2.45 to 5.12 % [124]. Similarly, Kazakhstani coals are also high in sulfur (0.49–6.31 %) [125]. Besides the three types mentioned above, there are superhigh-organic-sulfur (SHOS) coals. This is a class of coal in which the sulfur content usually ranges from 4 % to 11 % and is dominantly enriched in organic sulfur. In general, the content of different forms of sulfur varies significantly in coal samples formed during various periods of coal formation. For example, early carboniferous coals contained more sulfides. In contrast, late Permian, early Jurassic, and Tertiary coals contain more organic sulfur [126]. Besides this, it was mentioned that Early Carboniferous, Late Permian, and Early Jurassic coals are composed predominantly of high-sulfur coals. In contrast, Neogene coal is low in sulfur. In addition, interestingly, the link between the sulfur content and the size fraction of coals was detected in [127], which is essential in choosing and optimising an appropriate desulfurisation method. It was found that the content of organic sulfur does not change with the size of the fraction, but inorganic sulfur is dependent on this parameter of coals. As reported, the finer the coal, the higher the inorganic sulfur content.

The sulfur content and other factors also affect the coal price [128,129]: the higher the sulfur content, the cheaper the coal.

An important point is that each form's total sulfur content and proportion should be known. There are three primary forms of sulfur in coal: pyritic, organic, and sulfate sulfur (Fig. 13) [122,130–132], and their content can be expressed as follows [133]:

$$S_{IN} = 0.54 \times S_{TOT}$$

$$S_{PYR} = 0.49 \times S_{TOT}$$

$$S^0 = 0.05 \times S_{TOT}$$

$$S_{AL} = [0.276 - 0.69 \times (w_c - 0.6)] \times S_{TOT}$$

$$S_{ARO} = [0.184 - 0.345 \times (w_c - 0.6)] \times S_{TOT}$$

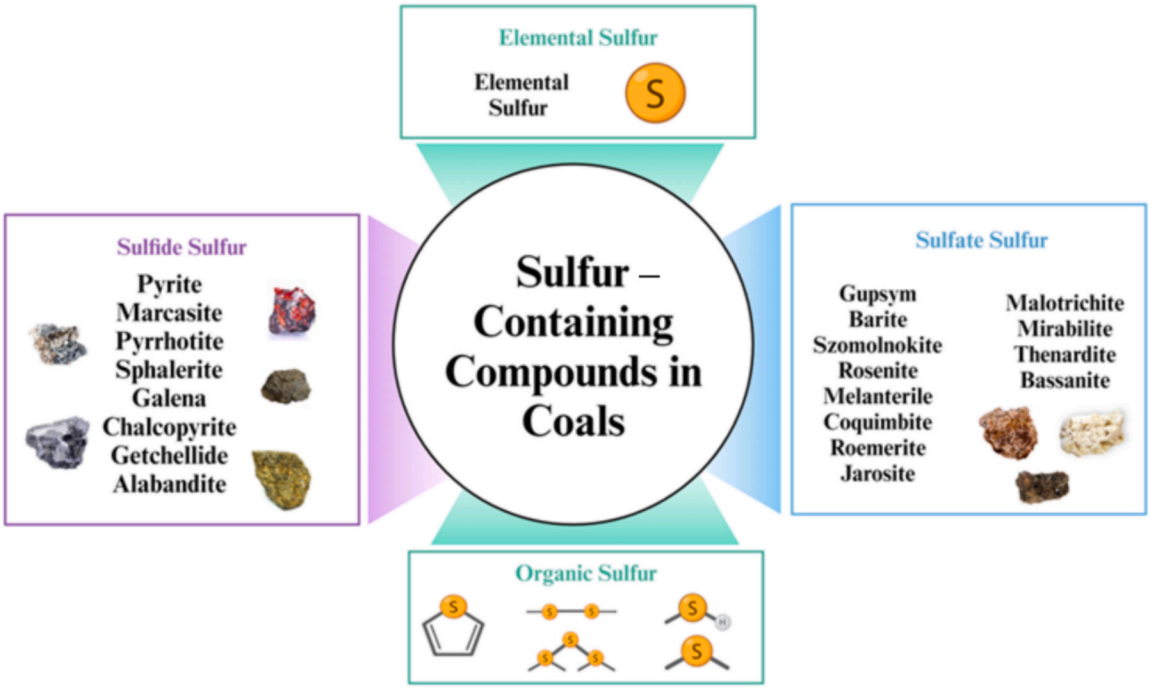

Fig. 13. Sulfur speciation in coal. The figure illustrates the three primary forms of sulfur in coal: pyritic (FeS_2), organic (C–S bonds), and sulfate ($CaSO_4$). The data used to build this figure were adapted from [122,130]

$$S_{THIO} = [1.035 \times (w_c - 0.6)] \times S_{TOT}$$

where S_{TOT} is total amount of sulfur, S_{AL} is aliphatic sulfur fraction, S_{ARO} is the aromatic fraction, S_{THIO} is the thiophenic fraction, and w_c is the carbon weight fraction in the coal.

The bulk of coal's sulfur is pyritic and organic sulfur. Small amounts of sulfate are present in weathered coals. According to the ASTM method D2492-84, organic sulfur in coal is traditionally calculated as the difference between the total sulfur and the sum of pyritic plus sulfate sulfur [134]. Zhang et al. highlighted the correlation between the distribution of organic sulfur in coal and the degree of metamorphism of coal [135]. In particular, thiophenic sulfur content is reduced with decreasing metamorphic degree. However, sulfonic acid content rises with decreasing metamorphic degree. At the same time, the contents of sulfate sulfur, sulfoxide, and sulfone are uncommonly related to this degree. Besides, it was shown that small free organic sulfur molecules in coal with a low metamorphic degree are mainly composed of aliphatic sulfides. In contrast, those in the coal of medium and high metamorphic degrees primarily comprise thiophenes. Also, as stated, the aromatisation of organic sulfur molecules rises with increasing coalification.

Coal also has elemental sulfur of minor to trace quantities, although coal analysis does not always determine it regularly. In general, the content of elemental sulfur presented in many coals might be up to 5 % of the total amount of sulfur in the coal sample [136]. There are several theories for the appearance of elemental sulfur in coal. Chou stated that S^o is a primary substance formed during coal formation [130]. Contrary to this, Duran et al. suggested that the reason for the S^o appearance in coals is atmosphere due to explosion, because, as reported, S^o was absent in pristine samples that had been processed and sealed under a nitrogen atmosphere [136,137]. Beyer et al. [137] demonstrated that microbial desulfurisation in an acidic medium results in inorganic sulfides (S_p) decreasing and S^o increasing with time, whereas the organic sulfur (S_{ORG}) remains unchanged. According to them, firstly, microbial oxidation of pyrite produces ferric sulfate; after this, a simultaneous inorganic reaction, leading to S^o and ferrous iron, between ferric iron and pyrite (FeS_2) takes place, as follows (Eq. (14)):

$$2Fe^{3+} + FeS_2 \rightarrow 3Fe^{2+} + 2S^0 \quad (14)$$

Another study on microbial desulfurisation of coals showed that the morphology and distribution of pyrites in coal play a major role in biodesulfurisation experiments [138]. The coal-pyrite link is weak in those coals in either a framboidal form, a spherical aggregate of anhedral to euhedral crystals, or isolated euhedral crystals. This makes coals most susceptible to oxidation.

Maffei et al. [133] proposed a predictive kinetic model of sulfur release from coal. As reported, the different organic sulfur component release rates are related to the weakness of the C–S bonds. As noted, the energy of C-S_{AL} and C-S_{ARO} bonds are 50.3 kcal mol^{-1} and 79 kcal mol^{-1}, respectively. This means that C–S bonds are 25–30 kcal mol^{-1} weaker than the corresponding C–C bonds. Based on this energy difference, researchers suggested that aliphatic sulfur is released from coal first because of weaker bonds, followed by S_{ARO} and S_{THIO}. Aliphatic sulfur mainly releases sulfur gas species, particularly H_2S. In contrast, thiophenic sulfur comes from a prevalent sulfur char, forming sulfur tar and light mercaptans. As for inorganic sulfur, its release is significantly slower than that of the organic fraction.

3.2. *Conventional (modified) chemistry methods of sulfur separation from coals and its purification*

Conventional or classic techniques such as extraction, whether aqueous or organic systems, can separate and concentrate SCCs from coals.

The first group of methods is based on pyrolysis. Increasing the pyrolysis temperature of Guizhou high-sulfur coal has demonstrated that raising the temperature from 700 °C to 1200 °C transforms various forms of sulfur into thiophenic sulfur [139]. The machine learning-based predictions [140] indicate that enhancing the hydrogen, the most significant factor influencing the sulfur content of thiophene, and volatile contents within a specific range improves desulfurisation. In [141], the addition of chromium effectively improves selective sulfur removal during the pyrolysis-based separation of sulfur from coal. Specifically, Cr_2O_3 plays a crucial role by capturing sulfur radicals to form sulfides

and facilitating the cleavage of O-S bonds in sulfoxides at the bottom of the coke. Furthermore, the concentration of Cr_xS_y exhibited a negative correlation with the level of thiophenic sulfur.

Grydlewicz and Grydlewicz [142] described a method for S° extraction from coals using organic solvents. The S° extractability (wt. %) for different solvents was reported as follows: 0.060 (acetone), 0.111 (cyclohexane), 0.098 (ethanol), 0.059 (hexane), 0.055 (methanol), 0.105 (tetrachloroethene), 0.026 (tetrahydrofuran), and 0.056 (toluene). The extracted S° was in three allotropic forms, i.e., S_8, S_7 and S_6. Hot tetrachloroethene extracted elemental sulfur (S°) from weathered coals but not from pristine coals [143]. Similarly, perchloroethylene (PCE) was employed to recover elemental sulfur from sludge contained approximately 40–60 % S° [105]. Sulfur was extracted with PCE at 80 °C and then separated from the residue by hot filtration. As noted, 15 min of extraction was sufficient to recover more than 90 % of the elemental sulfur with 5 ml PCE:1 g sludge ratio. The recovered sulfur was of 98–99.9 % purity.

Gonsalvesh et al. [144] proposed a new procedure to evaluate elemental sulfur in biodesulfurised low-rank coals (its scheme with full details is given in Fig. 14). As reported, the highest presence of S° was registered for the preliminary demineralised and depyritized coals due to their natural weathering. The offered experimental strategy allowed to achieve 16.1–53.8 % in the S° removal. Also, it was effective in assessing the S° content as a part of the total sulfur and organic sulfur that were 0.3–4.6 % and 0.3–5.1 %, respectively [137]. In [145], the chemical de-pyritisation of coal through the following biodesulfurisation process removed approximately 61 % of organic sulfur and 86.57 % of total sulfur from the coal sample.

Hao offered a novel method using carbon disulfide as an extracting agent to extract sulfur from coal-coking waste [146]. In this work, under the following optimised laboratory-scale technological conditions, more than 98 % sulfur yield could be obtained under the following conditions: the granularity of raw sulfur powder of 200 mesh, liquid–solid ratio of 3:1 $g \bullet g^{-1}$, extraction temperature of 40 °C, stirring velocity of 200 rpm, and stirring time of 30 min.

Elemental sulfur was also extracted from coal and other carbonaceous materials by treating an aqueous slurry of coal at an elevated temperature below the oxidation temperature of the coal or other carbonaceous materials [147]. This process occurred in the presence of an oxidising agent capable of reducing pyritic sulfides to a soluble state with hypochlorites, a catalyst acid.

Ersahan et al. [148] detected elemental sulfur formation in the Meyers coal desulfurisation process during the leaching of lignite particles by acidic ferric chloride. As reported, the formation rate of S° was found to depend not only on the concentration and acidity of the ferric chloride but also on the particle size of the sample, temperature, and the stirring rate. Generally, the formation of S° increases and decreases during the first 40–45 min of leaching. With small particles and high acid content, it was more significant.

A sulfur recovery technology set up by Gansu Huating Coal Conversion Company improved the total sulfur removal ratio to 98–100 % [105], but the overall average sulfur removal ratio is $>$ 99.6 %. In general, the exit sulfur content ranged from 10 to 600 ppm. According to Andersson and Holwitt [149], polymeric triphenylphosphine is an effective reagent for removing elemental sulfur from environmental samples. As noted, this reagent is easy to handle, reacts quantitatively with sulfur and forms non-hazardous products, leads to a small number of adverse reactions with analytes, and the used reagent can be regenerated and reused. However, to provide a fully completed reaction, it was recommended to use ultrasonification instead of conventional stirring and shaking the reaction mixture.

Zhang et al. demonstrated the possibility of using tannin extracts to recover high-purity elemental sulfur from coal syngas by a liquid redox catalytic process [150]. It has been shown that pre-treatment of sulfur pastes with nitric acid reduces the accumulation of impurities and increases the purity of sulfur from 60 % to 99 %, which leads to cleaner sulfur production. Once extracted with different solvents, elemental sulfur must be removed from solvent extracts. Mechlin´ska et al.

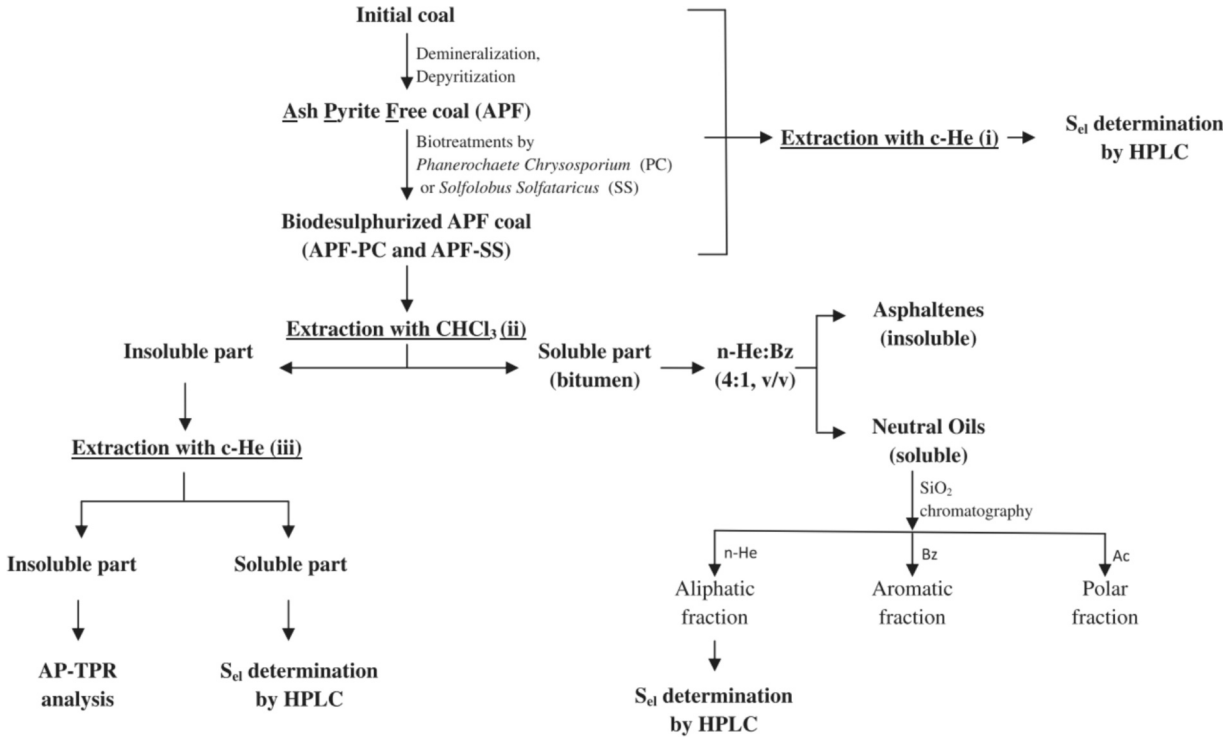

Fig. 14. Experimental strategy for elemental sulfur (S^o) determination in coal and its fractions. The approach involves extraction, separation, and quantitative analysis techniques, ensuring precise characterization of sulfur forms in coal samples [144]. Reprinted from Fuel 90(9) L. Gonsalvesh, S.P. Marinov, M. Stefanova, R. Carleer, J. Yperman, Evaluation of elemental sulphur in biodesulphurized low rank coals, 2923–2930, Copyright (2011), with permission from Elsevier.

discussed methods for removing sulfur from solvent extracts and their advantages and disadvantages [151].

The next type of extracting agent employed in sulfur extraction from coals is ILs. Binoy et al. [152] proposed an experimental strategy using 1-n-butyl, 3-methylimidazolium tetrafluoro borate (IL1) and 1-n-butyl, 3-methylimidazolium chloride (IL2) in oxidative desulfurisation and deashing of high sulfur coals. The authors reported the maximum removal of total sulfur, pyritic sulfur, sulfate sulfur and organic sulfur are observed to be 37.36 %, 62.50 %, 83.33 % and 31.63 %, respectively. Similarly to this work, a mixture of 1-carboxymethyl-3-methyl imidazolium bisulfate ionic liquid and hydrogen peroxide solution was used for organic sulfur removal from bituminous coal [153]. Note that the reaction temperature and duration significantly affect the ILs-based desulfurisation rate of coal [154]: the maximum removal rates for inorganic and organic sulfur were 76.2 % and 16.5 %, respectively; specifically, the ILs-H_2O_2 treatment reduced the levels of mercaptans and thioethers in the coal. In [155], quantum calculations and experiments have highlighted the role of intermolecular hydrogen bond interactions between organic sulfur and ionic liquids employed to remove organic sulfur compounds from coal. The stronger the S-H…Cl hydrogen bond, the better the solubility of sulfur, thereby increasing the extraction efficiency.

Alongside conventional extraction methods, flotation can be employed for the same reason. For instance, Sahinoglu used kerosene as a flotation reagent to clean coals from pyritic sulfur and achieved 90.04 % sulfur separation [156]. Cho et al. used sodium sulfite in a two-stage coal flotation to separate pyrite from a solid hydrocarbon matrix [157]. However, the separated coal pyrite contained some trace elements, such as arsenic (As), selenium (Se), and mercury (Hg).

3.3. Alternative ways of sulfur removal from coals and its purification

Nowadays, great interest is shown in the new microwave and ultrasound irradiation techniques and magnetic treatment compared to conventional chemical-based extraction methods. Xia proposed a novel method of removing organic sulfur from low-ranking high-sulfur coals by pre-heating with the Fe powder and isolating using a dry magnetic separator [158]. This method was reported as effective, allowing the removal of approximately 75 % more sulfur from the coal char heated with Fe powder than without Fe powder. In comparison, microwave radiation also showed immense power in increasing extraction yields. To compare, combining low-temperature oxidative pyrolysis, high-temperature reductive pyrolysis, and magnetic separation removes all forms of sulfur [159]. As this occurs, the removal efficiency approaches nearly 100 % for pyrite and 74.8 % for organic sulfur, leading to a total sulfur removal rate of 84.0 %. The effectiveness of microwave heating technology in removing organic sulfur from coals was demonstrated by Ma et al. [160] This method is based on the sensitivity of three distinct types of organic SCCs (mercaptans, thioethers and thiophenes) to microwave irradiation because of relatively high dielectric constants. The microwave frequency of 915 MHz is reported for the most effective sulfur removal. To confirm it, desulfurisation experiments on the example of the Xinyang coal were done. According to Ambedkar et al., ultrasonic coal wash is a promising technique to remove sulfur from coal [161]. Ultrasonic aqueous-based desulfurisation was proposed to treat high-investigation porphyry coal composed mainly of sulfate sulfur. Compared to traditional chemistry methods, ultrasonic treatment takes less time, has less solvent volume, and has a lower solvent concentration. Also, ultrasonic coal-wash equipment is commercially available.

4. Sulfur from minerals/ores

4.1. Sulfur in copper minerals and polymetallic ores

Sulfur binds with 15 chalcophile elements in different ionic forms [2]. For example, in the sulfide minerals, S^{2-} functions as a simple anion and as a compound S_2 anion [162]. In the sulfosalts, S^{2-} ion functions as a component of a complex anion. S^{4+} ion occurs in triangular pyramidal coordination with oxygen in the sulfite minerals because four valence electrons of sulfur are available for chemical bonding. In the case of sulfate minerals, S^{6+} has six valence electrons available for bonding, and due to this, it occurs in tetrahedral coordination with oxygen. Additionally, there are the thiosulfate minerals with sulfur in the hexavalent state but is coordinated by three O^{2-} anions and one S^{2-} anion. Krivovichev et al. [163] divided sulfur minerals into two groups based on their crystal-chemical features: the first group contains sulfides and sulfosalts, which are without S–O bonds, while the second ones are sulfites and sulfates, containing S–O bonds. In this term, sulfates and sulfites are more complex than sulfides and sulfosalts because of their chemical and structural complexity.

Sulfur binds in sulfides and some iron in pyrrhotite ($Fe_{1-x}S$, (x = 0 to 0.125)) or pyrite (FeS_2) [2]. It is known that about 90 % of the world's reserves in copper mining come from four sulfides – chalcopyrite ($CuFeS_2$), bornite (Cu_5FeS_4), chalcocite (Cu_2S) and cubanite ($CuFe_2S_3$) [164,165]. In addition to them, the main sulfide minerals of copper include enargite (Cu_3AsS_4) and covellite (CuS). The World Copper Factbook 2023 [166] informs that Chili, Peru and Congo, D.R. take the first three places in Copper Mine Production; alongside them, the list of top 10 countries includes China, USA, Indonesia, Russia, Australia, Zambia, and Kazakhstan. Kazakhstan is one of the world leaders in reserves of copper and other chemical elements of industrial value [167]. Kwon et al. emphasised that sulfide minerals predominate in Kazakhstan copper-bearing ores, namely chalcopyrite, bornite and chalcosiderite [168]. Atakhanova and Azhibay [169] reported that the Aktogay mine (Kazakhstan) has an annual processing capacity of 50 million tons (average copper content of 0.25 % for oxide ore and 0.33 % for sulfide ore) at a net cost of 2.56 USD per kg with a remaining service life of 25 years. For example, in medium ores with a copper content of 0.40–0.43 %, the total sulfur content changes from 0.48 % to 1.09 % depending on the type of rocks, whether granitic or volcanic. In the case of a relatively rich ore with a copper content of 0.50–0.66 %, the total sulfur amount is up to 1.08 %, while a poor ore, in which the sulfur content is 0.20–0.31 %, is approximately 0.82 %. Similarly to these data, Beisembayev et al. [170] reported that an average representative sample of sulfide ores contains 1.34 % sulfur. In contrast, in oxide ores, the S content is 0.38 %. Regarding the chemical forms of sulfur in sulfide copper ores, it is shown that such minerals represent the ore mineralisation of the sulfide zone as chalcopyrite, molybdenite and pyrite. In contrast, chalcopyrite makes up 80–90 % of the sulfide part of copper minerals [170]. Besides copper minerals, polymetallic sulfides can also be considered a considerable source of sulfur. The mineral composition of the ores of the Zhairem deposit (Kazakhstan) is shown mainly by sulfides [171]. Regarding the sample's sulfide content, there are types characterised as moderate and significant. Pyrite, sphalerite, and galena are indicated as the primary sulfides. For example, the maximum sulfide content in barite-free ores reaches 21.2–22.9 %, while the pyrite content varies in the 4.8–16.5 % range depending on the type of ore. It should be noted that sulfides in the ore are closely associated, complicating the selective separation of minerals. Another large deposit of polymetallic ores is Shalkiya. The main ore minerals include sphalerite, galena, and pyrite, and it is emphasised that sulfide forms represent 80–90 % of galena and about 94 % of sphalerite. The ore is characterised by a layered texture with fine-grained mineralisation up to emulsion, galena, sphalerite, and pyrite. It should be noted that most polymetallic sulfide ores are complex to enrich due to the reasons, firstly, the variety of forms of occurrence of the primary metals in the ores: iron, zinc, copper, and lead, and secondly, the textural and structural characteristics of the ores [164].

4.2. Separation of elemental sulfur from copper and polymetallic ores

Elemental sulfur is typically produced in oxidative processes by hydrometallurgical recovery of metal values from sulfide concentrates

such as chalcopyrite, enargite, and sphalerite. The main disadvantage of the generation of sulfur is that it retards or hampers the efficiency of the leaching process [172–176]. Sulfur can be removed from ores, minerals, and hydrometallurgical residues via physical and/or chemical treatments [177–179]. Interestingly, X-ray photoelectron spectroscopy studies of sulfide mineral surfaces showed that surfaces contain types of elemental sulfur (which are lost in a vacuum at room temperature), requiring cooling of the sample to < 200 K for preservation [180]. Some studies consider hydrometallurgical dissolution processes in terms of semiconductor electrochemistry [181,182]. For example, O'Connor and Eksteen highlighted the passivation and semiconductor mechanisms of chalcopyrite leaching [183]. Below, we consider the ways of separating/recovering elemental sulfur from some minerals.

Jorjani and Ghahreman [172] discussed various methods based on atmospheric leaching and medium temperature pressure oxidation to produce elemental sulfur from chalcopyrite. Oxidation leaching can be conducted in different environments; therein, the formation of elemental sulfur results in the following reactions (Eqs. (15)–(17)):

in chloride media [184]

$$CuFeS_2 + 3.5FeCl_3 \rightarrow 0.5CuCl_2 + 0.5CuCl + 4.5FeCl_2 + 2S^0 \quad (15)$$

in acidic ferric sulfate media [185]

$$CuFeS_2 + 2Fe_2(SO_4)_3 \rightarrow CuSO_4 + 5FeSO_4 + 2S^0 \quad (16)$$

in ammonia leaching solution [186]

$$CuFeS_2 + 4NH_3 + 6OH^- = Cu(NH_3)_4^{2+} + \frac{1}{2}S_2O_3^{2-} + S^0 + Fe(OH)_3 + \frac{3}{2}H_2O + 7e^- \quad (17)$$

According to Reilly and Scott [186], the sulfur recovery obtained during the oxidative ammoniacal leaching increases as the ratio of Cu/S in the crystal lattice increases in the series:

$$Cu_2S > CuS > CuFeS_2$$

Due to the dissolution of chalcopyrite in sulfuric acid, elemental sulfur was found on the surface of the mineral, along with bornite, chalcocite and covellite, which slows the dissolution. In this case, the staged nature of the process of dissolving chalcopyrite in sulfuric acid is represented by the following reactions (at the initial stage, the sulphate ion interacts with the ferric ion to form iron (III) sulphate) (Eqs. (18)–(22)) [170]:

$$6CuFeS_2 + 6Fe_2(SO_4)_3 \rightarrow Cu_5FeS_4 + CuSO_4 + 17FeSO_4 + 8S^0 \quad (18)$$

$$6Cu_5FeS_4 + 4Fe_2(SO_4)_3 \rightarrow Cu_2S + 3CuSO_4 + 9FeSO_4 + 3S^0 \quad (19)$$

$$Cu_2S + Fe_2(SO_4)_3 \rightarrow 3CuSO_4 + CuS + 2FeSO_4 \quad (20)$$

$$CuS + FeSO_4 \rightarrow CuSO_4 + 2FeSO_4 + S^0 \quad (21)$$

$$\sum: CuFeS_2 + 2Fe_2(SO_4)_3 \rightarrow CuSO_4 + 5FeSO_4 + 2S^0 \quad (22)$$

It is also shown that elemental sulfur was found on the surface of chalcopyrite when it was treated with sodium chloride. The distribution of sulfur on the surface of chalcopyrite treated with sodium chloride is as follows [170]:

On the surface without ionic cleaning – 3.82 wt% S.
On the surface after ionic cleaning – 6.82 wt% S.
On the surface after argon cleaning – 25.60 wt% S.
In the deep layer (200 nm) – 53.40 wt% S.

In this case, chalcopyrite dissolution occurs through the oxidation of sulfide sulfur to elemental sulfur and oxygen-containing anions and up to the sulfate ion. It was also noted that sodium chloride as a reagent does not affect the oxidation mechanism of chalcopyrite.

McGuire and Hamers [187] described the method to extract elemental sulfur in perchloroethylene from the oxidation of arsenopyrite, pyrite, marcasite, chalcopyrite, and chalcocite under various conditions. Elemental sulfur found at the mineral surface can be considered a close (99+%) approximation to the total amount of elemental sulfur. The reactions with ferric iron in solutions of perchloric acid or sulfuric acid (both at pH ~ 1 and 42 °C) produced S^0 in quantities greater than 50 % of the total reacted sulfur [188].

Like most sulfides, enargite should be intrinsically unstable in acidic environments. Dutrizac and MacDonald [189], also Lattanzi et al. [190] described enargite as ferric leaching results in elemental sulfur according to the following reaction (Eq. (23)):

$$Cu_3AsS_4 + 11Fe^{3+} + 4H_2O \rightarrow 3Cu^{2+} + AsO_4^{3-} + 4S^0 + 8H^+ + 11Fe^{2+} \quad (23)$$

Escobar et al. [191] compared bacterial and chemical leaching for enargite and informed that the latter one worked slower in leaching but resulted in elemental sulfur forming at the mineral surface (Eq. (24)):

$$Cu_3FeS_4 + 5.5Fe_2(SO_4)_3 + 4H_2O \rightarrow$$

$$\rightarrow 3CuSO_4 + 11FeSO_4 + 4S^0 + H_3AsO_4 + 2.5H_2SO_4 \quad (24)$$

Considering that 50 % of arsenic ions are presented in aqueous part according to the titration results, this reaction changes as (Eq. (25)):

$$Cu_3FeS_4 + 4.5Fe_2(SO_4)_3 + 2H_2O \rightarrow 3CuSO_4 + 9FeSO_4 + 4S^0 + HAsO_2 + 1.5H_2SO_4 \quad (25)$$

Kantar [192] stated that the stability of elemental sulfur formed during enargite leaching depends on solution pH and potential; the most stable elemental sulfur can be produced in acidic conditions. To confirm this, Escobar et al. [191] mentioned that a small fraction of the sulfur is oxidised to sulfate (Eq. (26):)

$$S^0 + 3Fe_2(SO_4)_3 + 4H_2O \rightarrow 6FeSO_4 + 4H_2SO_4 \quad (26)$$

In general, elemental sulfur converts to sulfate (SO_4^{2-}) in neutral and alkaline solutions as (Eq. (27)) [193]:

$$S^0 + 4H_2O \rightarrow SO_4^{2-} + 8H^+ + 6e^- \quad (27)$$

Lattanzi et al. [190] and Welham [194] informed that mechanical activation can partly oxidise enargite. This grinding resulted in the formation of elemental sulfur according to the following Eq. (28):

$$Cu_3AsS_4 + 6\frac{3}{4}O_2 \rightarrow 3CuSO_4 + \frac{1}{2}As_2O_3 + S^0 \quad (28)$$

Hol et al. [195] reported that grinding to a particle size with a p80 of 32 μm led to forming 3.3 wt% elemental sulfur during partial oxidation of enargite.

Another main source of sulfur compounds is polymetallic minerals and ores. Similarly to copper sulfide minerals, their leaching efficiency depends on the media. For instance, alkaline pre-treatment of a polymetallic sulfide (Fe-Pb-Mn) ore containing silver decreased elemental sulfur content and exposed sulfide surfaces [196]. Peng et al. [197] used an oxygenated $H_2SO_4 - HNO_3$ solution for leaching a sphalerite concentrate (74.7 % sphalerite, 5.7 % pyrite, and 2.3 % chalcopyrite) as follows (Eq. (29)):

$$3ZnS + 3H_2SO_4 + 2HNO_3 \rightarrow 3ZnSO_4 + 2NO + 3S^0 + 4H_2O \quad (29)$$

After that, various approaches were proposed to separate sulfur from the leaching residue, such as dissolving sulfur during leaching using organic solvents or sodium sulfide leaching and carbon dioxide precipitation, which allowed the recovery of elemental sulfur with a purity of 99.7 %. For the same purpose, solid sorbents, such as nano-silica, can be used.

Liu et al. [198] proposed flotation technology to extract elemental sulfur selectively from a high-sulfur pressure acid-leaching residue of zinc sulfide concentrate. As reported, the total sulfur content in sulfide was 46.21 %, and 81.97 % of total sulfur was elemental sulfur. The

proposed flotation scheme allowed to obtain an elemental sulfur concentrate product with 99.9 % recovery and 83.46 % purity.

Galena, PbS, can also produce elemental sulfur via oxidation in different mediums. Hu et al. [199] reported that elemental sulfur might be generated due to galena oxidation, also that oxidation in neutral or alkaline solution is more complex than in acid media (Eqs. (30)–(32)):

in acidic media

$$PbS \rightarrow Pb^{2+} + S^0 + 2e^- \quad (30)$$

in weak alkaline media:

$$PbS + 2H_2O \rightarrow Pb(OH)_2 + S^0 + 2H^+ + 2e^- \quad (31)$$

in alkaline media

$$PbS + 2H_2O \rightarrow HPbO^{2-} + S^0 + 3H^+ + 2e^- \quad (32)$$

Hu et al. [200] stated that mechanical activation of galena and pyrite produced elemental sulfur; however, this effect was not observed in the case of sphalerite and molybdenite. This feature of galena and pyrite is explained by the thermal stability of minerals under an inert atmosphere. For example, pyrite's initial thermal decomposition temperature is 713 K, which is lower than that of galena (1140 K). Tkáčová [201] explained this with the physical model of mechanical energy transformation, which stated that mechanical energy is transformed into chemical energy during mechanical activation of substances; chemical reaction happens on these "micro-contacting'' points where the temperature reaches about 1300 K. Also, this theory explained why more elemental sulfur is formed under pyrite's mechanical activation than in galena's case.

Cowan et al. [202] proposed an atmospheric oxidation of pyrite with a novel carbon catalyst for producing elemental sulfur with ultra-high yield. It was reported that the pyrite oxidation reached 60 % with a maximum 28 % S^0 yield without a catalyst. However, adding carbon-based catalyst made oxidation much more effective, for example, 96 % oxidation was achieved with a maximum 74 % S^0 yield thanks to the AF5 catalyst. To compare, activated carbons lead to 100 % oxidation with a maximum 64 % S^0 yield.

Another way to separate sulfur from industrial metallurgical residues is extraction. Fan et al. found that liquid paraffin worked to separate and purify elemental sulfur from sphalerite concentrate direct leaching residue [203]. According to Suárez-Gómez et al., toluene and carbon disulfide can also serve as solvents to obtain sulfur from sulfur concentrate [204]. They reported that up to 86.7 % of sulfur is recovered using toluene at 100 °C, and 96.3 % of high-purity sulfur is recovered at room temperature using carbon disulfide as solvent.

It was noted [205], that the chemical reaction between dissolved organic substances and dissolved sulfide in the presence of oxygen leads to the formation of elemental sulfur. This process is known as organo-mineralisation. Organic compounds likely play a role in stabilizing non-thermodynamically stable S^0 phases such as $\beta-$ and $\gamma - S_8$, which occur alone or in combination with the stable allotrope $\alpha - S_8$. Alongside ore minerals, polymetallic sulfur slag (PSS) can be considered an essential secondary resource for sulfur recovery. Chen et al. [206] proposed a recrystallisation method for efficiently separating sulfur and metals using organic solvents to control the particle size of sulfur crystals. It has been shown that the particle size of elemental sulfur is about 2000 μm, and the purity reaches 99.6 %. This method allowed efficient separation of sulfur from metal sulfides such as FeS_2 and ZnS using a new method of controlling recrystallisation.

5. Deep purification for obtaining ultrahigh-purity sulfur

Sulfur obtained for commercial use generally ranges from 99.5 % to 99.9 %. Yet, the purity plays an extremely significant role in sulfur-containing compounds, which could influence future technological breakthroughs in numerous areas, should not be dismissed [112]. Sulfur of high purity is an essential ingredient in the synthesis of materials used in energy storage devices [207]. Impurities strongly affect the performance and stability of sulfur-cathodes. Metals, chalcogens and bitumen impurities present in the sulfur cause the electrochemical polarization and decrease the stability. The presence of metal impurities such as sodium, magnesium, and calcium in ionomer membranes may hinder proton transport by exchanging with mobile protons [208]. Bitumen impurities have the potential to significantly affect the performance and longevity of sulfur batteries by obstructing operation, clogging electrode pores [209], forming insulating layers, and promoting corrosive reactions [210]. Indeed, chalcogen impurities could introduce redox-active species [211], slow down ion transport kinetics [212], and destabilise solid-electrolyte interfaces [213] in sulfur batteries, which demonstrates that the elimination of impurities is essential to achieve outstanding battery performance as well as safety. Hydrogen sulfide impurities increase the lithium anode polarization and self-discharge, thereby reducing the overall storage life and efficiency of the cells [214]. Modern requirements for ultrapure substances in semiconductor technology and infrared optics necessitate total impurity levels in sulfur ranging from 10^{-7} to 10^{-8} wt%, with individual impurities at 10^{-8} to 10^{-9} wt% [215].

Table 1 outlines various impurities in elemental sulfur and their impacts [112,216–219]. The source of sulfur is responsible for these impurities. For instance, sulfur extracted from petroleum products will contain hydrocarbons, amines, and bitumens, while sulfur mined may have different ash and metals. Some of these impurities can, in turn, impact the properties and performance of the sulfur-based materials.

High-purity sulfur is obtained through various methods, including chemical, distillation, and crystallization techniques, often employed individually or in combination. These methods effectively eliminate impurities while preserving the sulfur's integrity and desired properties.

Thermal purification methods are helpful since they can expel carbon impurities from sulfur. The process requires an extended boiling period, heating sulfur on a quartz rod, or directing sulfur vapour through a high-temperature zone, achieving efficiency from 10^{-3} wt% to 10^{-4} wt %. Similarly, Adamchik et al. [111,220] employed high-temperature oxidation to incorporate the total carbon content in sulfur to 10^{-5} wt% from $(2.8 \pm 0.1)\ 10^{-4}$ wt%. A comparative study conducted by Mochalov et al. [117] highlighted the superior efficacy of plasma distillation, with the lowest residual carbon content ($1{\cdot}10^{-5}$ wt%) achieved compared to methods without plasma. Brogdon et al. [221] also describe a comprehensive method for purifying elemental sulfur from hydrocarbon impurities. The process involves heating impure sulfur to prompt the reaction of hydrocarbons with sulfur, forming insoluble carbon–sulfur compounds and gaseous hydrogen sulfide. Subsequent separation and conversion steps yield elemental sulfur.

Chemical purification methods for elemental sulfur are challenged by the difficulty of removing impurities such as arsenic, selenium, and bitumens [222,223]. These methods typically involve oxidising the mentioned impurities and then separating them through washing or sorption techniques. Magnesite or lime milk can be employed to purify sulfur from arsenic, where sulfur is washed with them at 125 °C and a pressure of 2.5 atm with constant stirring. Alternatively, sulfur can be treated with ammonia, ammonium sulfate, or ammonium carbonate at 130 °C and a pressure of 3–4 atm, then decantation separates the resulting aqueous solution from sulfur. Separating selenium from sulfur often involves rapid oxidation of selenium at elevated temperatures. For instance, methods involving selenium oxidation in sulfur with nitric acid have been proposed, where sulfur is emulsified in a concentrated solution of magnesium chloride heated to 130 °C. However, this method does not entirely purify sulfur from selenium, as the selenium content in sulfur after six treatments with nitric acid remains at 0.01 %. Murphy et al. [224] outlined the method of producing highly purified sulfur, with a purity of 99.999 %, achieved by removing liquid-soluble, solid-insoluble impurities. This method involves treatment with concentrated sulfuric

Table 1
Summary of impurities present in elemental sulfur from various industrial sources, including their maximum content (ppmw) and effects on product quality and performance in energy storage applications [112,216–219].

A source for sulfur as an industrial by-product	Impurity	Maximum Content (ppmw)	Effect
Crude oil	Ash	< 500	Blocks liquid sulfur filters, may plug burner nozzles, discolors product.
Crude oil/ Petrochemical industry	Carbon/ Hydrocarbons	< 250	Weakens solid sulfur product strength, affects product colour, toxic when released.
Gaseous petrochemical industry	Amines	< 250	Corrosion of metal containment systems, production of acid, bulk instability when excessive, requires more heat for melting.
Gaseous petrochemical industry	Hydrogen Sulfide	< 10	Weakens structural sulfur products.
Sulfur recovery units	Polysulfide	< 10	Leads to loss in the capacity and cyclability of battery.
Crude Oil	Water	0.5—1.5 wt %	Swelling clays, soil dust contamination during storage.
Crude Oil	Acidity	0.020 wt%	Changes strength and grinding properties of solid (e.g., affects rubber makers).
Minerals/Coals	Metals	Varies	Corrosion of metal containment systems, formation of acid, affects product stability, lead to electrochemical polarization and reduce stability of battery.
Minerals	Chalcogen	Varies	Formation of volatile compounds, affects product quality and stability, slow down ion transport kinetics in energy storage system.
Minerals/Coals	Bitumens	Varies	Contamination of sulfur, reduce stability of battery.
Minerals/Coals	Arsenic	0.25	Toxic, Health Hazard.
Minerals/Coals	Selenium	1.00	Influences physical and chemical properties.
Minerals/Coals	Tellurium	1.00	Affects electrical conductivity, properties.

and nitric acids and rinsing with distilled water to remove entrapped acids, boiling the sulfur with helium or nitrogen, subsequent melting, extraction, and distillation steps, and sealing in glass ampoules under vacuum. The method successfully yields high purity, with the total impurities reduced to $1.3{\cdot}10^{-5}$ %, and organic matter minimised to 0.0002 % as carbon (active or not). Sulfur purification from selenium was based on the interaction of impurities with oxidising agents such as silver and copper oxides [225]. Selenium was preferentially bound during the passage of sulfur vapours at temperatures of 600–700 °C through a column filled with inert packing or granules of aluminium oxide, onto which copper or silver oxides were deposited, resulting in reducing the selenium content in sulfur from $1.3{\cdot}10^{-4}$ wt% to $6.5{\cdot}10^{-5}$ wt%.

Another method proposed for deep sulfur purification is counter-current crystallisation [226]. Sulfur purification is carried out in an apparatus where the temperature at the top is 4–5 °C lower and at the bottom is higher than the melting temperature of sulfur. The apparatus is filled with molten sulfur. Crystals of sulfur formed in the colder end (crystalliser) move into the purification zone, where mass transfer occurs between the liquid and crystalline phases. After passing through the purification zone, the crystals enter the melting zone, melting due to the higher temperature. The liquid sulfur rises upwards in counter current to the falling crystals. As a result of multiple phase reversals, impurity phases with a partition coefficient $\alpha < 1$ concentrate in the upper part of the apparatus, while purified sulfur collects in the lower part. Samples were obtained with the following concentration of impurities: bitumenes were $2{\cdot}10^{-5}$ wt%; Se was $1{\cdot}10^{-3}$ wt%; and As was $8.2{\cdot}10^{-4}$ wt %.

The presented data show that among the investigated methods, there is no single method capable of purifying sulfur from all impurities. The most difficult-to-remove impurities are carbon and elements closely resembling sulfur in properties, such as arsenic and selenium. Churbanov et al. [113] pointed out that combining the counter-current crystallisation from a melt method with multi-stage vacuum distillation yielded sulfur with a total impurity content of $2.5{\cdot}10^{-5}$ wt%. The purified sulfur contained carbon at $1{\cdot}10^{-6}$ wt%, arsenic at less than $5.3{\cdot}10^{-6}$ wt%, and selenium at less than $8{\cdot}10^{-6}$ wt% [227].

6. Sulfur for energy storage

One of the most promising directions of utilising excessive sulfur as byproducts is energy storage, including metal-sulfur batteries and thermal energy storage. This chapter delves into the various types of metal-sulfur batteries, also the critical role of sulfur-based electrolytes in enhancing battery performance and the significant advancements being made towards the commercialization of these technologies. Additionally, sulfur's application in thermal energy storage highlights its versatility and importance in the future of global energy storage systems.

6.1. Sulfur in batteries

Battery energy storage systems are crucial for addressing the intermittent nature of renewables, with a significant focus on electric vehicles. Amidst this backdrop, sulfur materials have emerged as potential candidates for high energy density and low-cost electricity storage applications. These materials prove environmental sustainability, cost-effectiveness, and abundance as a byproduct of the petroleum industry [228].

There are several types of metal-sulfur batteries, including lithium-sulfur (LSB), sodium-sulfur (NSB), potassium-sulfur (KSB), and aluminum-sulfur (ASB) batteries (Fig. 15). Among these, LSB have been extensively studied and have made significant progress due to sulfur's high theoretical capacity [229]. LSB technology is considered a 'next-generation' battery technology, along with innovations like all-solid-state, cumulatively promising greater energy density than commercial lithium-ion batteries (LIBs) [230]. The main challenges associated with the development of LSBs and other metal-sulfur batteries, causing low Coulombic efficiency, poor rate-capability, and limited cycle life, include the following [231–233]:

- insulating nature of the sulfur and its lithiated products Li_2S/Li_2S_2;
- high volume change during lithiation and delithiation;
- dissolution and shuttle of intermediate products, lithium polysulfides (Li_2S_x, $2 < x \leq 8$);
- side reactions with the metal anode and corrosion.

Strategies like designing micro/nanostructured sulfur hosts, separator modifications, interlayers, advanced binders, optimized electrolytes, and regulated metal anodes have been developed to address these issues and improve sulfur conversion efficiency [234–237]. For instance, our research group successfully incorporated the multifunctional Ni/NiO-embedded carbon nanofibers (Ni/NiO@CNFs), achieving high initial capacities and excellent capacity retention, effectively mitigating polysulfide dissolution and improving long-term cyclability (Fig. 16**a–b**).

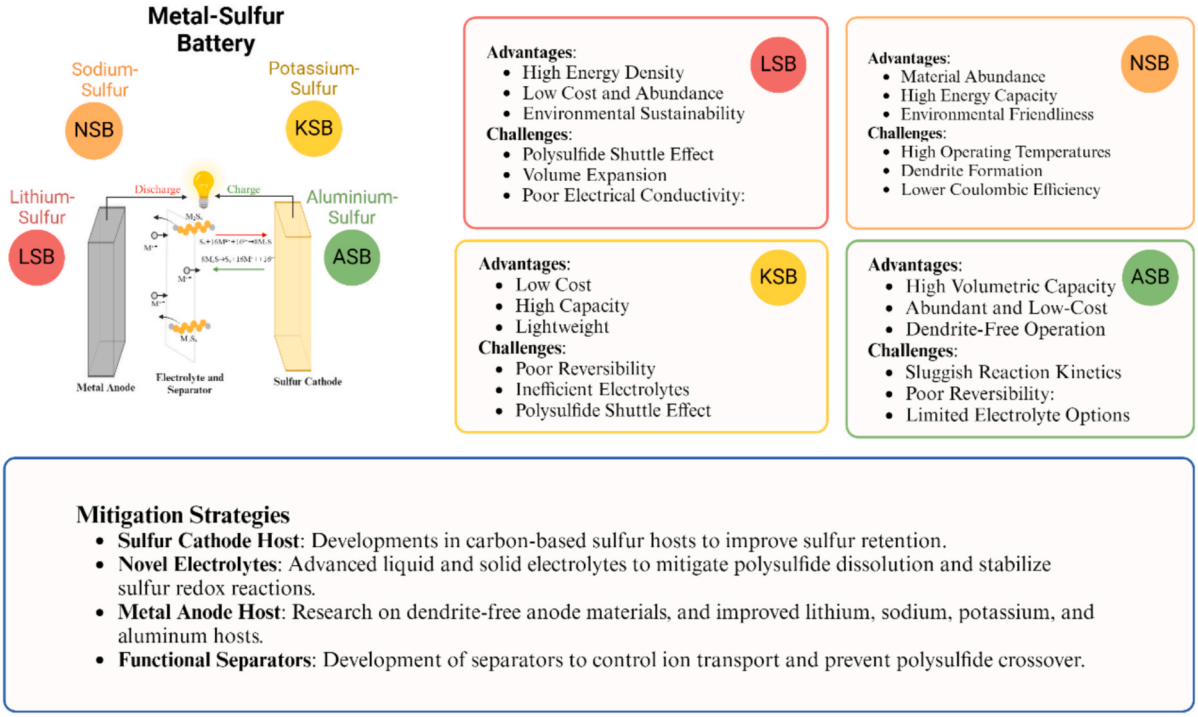

Fig. 15. Metal-sulfur battery types (Li–S, Na–S, K–S) with theoretical energy densities (Wh kg^{-1}). The figure summarizes the key challenges (e.g., shuttle effect, insulation) and solutions (e.g., cathode composites, solid electrolytes) for metal-sulfur batteries. Lithium-sulfur (Li–S) batteries, with a theoretical energy density of ~ 2600 Wh kg^{-1}, are the most extensively studied, but sodium-sulfur (Na–S) and potassium-sulfur (K–S) batteries also show promise for large-scale energy storage. The data used to build this figure were adapted from Chen et al. [229]

Fig. 17 provides a timeline of key advancements in LSBs from their initial concept to recent developments. The evolution begins in the 1960s–1970s with the introduction of metal-sulfur batteries and early rechargeable LSB prototypes. In the 1980s–1990s**,** improvements in materials and cell design emerged, incorporating conventional electrolytes like polyethylene oxide (PEO) polymer and 1,3-dioxolane (DOL) and 1,2-dimethoxyethane (DME). The 2000s saw the development of nanostructured materials, sulfur nanoparticles, and porous carbon hosts, along with innovations in doping, binary electrolytes, and interlayer design, leading to commercialization in aerospace and unmanned aerial vehicle applications. Between 2010–2015, research focused on scaling up production, optimizing manufacturing, and introducing all-solid-state LSBs with advanced cathode designs. In the 2016–2020 period, LSBs expanded into diverse markets such as aerospace, marine, and defense, with progress in MOF-based materials, composite binders, and alloy anodes. The most recent advancements **(**2021–2024**)** include the development of ZnS-SnS@NC heterostructure separators, artificial hybrid interphases, 3D electrolyte designs, and efforts to integrate LSBs into electric vehicle platforms [238–242].

With the growing demand for higher-energy batteries, all forms of sulfur (elemental sulfur, metal sulfides, and organic and inorganic sulfur) are increasingly appealing for energy applications beyond metal-sulfur batteries, such as cathodes, anodes, and electrolytes [243]. Sulfur doping is an effective strategy for optimising MIBs' rate performance and reversible capacity. Within the carbon structure, sulfur can be represented in three configurations: C-S-C, C-SO_x-C (where x = 2, 3, or 4), and C-SH [244]. The C-S bond length is longer than the C-C bond length due to the larger radius of sulfur (1.78 Å). The sulfur atom forms two σ-bonds with the nearest carbon atoms in the C-S-C bonding configuration. S atom within the C-S-C structure possesses two lone pairs and demonstrates sp^3 hybridisation, resulting in an angle of less than 109.5°. This angle is smaller than that observed in an ideal hexagonal carbon configuration. The combination of extended bond lengths and reduced bond angles affects the stability of the aromatic structure. Moreover, although sulfur (S) and carbon (C) possess similar electronegativities—2.58 for S and 2.55 for C—sulfur doping alters the charge density. Also, In the C-SO_x-C and C-SH configurations, it has been demonstrated that the sp2 carbon becomes asymmetric with the higher binding energy as the number of functional groups increases [245]. Additionally, the S-doping can modulate the intrinsic crystal structure of active materials and affect the crystal structure's charge/ion state, bandgap, and stability [246]. All these factors, including the shifts in aromatic structure, the rearrangements in electronic and crystallographic structure, as well as charge distribution, contribute to the improved electrical conductivity and chemical reactivity of S-doped carbon, increase carbon interlayer spacing, boost active sites and metal ion adsorption [246]. Numerous experimental studies support this, demonstrating significant enhancements in the electrochemical performance of carbon materials in the presence of S. In [247], sulfur-doped carbonaceous material, with an S mass loading of 27.05 at%, has demonstrated a long cyclability (over 5200 cycles) with a reverse capacity of 220.2 mAh·g^{-1} and a reverse CE of > 99 % at 0.5 A·g^{-1} (Fig. 16**c–d**). The exceptional electrochemical performances have been demonstrated by elemental S-coated-rGO [248], transition-metal sulfides [249], organic sulfur [250], and inorganic sulfur [251], sulfur in a mixed form [252] in MIBs. Recent studies have also highlighted the essential role of S and S-containing compounds in alleviating undesirable electrostatic interactions between the host material and Mg^{2+} ions in the Mg-ion battery [249] and reducing the expansion degree during the material's charging or discharging [243], etc. However, when transferring (industrial) sulfur into energy storage systems, the desired purity level for sulfur and sulfur-containing compounds is crucial to the capacity and performance of MIBs. For instance, in [253], elemental sulfur with 68.61 % purity and 99.5 % crystallisation (orthorhombic crystal structure) has been recommended for LSBs. Yamano et al. [254] reported that the rubber-derived sulfur composite cathode (with an S purity > 99.9 %), together with the SiO anode, exhibits outstanding electrochemical properties by showing superior performance from

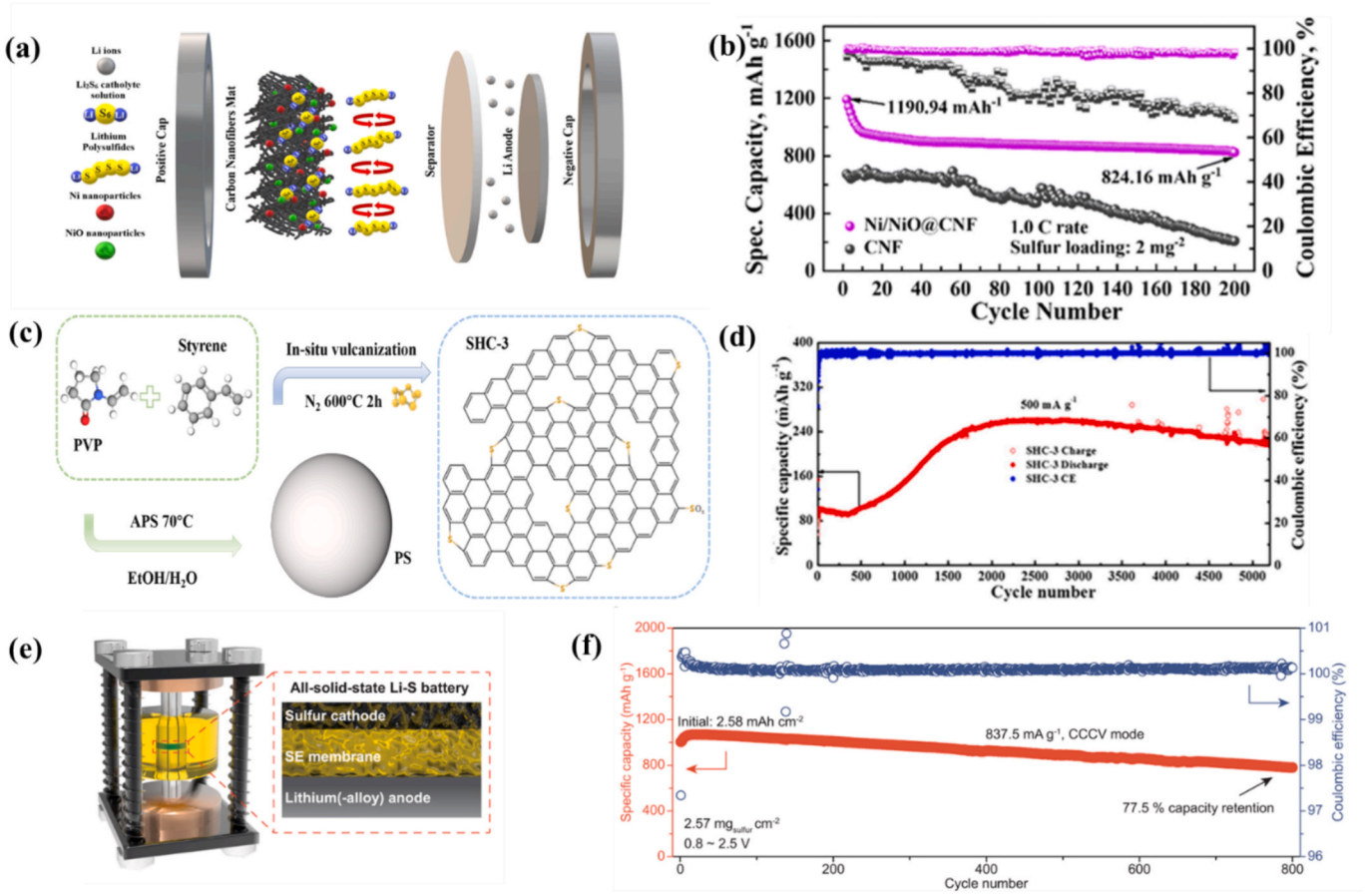

Fig. 16. (a) Schematic illustration of the fabrication process of Ni/NiO@CNFs, highlighting the incorporation of Ni and NiO nanoparticles into carbon nanofiber matrices for enhanced electrochemical performance. (b) Cycling performance of Ni/NiO@CNFs compared to pristine CNFs at a 1.0C rate, demonstrating superior specific capacity and stability with Ni/NiO modification. (c) Schematic representation of the synthesis of SHC-3, illustrating the polymerization process leading to the final hierarchical carbon structure. (d) Long-term cycling stability of SHC-3 at 500 mA g^{-1}, showing stable charge–discharge performance and high Coulombic efficiency over extended cycles. (e) Schematic illustration of an all-solid-state Li-S battery (ASSB) architecture, detailing the sulfur cathode, solid electrolyte (SE) membrane, and lithium alloy anode for enhanced safety and stability. (f) Cycling performance of the Li-In|LPB|S-C-LPB cell, demonstrating high initial capacity, stable long-term operation, and capacity retention under CCCV mode. (a-b) Licensed under CC-BY-NC 3.0 [235]. Copyright © 2024 Nanoscale Advances. (c–d) Reproduced with permission [245]. (e–f) Licensed under CC-BY-NC-SA 4.0 [264]. Copyright © 2023 Nature Communication.

−20°C to 80°C for over 100 cycles. In a patented study [255], battery-grade high-purity manganese sulfate was derived from industrial-grade manganese sulfate containing light metal impurities (such as Ca and Mg) of < 30 ppm, Fe content of < 3 ppm and other heavy metal impurities of < 8 ppm.

All-solid-state batteries (ASSBs) are a promising alternative to conventional liquid electrolyte-based systems due to their improved safety, desired mechanical properties, wider electrochemical stability windows, and potential for higher energy density. Among ASSBs, all-solid-state lithium-sulfur batteries (ASSLSBs) are gaining significant attention for their ability to overcome the polysulfide shuttle effect that plagues conventional lithium-sulfur batteries [256]. By incorporating solid sulfide electrolytes, ASSLSBs can enable stable long-term cycling, higher sulfur utilization, and enhanced safety [257]. These innovations are critical in the continued development of high-energy, long-cycle-life batteries that can meet the demands of emerging energy storage markets.

6.1.1. *Sulfur – Based electrolytes*

Sulfur-containing electrolytes, both in liquid and solid forms, are emerging as pivotal components in advancing metal-sulfur batteries due to their ability to enhance electrochemical performance, safety, and energy density [258]. The electrolyte directly affects polysulfide solubility, shuttle effects, and the formation of the solid electrolyte interphase (SEI), influencing both the sulfur reaction pathways and metal anode protection [259]. In particular, liquid sulfur-containing electrolytes can facilitate better ion transport and lower impedance [260]. Liquid sulfur-containing electrolytes, particularly those based on ether solvents like DOL/DME in bis(trifluoromethanesulfonyl)imide (TFSI) salts, facilitate fast redox kinetics via a dissolution-precipitation mechanism. While these liquid electrolytes enhance sulfur utilization and lower impedance, they are prone to the polysulfide shuttle effect, which causes capacity fading and reduces the efficiency of Li-S batteries [259,261]. Recent innovations in high-solvating electrolytes such as dimethyl sulfoxide (DMSO) show promise in addressing these issues by improving polysulfide solubility. However, the high reactivity of DMSO with lithium metal poses challenges, necessitating advanced anode protection strategies [259].

Solid-state sulfur electrolytes have shown tremendous promise due to their high ionic conductivity at room temperature, rivalling that of liquid electrolytes, while offering enhanced thermal stability and safety by eliminating the need for flammable solvents. Electrolytes such as Li_6PS_5Cl and $Li_{9.54}Si_{1.74}P_{1.44}S_{11.7}Cl_{0.3}$ have been developed to offer superior ionic conductivities at room temperature, enabling fast lithium-ion transport [262]. However, one of the main challenges with solid electrolytes is their mechanical brittleness. To address the brittleness of solid sulfide electrolytes, polymer-sulfide composite electrolytes have been developed, combining the high ionic conductivity of sulfide

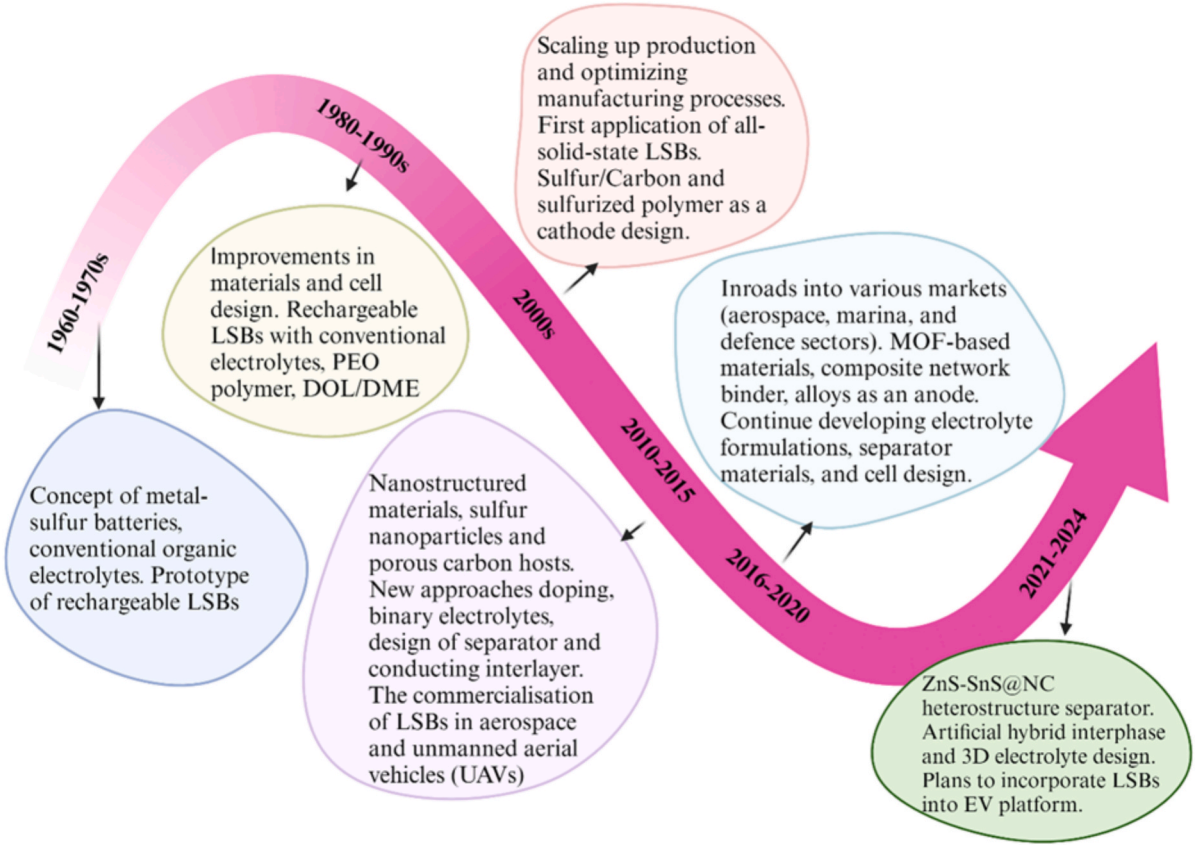

Fig. 17. Timeline of lithium-sulfur battery milestones. The figure traces the development of lithium-sulfur (Li–S) batteries from early prototypes in the 1960s to modern innovations in cathode design, electrolytes, and commercialization efforts in the 2020s. Key advancements include the introduction of nanostructured sulfur hosts, solid-state electrolytes, and strategies to mitigate the polysulfide shuttle effect. The data used to build this figure were adapted from [238–242]

materials with the mechanical flexibility of polymers. These composites offer a balance between structural stability and ionic transport, making them a promising solution for fabricating thin, flexible electrolyte films. For example, the combination of sulfide phases like Li_6PS_5Cl or $Li_7P_3S_{11}$ with polymer binders such as PEO or nitrile-butadiene rubber (NBR) significantly enhances flexibility while ensuring stable ion transport pathways [263]. Additionally, the Li_3PS_4-2$LiBH_4$ glass–ceramic solid electrolyte offers a lower density (1.491 g cm^{-3}) and small particle size, which improves the overall ionic transport within the battery and leads to enhanced sulfur utilisation in high-sulfur-content cathodes. The S-C-LPB cathode demonstrated high discharge capacities across various current densities (1144.6–663.0 mAh g^{-1} at 167.5–1675 mA g^{-1}) with excellent reversibility at 60 °C, cycling stably for over 800 cycles (Fig. 16**e–f**) [264]. These innovations are critical in the continued development of high-energy, long-cycle-life batteries that can meet the demands of emerging energy storage markets.

6.1.2. *The path towards commercialisation of lithium-sulfur batteries*

LSBs are very close to commercialisation despite not reaching this level compared to existing batteries. Advancements in emerging trends in LSB technology, along with a rise in government funding for light-weight, high energy density batteries for military, aviation, and other industries, are anticipated to open new doors to growth for key industry players. Over the last two decades, most big conglomerates like Bosch, LG Chem and Samsung started significant research activities to develop LSBs, including some SMEs like OXIS Energy Ltd. in the United Kingdom. The number of granted patents has notably risen over the last decades, proving the advanced level of development in the field of LSBs [265]. Recent research suggests that the market size, valued at 233 billion USD in 2024, is set to soar to 499.79 billion USD by 2029 [266]. In June 2023, Lyten Inc., a battery manufacturer based in the United States, made a significant announcement regarding launching their latest innovation: Lyten's 800 V LSB featuring the Lyten 3D graphene. Lyten's 800 V LSB boast an impressive energy density ranging between 3000 Wh kg^{-1} and 600 Wh kg^{-1} [267]. In May 2023, Li-S Energy, an Australian battery technology company, unveiled a groundbreaking innovation in the form of 20-layer battery cells utilising third-generation semi-solid-state LSB technology [268]. Despite the advancements, the market of LSB is relatively fragmented, and critical companies like GS Yuasa Corporation, LG Energy Solutions Ltd, Saft Groupe SA, Gelion PLC, and Sion Power Corporation, *etc.* are actively contributing to the development of this emerging technology, pushing the industry toward new frontiers in battery innovations [265].

6.2. *Thermal energy storage*

Sulfur also has gained attention for thermal energy storage (TES) applications, offering a range of advantages that make it an attractive option for both low and high-temperature applications. Thus, its chemical stability, efficient heat transfer properties and low cost make sulfur a good substitute for conventional TES materials. Integrating sulfur TES with renewable energy systems, including solar and wind power, presents exciting opportunities to enhance grid stability and reliability, bridging the gap between energy supply and demand. Studies have demonstrated sulfur's viability, for instance, Barde et al. [269] examine the ability of elemental sulfur TES for high temperature, such as concentrated solar power (CSP) and combined heat and power (CHP) plants. The sulfur TES battery was tested in terms of its ability to be safely and stably cycled over temperatures of 200–600 °C, and it was able to endure twelve thermal cycles. The Sulfur TES battery could store

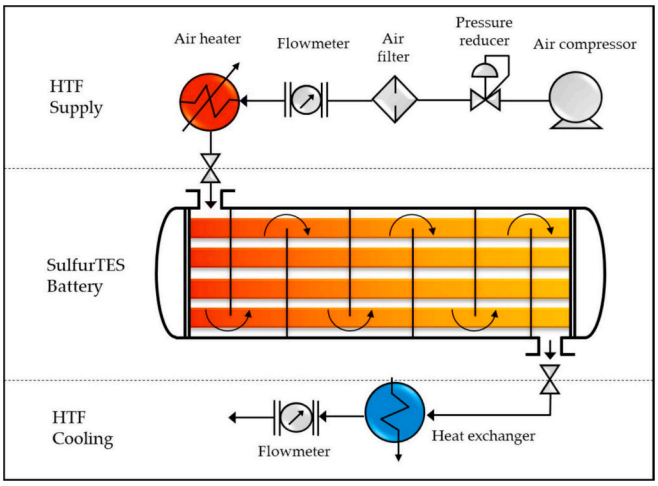

Fig. 18. Sulfur-based thermal energy storage (TES) system. The diagram illustrates a sulfur TES system designed for high-temperature applications, such as concentrated solar power (CSP) and combined heat and power (CHP) plants. The system can store up to 7.6 kWh^{-1} of thermal energy and achieves a volumetric energy density of 200–255 kWh m^{-3}. Reproduced with permission [269]. Copyright © 2018 Barde et al. Published by Elsevier.

up to 7.6 kW h^{-1} of thermal energy in the same preceding cycles. In Fig. 18 the scheme of sulfur TES system is presented. In addition, a significantly high volumetric energy density of 200–255 kW h m^{-3} was achieved [9,270,271].

On the other hand, high melting point of sulfur, around 115 °C, limits its suitability for low-temperature thermal energy storage applications, as maintaining such temperatures requires additional energy input, reducing overall system efficiency [272]. Its low thermal conductivity further complicates matters by slowing down heat transfer during charging and discharging, making it challenging to achieve quick thermal responses in large-scale systems [273].

Safety concerns also play a critical role in limiting widespread adoption of sulfur. At elevated temperatures, sulfur can release hydrogen sulfide (H_2S) and sulfur dioxide (SO_2), toxic and corrosive gases that pose serious health and environmental risks [9]. Additionally, in the presence of oxygen, sulfur is flammable, increasing the risk of fire in case of containment failure or system malfunctions [274]. Molten sulfur can also react with storage materials, causing corrosion or degradation that compromises the longevity of system components [275,276].

These challenges necessitate the use of specialized materials, corrosion-resistant coatings, and advanced sealing technologies, which significantly increase the cost and complexity of the system [277]. Designing robust safety protocols to manage the risks of toxic emissions and fire hazards further adds to operational expenses. Additionally, regular maintenance becomes essential to monitor material degradation and ensure the reliability of thermal storage performance over extended cycles.

Sulfur-based technology has introduced enhanced forms of energy production and storage; hence, it has the potential to aid the international energy revolution, emphasising renewable energy. However, the factors mentioned above create a range of technical and economic barriers that must be addressed to make sulfur a viable option for large-scale energy storage applications.

7. Conclusions and perspectives

Sulfur, a widely available by-product of industrial processes, requires efficient purification to meet the stringent material requirements of advanced energy storage technologies. The source and method of sulfur purification significantly impact its availability, cost, and purity. The highest purity sulfur (99.6–99.999 %) is obtained through advanced techniques such as recrystallization, plasma distillation, and thermochemical processing, including vacuum extraction. In contrast, the most economically viable and abundant sulfur is derived from petroleum refining processes, particularly via the Claus process, which recovers sulfur from hydrogen sulfide gas with an efficiency of up to 99.5 %. Given the global sulfur oversupply—estimated at seven million tons annually—developing cost-effective and environmentally friendly purification processes is essential. Green chemistry-based desulfurization methods, enhanced catalysts, and AI-driven process optimization offer promising pathways to improve sulfur purity while maintaining economic feasibility. Future research should focus on the design of novel catalytic materials that enhance the efficiency of sulfur purification while reducing energy consumption and chemical waste.

Beyond purification, sulfur plays a critical role in energy storage applications. In lithium-sulfur batteries, battery-grade sulfur is essential due to its low cost, lightweight nature, and exceptionally high volumetric and gravimetric energy densities, making LSBs strong candidates for commercialization. Sulfur is also a key component of both liquid and solid electrolytes. In liquid electrolytes, sulfur-containing species influence polysulfide solubility and redox kinetics, directly impacting battery performance and cycle life. The development of advanced electrolyte formulations, including high-donor-number solvents and functional additives, is crucial for mitigating polysulfide shuttle effects and improving long-term stability. In sulfide-based solid electrolytes, sulfur plays a central role in achieving high lithium-ion conductivity, making these materials essential for next-generation all-solid-state lithium-ion and lithium-sulfur batteries. Continued research on electrolyte stability, electrochemical compatibility, and scalable manufacturing processes will be key to unlocking the full potential of LSBs and solid-state battery technologies.

Looking ahead, several key research directions are expected to shape the future of sulfur-based energy storage. In sulfur purification, new methods aimed at improving efficiency while reducing environmental impact will be crucial, including solvent-free purification processes and electrochemical refining techniques. Artificial intelligence and machine learning could further optimize purification pathways, reducing energy consumption and operational costs. In battery technologies, solid-state lithium-sulfur batteries are expected to receive increasing attention, with a focus on enhancing sulfide-based solid electrolytes to improve their ionic conductivity, electrochemical stability, and manufacturability. The development of novel sulfur cathode architectures, including high-surface-area carbon scaffolds, sulfurized polymers, and hierarchical porous materials, could address issues related to active material utilization and capacity fading. Additionally, breakthroughs in interfacial engineering, such as the design of artificial solid-electrolyte interphases and protective coatings, may significantly enhance the cycling stability and lifespan of lithium-sulfur batteries.

Futhermore, sulfur's role in alternative battery chemistries is expected to grow, particularly in sodium-sulfur, magnesium-sulfur, and calcium-sulfur systems, which offer promise for grid-scale energy storage. The further development of sulfide-based solid electrolytes will also be critical for expanding their use in multivalent ion batteries, providing new opportunities for high-performance, low-cost storage solutions. Additionally, sulfur-based thermal energy storage is likely to benefit from new materials and design strategies that improve thermal stability, energy density, and integration with renewable energy systems such as concentrated solar power. Advances in sulfur composites and phase-change materials could lead to more efficient and scalable TES solutions.

As sulfur-based technologies advance, careful consideration must be given to their environmental impact. Increased sulfur utilization in energy storage raises concerns regarding resource sustainability, waste management, and potential emissions from large-scale sulfur processing. Future research should prioritize the development of closed-loop recycling processes for spent sulfur materials, minimizing the environmental footprint of both extraction and disposal. Additionally, the

environmental impact of sulfur-based electrolytes, particularly sulfide solid electrolytes, should be assessed to ensure their safe large-scale deployment. The design of biodegradable or recyclable sulfur-containing materials could provide a sustainable pathway for mitigating long-term environmental concerns. A comprehensive life-cycle assessment of sulfur applications in energy storage could provide critical insights into optimizing resource efficiency and reducing environmental footprints.

By addressing these challenges and opportunities, sulfur-based materials and technologies can play a transformative role in the transition to sustainable energy storage solutions. Interdisciplinary collaboration between materials scientists, chemists, and engineers will be essential to realizing the full potential of sulfur as a key component of next-generation energy systems. The continued advancement of purification technologies, battery materials, and scalable manufacturing processes will drive the commercialization of sulfur-based storage, paving the way for more efficient and cost-effective energy solutions in the future.

Notes. *The original figures and a graphical abstract were created with* BioRender.com.

CRediT authorship contribution statement

Aitolkyn Uali: Writing – review & editing, Writing – original draft, Visualization, Methodology, Investigation. **Aizhan Kazymbetova:** Writing – review & editing, Writing – original draft, Visualization, Software, Investigation, Data curation. **Ayaulym Belgibayeva:** Writing – review & editing, Supervision. **Arailym Nurpeissova:** Writing – review & editing, Validation, Supervision, Project administration, Funding acquisition, Conceptualization. **Zhumabay Bakenov:** Writing – review & editing, Supervision, Funding acquisition, Conceptualization. **Aliya Mukanova:** Writing – review & editing, Writing – original draft, Validation, Supervision, Project administration, Conceptualization.

Declaration of competing interest

The authors declare the following financial interests/personal relationships which may be considered as potential competing interests: Zhumabay Bakenov reports financial support was provided by Ministry of Science and Higher Education of the Republic of Kazakhstan. If there are other authors, they declare that they have no known competing financial interests or personal relationships that could have appeared to influence the work reported in this paper.

Acknowledgements

This work was supported by the research-targeted program BR21882402 “Development of new technologies of materials and energy storage systems for a green economy” from the Ministry of Science and Higher Education of the Republic of Kazakhstan.

Data availability

Data will be made available on request.

References

[1] R.R. Seal, Sulfur isotope geochemistry of sulfide minerals, Rev. Mineral. Geochem. 61 (2006) 633–677, https://doi.org/10.2138/rmg.2006.61.12.
[2] A. Malyshev, L. Malysheva, Sulfur in ore formation, Ore Geol. Rev. 150 (2022) 105199, https://doi.org/10.1016/J.OREGEOREV.2022.105199.
[3] G. Kutney, Sulfur. History, Technology, Applications and Industry, ChemTec, Toronto, 2007.
[4] T.A. Rappold, K.S. Lackner, Large scale disposal of waste sulfur: From sulfide fuels to sulfate sequestration, Energy 35 (2010) 1368–1380, https://doi.org/10.1016/J.ENERGY.2009.11.022.
[5] J.G. Wagenfeld, K. Al-Ali, S. Almheiri, A.F. Slavens, N. Calvet, Sustainable applications utilizing sulfur, a by-product from oil and gas industry: A state-of-the-art review, Waste Manag. 95 (2019) 78–89, https://doi.org/10.1016/J.WASMAN.2019.06.002.
[6] S.M. Justin Chalker, M.J.H. Worthington, R.L. Kucera, J.M. Chalker, Green chemistry and polymers made from sulfur, Green Chem. 19 (12) (2017) 2748–2761, https://doi.org/10.1039/c7gc00014f.
[7] H. Mutlu, E. Berfin Ceper, X. Li, J. Yang, W. Dong, M. Murat Ozmen, P. Theato, H. Mutlu, P. Theato, E.B. Ceper, M.M. Ozmen, X. Li, J. Yang, W. Dong, Sulfur chemistry in polymer and materials science, Macromol. Rapid Commun. 40 (1) (2018) 1800650, https://doi.org/10.1002/marc.201800650.
[8] M. Shinn, K. Nithyanandam, A. Barde, R.E. Wirz, Sulfur-based thermal energy storage system using intermodal containment: Design and performance analysis, Appl. Therm. Eng. 128 (2018) 1009–1021, https://doi.org/10.1016/J.APPLTHERMALENG.2017.08.167.
[9] Y. Wang, A. Barde, K. Jin, R.E. Wirz, System performance analyses of sulfur-based thermal energy storage, Energy 195 (2020) 116996, https://doi.org/10.1016/J.ENERGY.2020.116996.
[10] M. Costa, W. El Mofid, T. Sörgel, Sulfur Loading as a Manufacturing Key Factor of Additive-Free Cathodes for Lithium-Sulfur Batteries Prepared by Composite Electroforming (2023), https://doi.org/10.3390/en16031134.
[11] S. Dörfler, S. Walus, J. Locke, A. Fotouhi, D.J. Auger, N. Shateri, T. Abendroth, P. Härtel, H. Althues, S. Kaskel, Recent Progress and Emerging Application Areas for Lithium-Sulfur Battery Technology (2020), https://doi.org/10.1002/ente.202000694.
[12] A. Manthiram, Y. Fu, Y.-S. Su, Challenges and Prospects of Lithium–Sulfur Batteries, Acc. Chem. Res. 46 (2012) 1125–1134, https://doi.org/10.1021/ar300179v.
[13] P. Chen, C. Wang, T. Wang, Review and prospects for room-temperature sodium-sulfur batteries, Mater Res Lett 10 (2022) 691–719, https://doi.org/10.1080/21663831.2022.2092428.
[14] J. Shan, H. Sun, J. Liu, Z. Yan, K. Zhu, X. Yu, Y. Dou, Application of Activated Carbon based on High-sulfur Petroleum Coke in Potassium-ion Batteries, in: 2022 2nd International Conference on Electrical Engineering and Control Science (IC2ECS), 2022, pp. 1–4, https://doi.org/10.1109/IC2ECS57645.2022.10087943.
[15] E.V. Kuz’mina, E.V. Karaseva, N.V. Chudova, A.L. Ivanov, V.S. Kolosnitsyn, Petroleum coke as the active material for negative electrodes in lithium–sulfur batteries, Russ. J. Electrochem. 57 (2021) 131–141, https://doi.org/10.1134/S102319352103006X.
[16] S.S. Shah, M.A. Aziz, Z.H. Yamani, High-yield petroleum coke derived activated carbon with self-sulfur confinement for high-performance supercapacitor, Diam. Relat. Mater. 140 (2023) 110450, https://doi.org/10.1016/J.DIAMOND.2023.110450.
[17] Y. Han, Y. Zhang, C. Xu, C.S. Hsu, Molecular characterization of sulfur-containing compounds in petroleum, Fuel 221 (2018) 144–158, https://doi.org/10.1016/J.FUEL.2018.02.110.
[18] Z. Xi, K. Xi, L. Lu, M. Zhang, Study on oxidation characteristics and conversion of sulfur-containing model compounds in coal, Fuel 331 (2023) 125756, https://doi.org/10.1016/J.FUEL.2022.125756.
[19] R. Javadli, A. De Klerk, Desulfurization of heavy oil, Appl. Petrochem. Res. 1 (2012) 3–19, https://doi.org/10.1007/s13203-012-0006-6.
[20] H. Al-Haj-Ibrahim, B.I. Morsi, Desulfurization of petroleum coke: a review, Industr. Eng. Chem. Res. 31 (2002) 1835–1840, https://doi.org/10.1021/ie00008a001.
[21] B. Saha, S. Vedachalam, A.K. Dalai, Review on recent advances in adsorptive desulfurization, Fuel Process. Technol. 214 (2021) 106685, https://doi.org/10.1016/J.FUPROC.2020.106685.
[22] A.W. Bhutto, R. Abro, S. Gao, T. Abbas, X. Chen, G. Yu, Oxidative desulfurization of fuel oils using ionic liquids: A review, J. Taiwan Inst. Chem. Eng. 62 (2016) 84–97, https://doi.org/10.1016/J.JTICE.2016.01.014.
[23] J. Chen, Y. Zhang, J. Yang, Y. Nuli, J. Wang, Rechargeable Battery Technology Post lithium-sulfur battery era: challenges and opportunities towards practical application, Science China-Chemistry 67 (2024) 106–121, https://doi.org/10.1007/s11426-022-1421-7.
[24] W.L. Orr, J.S. Sinninghe Damsté, Geochemistry of Sulfur in Petroleum Systems, 2009. https://doi.org/10.1021/bk-1990-0429.ch001.
[25] M.A. Fahim, T.A. Alsahhaf, A. Elkilani, Refinery Feedstocks and Products, Fundamentals of Petroleum Refining (2010) 11–31, https://doi.org/10.1016/B978-0-444-52785-1.00002-4.
[26] P.Y. Hsieh, T.J. Bruno, Measuring sulfur content and corrosivity of North American petroleum with the advanced distillation curve method, Energy Fuels 28 (3) (2014) 1868–1883, https://doi.org/10.1021/ef402489c.
[27] World Oil Outlook 2045 Organization of the Petroleum (2023) Exporting Countries, n.d.
[28] World Oil Outlook 2045 Organization of the Petroleum Exporting Countries (2021), n.d.
[29] Crude Oil Price Differentials and Differences in Oil Qualities: A Statistical Analysis, 2005. www.esmap.org.
[30] R. Uria-Martinez, J.J. Corbett, Z. Wang, Primer on the Cost of Marine Fuels Compliant with IMO 2020 Rule, (n.d.). https://doi.org/10.13140/RG.2.2.28660.88963.
[31] Q. Shi, J. Wu, Review on Sulfur Compounds in Petroleum and Its Products: State-of-the-Art and Perspectives, Energy Fuel 35 (2021) 14445–14461, https://doi.org/10.1021/acs.energyfuels.1c02229.
[32] M. Shahbaz, N. Rashid, J. Saleem, H. Mackey, G. McKay, T. Al-Ansari, A review of waste management approaches to maximise sustainable value of waste from the

oil and gas industry and potential for the State of Qatar, Fuel 332 (2023), https://doi.org/10.1016/j.fuel.2022.126220.
[33] A. Demirbas, H. Alidrisi, M.A. Balubaid, A.P.I. Gravity, Sulfur Content, and Desulfurization of Crude Oil, Pet. Sci. Technol. 33 (2015) 93–101, https://doi.org/10.1080/10916466.2014.950383.
[34] V.V. Lobodin, W.K. Robbins, J. Lu, R.P. Rodgers, Separation and Characterization of Reactive and Non-Reactive Sulfur in Petroleum and Its Fractions, Energy&fuels 29 (2015) 6177–6186, https://doi.org/10.1021/acs.energyfuels.5b00780.
[35] D. Singh, A. Chopra, P.K. Mahendra, V. Kagdiyal, D. Saxena, Sulfur compounds in the fuel range fractions from different crude oils, Pet. Sci. Technol. 34 (2016) 1248–1254, https://doi.org/10.1080/10916466.2016.1196218.
[36] R. Weast (Ed.), CRC Handbook of Chemistry and Physics, CRC Press, Boca Raton, 1988.
[37] L. Šindelářová, E.N. Luu, P. Vozka, Comparison of gas and kerosene oils chemical composition before and after hydrotreating using comprehensive two-dimensional gas chromatography, Journal of Chromatography Open 2 (2022) 100068, https://doi.org/10.1016/j.jcoa.2022.100068.
[38] Y.S. Al-Degs, A.H. El-Sheikh, R.Z. Al Bakain, A.P. Newman, M.A. Al-Ghouti, Conventional and Upcoming Sulfur-Cleaning Technologies for Petroleum Fuel: A Review, Energy Technol. 4 (2016) 679–699, https://doi.org/10.1002/ente.201500475.
[39] A. Haruna, Z.M.A. Merican, S.G. Musa, S. Abubakar, Sulfur removal technologies from fuel oil for a safe and sustainable environment, Fuel 329 (2022) 125370, https://doi.org/10.1016/J.FUEL.2022.125370.
[40] J.H. Gary, G.E. Handwerk, M.J. Kaiser, Petroleum refining : technology and economics, CRC Press, 2007.
[41] S.A. Ganiyu, S.A. Lateef, Review of adsorptive desulfurization process: Overview of the non-carbonaceous materials, mechanism and synthesis strategies, Fuel 294 (2021) 120273, https://doi.org/10.1016/J.FUEL.2021.120273.
[42] S. Ding, S. Jiang, Y. Zhou, Q. Wei, W. Zhou, Catalytic characteristics of active corner sites in CoMoS nanostructure hydrodesulfurization – A mechanism study based on DFT calculations, J. Catal. 345 (2017) 24–38, https://doi.org/10.1016/j.jcat.2016.11.011.
[43] Y. Liang, B. Zhang, Y. Shi, R. Jiang, H. Zhang, Research on wide-temperature rechargeable sodium-sulfur batteries: features, challenges and solutions, Materials 16 (2023) 4263, https://doi.org/10.3390/ma16124263.
[44] V.A. Valles, Y. Sa-ngasaeng, M.L. Martínez, S. Jongpatiwut, A.R. Beltramone, HDT of the model diesel feed over Ir-modified Zr-SBA-15 catalysts, Fuel 240 (2019) 138–152, https://doi.org/10.1016/j.fuel.2018.11.148.
[45] J. Fu, P. Zheng, P. Du, A. Duan, Z. Zhao, G. Jiang, J. Liu, Y. Wei, C. Xu, K. Chi, Zirconium modified TUD-1 mesoporous catalysts for the hydrodesulfurization of FCC diesel, Appl. Catal. A 502 (2015) 320–328, https://doi.org/10.1016/j.apcata.2015.06.026.
[46] N.N. Tomina, P.A. Nikul'Shin, V.S. Tsvetkov, A.A. Pimerzin, Thiophene hydrodesulfurization and diesel fuel hydrorefining activities of XMo6(S)/γ-Al2O3 and Ni-XMo6(S)/γ-Al2O3 (X = Al, Ga, In, Fe, Co, and Ni) catalysts, Kinet. Catal. 50 (2009) 220–227, https://doi.org/10.1134/S0023158409020116.
[47] P. Toro, J. Casierra, E. Bastardo, M. Ricaurte, Diesel hydrodesulfurization and its impact on the fuel market in ecuador: A review, ESPOCH Congresses: the Ecuadorian Journal of s.t.e.a.m. 3 (2023) 355–382, https://doi.org/10.18502/espoch.v3i1.14456.
[48] M. Wang, S. Zhao, K.H. Chung, C. Xu, Q. Shi, Approach for selective separation of thiophenic and sulfidic sulfur compounds from petroleum by methylation/demethylation, Anal. Chem. 87 (2015) 1083–1088, https://doi.org/10.1021/ac503670k.
[49] M.O. Azeez, S.A. Ganiyu, Review of biomass derived-activated carbon for production of clean fuels by adsorptive desulfurization: Insights into processes, modifications, properties, and performances, Arab. J. Chem. 16 (2023) 105182, https://doi.org/10.1016/j.arabjc.2023.105182.
[50] S. Wang, Y. Peng, Natural zeolites as effective adsorbents in water and wastewater treatment, Chem. Eng. J. 156 (2010) 11–24, https://doi.org/10.1016/j.cej.2009.10.029.
[51] M. Wdowin, M. Franus, R. Panek, L. Badura, W. Franus, The conversion technology of fly ash into zeolites, Clean Technol Environ, Policy 16 (2014) 1217–1223, https://doi.org/10.1007/s10098-014-0719-6.
[52] M. Moradi, R. Karimzadeh, E.S. Moosavi, Modified and ion exchanged clinoptilolite for the adsorptive removal of sulfur compounds in a model fuel: New adsorbents for desulfurization, Fuel 217 (2018) 467–477, https://doi.org/10.1016/j.fuel.2017.12.095.
[53] J. Rui, F. Liu, R. Wang, Y. Lu, X. Yang, D.J. McPhee, Adsorptive desulfurization of model gasoline by using different Zn sources exchanged NaY zeolites, Molecules 22 (2017) 305, https://doi.org/10.3390/molecules22020305.
[54] Z.Y. Zhang, T.B. Shi, C.Z. Jia, W.J. Ji, Y. Chen, M.Y. He, Adsorptive removal of aromatic organosulfur compounds over the modified Na-Y zeolites, Appl Catal B 82 (2008) 1–10, https://doi.org/10.1016/j.apcatb.2008.01.006.
[55] G. Blanco-Brieva, J.M. Campos-Martin, S.M. Al-Zahrani, J.L.G. Fierro, Effectiveness of metal-organic frameworks for removal of refractory organo-sulfur compound present in liquid fuels, Fuel 90 (2011) 190–197, https://doi.org/10.1016/j.fuel.2010.08.008.
[56] N.A. Khan, J.W. Jun, J.H. Jeong, S.H. Jhung, Remarkable adsorptive performance of a metal-organic framework, vanadium-benzenedicarboxylate (MIL-47), for benzothiophene, Chem. Commun. 47 (2011) 1306–1308, https://doi.org/10.1039/c0cc04759g.
[57] J.X. Qin, P. Tan, Y. Jiang, X.Q. Liu, Q.X. He, L.B. Sun, Functionalization of metal-organic frameworks with cuprous sites using vapor-induced selective reduction: Efficient adsorbents for deep desulfurization, Green Chem. 18 (2016) 3210–3215, https://doi.org/10.1039/c6gc00613b.
[58] D. Peralta, G. Chaplais, A. Simon-Masseron, K. Barthelet, G.D. Pirngruber, Metal-organic framework materials for desulfurization by adsorption, Energy Fuels 26 (8) (2012) 4953–4960, https://doi.org/10.1021/ef300762z.
[59] I.S. Ali, O.Y.T. Al-Janabi, E.T.B. Al-Tikrity, P.J.S. Foot, Adsorptive desulfurization of model and real fuel via wire-, rod-, and flower-like Fe3O4@MnO2@activated carbon made from palm kernel shells as newly designed magnetic nanoadsorbents, Fuel 340 (2023) 127523, https://doi.org/10.1016/j.fuel.2023.127523.
[60] R. Abro, A.A. Abdeltawab, S.S. Al-Deyab, G. Yu, A.B. Qazi, S. Gao, X. Chen, A review of extractive desulfurization of fuel oils using ionic liquids, RSC Adv. 4 (2014) 35302–35317, https://doi.org/10.1039/c4ra03478c.
[61] D. Jha, P. Maheshwari, Y. Singh, M.B. Haider, R. Kumar, M.S. Balathanigaimani, A comparative review of extractive desulfurization using designer solvents: Ionic liquids & deep eutectic solvents, J. Energy Inst. 110 (2023) 101313, https://doi.org/10.1016/J.JOEI.2023.101313.
[62] R. Abro, N. Kiran, S. Ahmed, A. Muhammad, A.S. Jatoi, S.A. Mazari, U. Salma, N. V. Plechkova, Extractive desulfurization of fuel oils using deep eutectic solvents – A comprehensive review, J Environ Chem Eng 10 (2022) 107369, https://doi.org/10.1016/J.JECE.2022.107369.
[63] P. Makoś, G. Boczkaj, Deep eutectic solvents based highly efficient extractive desulfurization of fuels – Eco-friendly approach, J. Mol. Liq. 296 (2019) 111916, https://doi.org/10.1016/J.MOLLIQ.2019.111916.
[64] Z. Zhu, H. Lü, M. Zhang, H. Yang, Deep eutectic solvents as non-traditionally multifunctional media for the desulfurization process of fuel oil, PCCP 23 (2021) 785, https://doi.org/10.1039/d0cp05153e.
[65] Z. Jiang, X. Wang, H. Deng, J. Zhao, Y. Li, Molecular mechanism and experimental study of fuel oil extractive desulfurization technology based on ionic liquid, J. Energy Inst. 112 (2024) 101452, https://doi.org/10.1016/j.joei.2023.101452.
[66] M.S. Aminuddin, M.A. Bustam, K. Johari, In silico COSMO-RS screening and experimental validation of metal chloride functionalized ionic liquids as dual-functional catalysts and solvents for H2S conversion to elemental sulfur, J. Mol. Liq. 423 (2025) 127002, https://doi.org/10.1016/J.MOLLIQ.2025.127002.
[67] G. Yu, D. Jin, F. Zhang, S. Tian, Z. Zhou, Z. Ren, Extraction-adsorption coupled desulfurization of fuel oil by novel functionalized porous liquids, Chem. Eng. J. 453 (2023) 139935, https://doi.org/10.1016/j.cej.2022.139935.
[68] Z.S. Gano, F.S. Mjalli, T. Al-Wahaibi, Y. Al-Wahaibi, I.M. Alnashef, Desulfurization of liquid fuel via extraction with imidazole-containing deep eutectic solvent, Green Process. Synth, 6 (2017) 511–521, https://doi.org/10.1515/gps-2016-0124.
[69] S. Houda, C. Lancelot, P. Blanchard, L. Poinel, C. Lamonier, Oxidative Desulfurization of Heavy Oils with High Sulfur Content: A Review, Catalysts 8 (2018) 344, https://doi.org/10.3390/catal8090344.
[70] A.M. Dehkordi, Z. Kiaei, M.A. Sobati, Oxidative desulfurization of simulated light fuel oil and untreated kerosene, Fuel Process. Technol. 90 (2009) 435–445, https://doi.org/10.1016/j.fuproc.2008.11.006.
[71] M.C. Capel-Sanchez, P. Perez-Presas, J.M. Campos-Martin, J.L.G. Fierro, Highly efficient deep desulfurization of fuels by chemical oxidation, Catal. Today 157 (1-4) (2010) 390–396, https://doi.org/10.1016/j.cattod.2010.01.047.
[72] B. Zapata, F. Pedraza, M.A. Valenzuela, Catalyst screening for oxidative desulfurization using hydrogen peroxide, Catal. Today 106 (1-4) (2005) 219–221, https://doi.org/10.1016/j.cattod.2005.07.134.
[73] M. Haghighi, S. Gooneh-Farahani, Insights to the oxidative desulfurization process of fossil fuels over organic and inorganic heterogeneous catalysts: advantages and issues, Environ. Sci. Pollut. Res. 27 (2020) 39923–39945, https://doi.org/10.1007/s11356-020-10310-4.
[74] A. Haruna, Z.M.A. Merican, S.G. Musa, Recent advances in catalytic oxidative desulfurization of fuel oil – A review, J. Ind. Eng. Chem. 112 (2022) 20–36, https://doi.org/10.1016/j.jiec.2022.05.023.
[75] Y. Lv, J. Jiao, R. Wang, W. Jiao, Silicotungstic acid-supported C@SiO2 nanospheres as an efficient oxidative desulfurization catalyst, Chem. Eng. Sci. 248 (2022) 117225, https://doi.org/10.1016/j.ces.2021.117225.
[76] M. Shi, D. Zhang, X. Yu, Y. Li, X. Wang, W. Yang, Deep oxidative desulfurization catalyzed by (NH4)5H6PV8Mo4O40 using molecular oxygen as an oxidant, Fuel Process. Technol. 160 (2017) 136–142, https://doi.org/10.1016/j.fuproc.2017.02.038.
[77] C. Kwak, J.J. Lee, J.S. Bae, K. Choi, S.H. Moon, Hydrodesulfurization of DBT, 4-MDBT, and 4,6-DMDBT on fluorinated CoMoS/Al2O3 catalysts, Appl. Catal. A 200 (2000) 233–242.
[78] B. Yuan, X. Li, Y. Sun, A Short Review of Aerobic Oxidative Desulfurization of Liquid Fuels over Porous Materials, Catalysts 12 (2022) 129, https://doi.org/10.3390/catal12020129.
[79] T. Zhang, J. Zhang, Z. Wang, J. Liu, G. Qian, D. Wang, X. Gong, Review of electrochemical oxidation desulfurization for fuels and minerals, Fuel 305 (2021) 121562, https://doi.org/10.1016/j.fuel.2021.121562.
[80] M.N. Hossain, H.C. Park, H.S. Choi, A Comprehensive Review on Catalytic Oxidative Desulfurization of Liquid Fuel Oil (2019), https://doi.org/10.3390/catal9030229.
[81] O.O. Sadare, F. Obazu, M.O. Daramola, Biodesulfurization of petroleum distillates—current status, opportunities and future challenges, Environments 4 (2017) 1–20, https://doi.org/10.3390/environments4040085.
[82] K. Kodama, K. Umehara, K. Shimizu, S. Nakatani, Y. Minoda, K. Yamada, Identification of microbial products from dibenzothiophene and its proposed

oxidation pathway, Agric. Biol. Chem. 37 (1973) 45–50, https://doi.org/10.1080/00021369.1973.10860640.
[83] M. Kalita, P.A. Sangannavar, M. Chutia, D.K. Jha, K. Sathyanarayana, J.S. Kumar, G. Subrahmanyam, Microbial biodesulfurization: a sustainable technology for refining fossil fuels, Microbial Resource Technologies for Sustainable Development (2022) 333–351, https://doi.org/10.1016/B978-0-323-90590-9.00019-5.
[84] F. Davoodi-Dehaghani, M. Vosoughi, A.A. Ziaee, Biodesulfurization of dibenzothiophene by a newly isolated Rhodococcus erythropolis strain, Bioresour. Technol. 101 (2010) 1102–1105, https://doi.org/10.1016/j.biortech.2009.08.058.
[85] R.Y. Mamuad, A.E.S. Choi, Biodesulfurization Processes for the Removal of Sulfur from Diesel Oil: A Perspective Report, Energies (basel) 16 (2023) 2738, https://doi.org/10.3390/en16062738.
[86] P. Derikvand, Z. Etemadifar, D. Biria, Taguchi optimization of dibenzothiophene biodesulfurization by Rhodococcus erythropolis R1 immobilized cells in a biphasic system, Int. Biodeter. Biodegr. 86 (2014) 343–348, https://doi.org/10.1016/j.ibiod.2013.10.006.
[87] H.N. Nassar, S.S. Abu Amr, N.S. El-Gendy, Biodesulfurization of refractory sulfur compounds in petro-diesel by a novel hydrocarbon tolerable strain Paenibacillus glucanolyticus HN4, Environ. Sci. Pollut. Res. 28 (2021) 8102–8116, https://doi.org/10.1007/s11356-020-11090-7.
[88] D. Maass, D. de Oliveira, A.A.U. de Souza, S.M.A.G.U. Souza, Biodesulfurization of a system containing synthetic fuel using rhodococcus erythropolis ATCC 4277, Appl Biochem Biotechnol 174 (2014) 2079–2085, https://doi.org/10.1007/s12010-014-1189-3.
[89] M.A. Abo-State, N.S. El-Gendy, S.A. El-Temtamy, H.M. Mahdy, H.N. Nassar, Modification of basal salts medium for enhancing dibenzothiophene biodesulfurization by Brevibacillus invocatus C19 and Rhodococcus erythropolis IGTS8, World Appl. Sci. J. 30 (2014) 133–140, https://doi.org/10.5829/idosi.wasj.2014.30.02.14023.
[90] I. Shafiq, S. Shafique, P. Akhter, W. Yang, M. Hussain, Recent developments in alumina supported hydrodesulfurization catalysts for the production of sulfur-free refinery products: A technical review, Catal. Rev. Sci. Eng. 64 (2022) 1–86, https://doi.org/10.1080/01614940.2020.1780824.
[91] O.N. Katasonova, E.Y. Savonina, T.A. Maryutina, Extraction Methods for Removing Sulfur and Its Compounds from Crude Oil and Petroleum Products, Russ. J. Appl. Chem. 94 (2021) 411–436, https://doi.org/10.1134/S1070427221040017.
[92] H. Jiang, J. Zhang, J. Shao, T. Fan, J. Li, F. Agblevor, H. Song, J. Yu, H. Yang, H. Chen, Desulfurization and upgrade of pyrolytic oil and gas during waste tires pyrolysis: The role of metal oxides, Waste Manag. 182 (2024) 44–54, https://doi.org/10.1016/J.WASMAN.2024.04.020.
[93] F. Shen, S. Qu, J. Li, Z. Yang, C. Zhou, F. Yang, Z. He, K. Xiang, M. Shi, H. Liu, Development of chemical looping desulfurization method for high sulfur petroleum coke, Fuel 357 (2024) 129658, https://doi.org/10.1016/J.FUEL.2023.129658.
[94] P. Luo, Z. Chen, X. Chen, W. Ma, X. Gan, R. Xie, Study on desulfurization and modification of high-sulfur petroleum coke via reduced iron powder catalytic roasting, J. Environ. Chem. Eng. 12 (2024) 114860, https://doi.org/10.1016/J.JECE.2024.114860.
[95] Y.N. Kitashov, A.V. Nazarov, E.I. Zorya, A.V. Muradov, Alternative methods for the removal of sulfur compounds from petroleum fractions, Chem. Technol. Fuels Oils 55 (2019) 584–589, https://doi.org/10.1007/s10553-019-01070-0.
[96] B. Borca, T. Michnowicz, R. Pétuya, M. Pristl, V. Schendel, I. Pentegov, U. Kraft, H. Klauk, P. Wahl, R. Gutzler, A. Arnau, U. Schlickum, K. Kern, Electric-Field-Driven Direct Desulfurization, ACS Nano 11 (2017) 4703–4709, https://doi.org/10.1021/acsnano.7b00612.
[97] R.A. Pandey, S. Malhotra, Desulfurization of gaseous fuels with recovery of elemental sulfur: An overview, Crit. Rev. Environ. Sci. Technol. 29 (1999) 229–268, https://doi.org/10.1080/10643389991259236.
[98] D. Muktaly, A. Akopyan, Z. Myltykbaeva, Y. Imanbayev, Gasoline Fraction High-Efficient Sweetening by Gas Condensate Oxidation and Rectification (2023), https://doi.org/10.3390/pr11103017.
[99] R.F. Bacon, R. Fanelli, Purification of Sulfu, Ind Eng Chem 34 (1942) 1043–1048. https://pubs.acs.org/sharingguidelines.
[100] L. Kohl, R. Nielsen, Gas Purification (1997).
[101] M.I. Stewart, Gas sweetening, in: Surface production operations, Elsevier, 2014, pp. 433–539, https://doi.org/10.1016/b978-0-12-382207-9.00009-3.
[102] M.A. Fahim, T.A. Alsahhaf, A. Elkilani, Acid Gas Processing and Mercaptans Removal, in: Fundamentals of petroleum refining, 2010, pp. 377–402, https://doi.org/10.1016/B978-0-444-52785-1.00016-4.
[103] H. Ghahraloud, M. Farsi, M.R. Rahimpour, Modification of Claus Sulfur Recovery Unit by Isothermal Reactors to Decrease Sulfur Contaminant Emission: Process Modeling and Optimization 14 (2019), https://doi.org/10.1515/cppm-2017-0049.
[104] P.R. Robinson, Sulfur Removal and Recovery, in: C.S. Hsu, P.R. Robinson (Eds.), Springer Handbook of Petroleum Technology, Springer International Publishing, Cham, 2017, pp. 649–673, https://doi.org/10.1007/978-3-319-49347-3_20.
[105] Y. Huang, H. Chen, Y. Lu, B. Liu, H. Shi, T. Xiao, A novel process to recover sulfur in aqueous phase under ambient conditions, Appl. Petrochem. Res. 5 (3) (2015) 207–213, https://doi.org/10.1007/s13203-015-0106-1.
[106] A.R. Mol, D.J. Meuwissen, S.D. Pruim, V. van Zhou Chenyu, J.B. Vught, C.J. Klok, R.D. van der Buisman Weijden, Novel agglomeration strategy for elemental sulfur produced during biological gas desulfurization, ACS Omega 6 (2021) 27913–27923, https://doi.org/10.1021/acsomega.1c03701.
[107] Z. Chen, T. Mu, M. Yang, N.A. Samak, X. Hao, Y. Jia, G. Yang, Q. Wen, J. Shen, S. Peh, J. Xing, Biologically produced elemental sulfur clogging induced by thiols in gas biodesulfurization systems, Chem. Eng. J. 462 (2023) 142196, https://doi.org/10.1016/J.CEJ.2023.142196.
[108] R.J. Falkiner, M.A. Poirier, I.D. Campbeli, Process for removing elemental sulfur from fluids, 5160045, 1992.
[109] I. Al-Zahrani, M.H.A. Mohammed, C. Basheer, M.N. Siddiqui, A. Al-Arfaj, Membrane Assisted Simultaneous Extraction and Derivatization with Triphenylphosphine of Elemental Sulfur in Arabian Crude Samples by Gas Chromatography/mass Spectrometry (2015), https://doi.org/10.1155/2015/792914.
[110] E.N. Kiseleva, N.Y. Smykova, Sulfur Purification by Multiple Distillations through a High-Temperature Zone, Zh. Prikl. Khim. 47 (1974) 447–448.
[111] S.A. Adamchik, P.G. Sennikov, A.D. Bulanov, Thermochemical Purification of Sulfur from Hydrocarbons, Russian, J. Inorg. Mater. 36 (2000) 725–729.
[112] S. Susman, S. Clark Rowland, K.J. Volin, The purification of elemental sulfur, J. Mater. Res. 7 (1992) 1526–1533, https://doi.org/10.1557/JMR.1992.1526.
[113] M.F. Churbanov, G.E. Snopatin, A.Y. Sozin, I.V. Skripachev, Molecular Composition of Organic Impurities in Extrapure Sulfur 53 (2017) 989–992, https://doi.org/10.1134/S0020168517090047.
[114] M.V. Sukhanov, T.I. Storozheva, I.I. Evdokimov, V.G. Pimenov, A. Yu Sozin, T. V. Kotereva, Fine Purification of Monoisotopic 32 S and 34 S, Original Russian Text © 53 (2017) 126–131, https://doi.org/10.1134/S0020168517020145.
[115] I.K.S. Altayi, I.A. Aldobouni, Catalytic purification of sulfur from bituminous impurity, Pak. J. Anal. Environ. Chem. 24 (2023) 155–166, https://doi.org/10.21743/PJAEC/2023.12.04.
[116] A. Logunov, L. Mochalov, A. Mashin, Plasma-Chemical purification of sulfur, in: Advanced Photonics 2018 (BGPP, IPR, NP, NOMA, Sensors, Networks, SPPCom, SOF), Optica Publishing Group, Zurich, 2018: p. JTu2A.30. https://doi.org/10.1364/BGPPM.2018.JTu2A.30.
[117] L. Mochalov, R. Kornev, A. Logunov, M. Kudryashov, A. Mashin, A. Vorotyntsev, V. Vorotyntsev, Behavior of carbon-containing impurities in the process of plasma-chemical distillation of sulfur, Plasma Chem. Plasma Process. 38 (2018) 587–598, https://doi.org/10.1007/s11090-018-9879-1.
[118] T.A.N.R. Gunaratna, P.K. Prajapati, K.M.N. de Silva, W.R.M. de Silva, Comparision of traditional and laboratory methods of sulphur processing, J Ayurveda Integr Med 14 (2023) 100751, https://doi.org/10.1016/J.JAIM.2023.100751.
[119] PUB_Sustainable_Global_Energy_Development_The_Case_for_Coal_2004_Exec_summary_WEC, (n.d.).
[120] W.H. Calkins, The chemical forms of sulfur in coal: a review, Fuel 73 (1994) 475–484, https://doi.org/10.1016/0016-2361(94)90028-0.
[121] S. Dai, R.B. Finkelman, D. French, J.C. Hower, I.T. Graham, F. Zhao, Modes of occurrence of elements in coal: A critical evaluation, Earth Sci. Rev. 222 (2021) 103815, https://doi.org/10.1016/J.EARSCIREV.2021.103815.
[122] C.L. Chou, Sulfur in coals: A review of geochemistry and origins, Int. J. Coal Geol. 100 (2012) 1–13, https://doi.org/10.1016/J.COAL.2012.05.009.
[123] H.Y. Xiao, C.Q. Liu, The elemental and isotopic composition of sulfur and nitrogen in Chinese coals, Org Geochem. 42 (2011) 84–93, https://doi.org/10.1016/J.ORGGEOCHEM.2010.10.011.
[124] B.K. Saikia, P. Wang, A. Saikia, H. Song, J. Liu, J. Wei, U.N. Gupta, Mineralogical and Elemental Analysis of Some High-Sulfur Indian Paleogene Coals: A Statistical Approach, Energy Fuel 29 (2015) 1407–1420, https://doi.org/10.1021/ef502511t.
[125] Y.N. Pak, M.V. Ponomaryova, D. Yu Pak, Monitoring the Sulfur Content of Coal COAL, Koks Khim. 59 (2016) 10–16, https://doi.org/10.3103/S1068364X16010051.
[126] B. Xu, Y. Song, Y. Tian, R. Yang, F. Xu, S. Ding, P. Sun, Sulfur content in coal formed during different geologic periods in the Guangxi Province and the relationship with the depositional environment, Arab. J. Geosci. 13 (2020) 294, https://doi.org/10.1007/s12517-020-5246-7.
[127] X.G. Mu, Z.X. Jin, C.B. Deng, F. Gao, Variation of Sulfur Content in Coking Coal as Function of Its Particle Size, Solid Fuel Chem. 54 (2020) 326–336, https://doi.org/10.3103/S0361521920050079.
[128] R. Tiwari, S. Bhattacharya, P. Raghav, A Discussion on Non-coking Coal Pricing Systems Adopted in Different Countries, Vikalpa 40 (2015) 62–73, https://doi.org/10.1177/0256090915573615.
[129] U. Lorenz, Z. Grudziński, Hard coal for energetic purposes: price-quality relationships; international coal market observations and Polish practice, n.d.
[130] C.-L. Chou, Geochemistry of Sulfur in Coal, in: 1990: pp. 30–52. https://doi.org/10.1021/bk-1990-0429.ch002.
[131] H.J. Gluskoter, Inorganic Sulfur in Coal, Energy Source. 3 (1977) 125–131, https://doi.org/10.1080/00908317708945974.
[132] Clarence. Karr, Analytical methods for coal and coal products, Academic Press, 1978.
[133] T. Maffei, S. Sommariva, E. Ranzi, T. Faravelli, A predictive kinetic model of sulfur release from coal, Fuel 91 (2012) 213–223, https://doi.org/10.1016/J.FUEL.2011.08.017.
[134] M. (ASTM) American Society for Testing, Standard test method for forms of sulfur in coal, D2492-84. Annual Book of ASTM Standards, 1989.
[135] L. Zhang, Z. Li, Y. Yang, Y. Zhou, J. Li, L. Si, B. Kong, Research on the Composition and Distribution of Organic Sulfur in Coal (2016), https://doi.org/10.3390/molecules21050630.
[136] J.E. Duran, S.R. Mahasay, L.M. Stock, The occurrence of elemental sulphur in coals, Fuel 65 (1986) 1167–1168, https://doi.org/10.1016/0016-2361(86)90187-0.

[137] M. Beyer, H.G. Ebner, H. Assenmacher, J. Frigge, Elemental sulphur in microbiologically desulphurized coals, Fuel 66 (1987) 551–555, https://doi.org/10.1016/0016-2361(87)90162-1.

[138] C. Acharya, R.N. Kar, L.B. Sukla, Bacterial removal of sulphur from three different coals, Fuel 80 (2001) 2207–2216, https://doi.org/10.1016/S0016-2361(01)00100-4.

[139] M. Wang, Q. Du, Y. Li, J. Gao, B. Xiao, H. Wang, Transformation of sulfur in coal during rapid pyrolysis at high temperatures, Energy Sources Part A 46 (2024) 7547–7559, https://doi.org/10.1080/15567036.2020.1757789.

[140] J. Yao, H. Shui, Z. Li, H. Yan, J. Yan, Z. Lei, S. Ren, Z. Wang, S. Kang, Machine learning prediction of pyrolytic sulfur migration based on coal compositions, J. Anal. Appl. Pyrol. 177 (2024) 106316, https://doi.org/10.1016/J.JAAP.2023.106316.

[141] Y. Jia, Z. Bai, Z. Guo, L. Kong, J. Bai, W. Li, Effect of chromium on the spatial distribution of sulfur during pyrolysis of coal with high organic sulfur, Fuel 357 (2024) 129750, https://doi.org/10.1016/J.FUEL.2023.129750.

[142] G. Gryglewicz, S. Gryglewicz, Determination of elemental sulfur in coal by gas chromatography – mass spectrometry, Fresenius J. Anal. Chem. 370 (2001) 60–63, https://doi.org/10.1007/s002160100756.

[143] K.C. Hackley, D.H. Buchanan, K. Coombs, C. Chaven, C.W. Kruse, Solvent extraction of elemental sulfur from coal and a determination of its source using stable sulfur isotopes, Fuel Process. Technol. 24 (1990) 431–436, https://doi.org/10.1016/0378-3820(90)90083-5.

[144] L. Gonsalvesh, S.P. Marinov, M. Stefanova, R. Carleer, J. Yperman, Evaluation of elemental sulphur in biodesulphurized low rank coals, Fuel 90 (2011) 2923–2930, https://doi.org/10.1016/j.fuel.2011.04.041.

[145] J. Khan, M. Ishtiaq Ali, J. Khan Achakzai, A. Jamal, I. Ahmed, A. Manan Kakar, S. Uddin, Sequential Chemical and Biological Desulphurization of High Sulfur Containing Pakistani Coal, Geomicrobiol J. 41 (2024) 959–965, https://doi.org/10.1080/01490451.2024.2407345.

[146] W. Hao, Experimental Investigation on Sulfur Extraction from Coal Coking Waste, American Journal of Applied Chemistry 5 (2017) 19, https://doi.org/10.11648/j.ajac.20170501.13.

[147] C.H. Simpson, Method for removing pyritic, organic, and elemental sulfur from coal, 0 230 500, 1987.

[148] H. Ersahan, R. Boncukcuoolu, M.M. Kocakerim, Elemental sulfur formation in the Meyers coal desulfurization process, 1995.

[149] J.T. Andersson, U. Holwitt, An advantageous reagent for the removal of elemental sulfur from environmental samples, Fresenius J. Anal. Chem. 350 (1994) 474–480, https://doi.org/10.1007/BF00321792.

[150] H. Zhang, X. Hu, Z. Liu, X. Yang, X.J. Yang, Recovery of high purity elemental sulfur from coal syngas by liquid redox catalytic process using tannin extracts, J. Clean. Prod. 142 (2017) 3204–3211, https://doi.org/10.1016/J.JCLEPRO.2016.10.149.

[151] A. Mechlińska, L. Wolska, J. Namieśnik, L. Wolska, Removal of sulfur from a solvent extract, TrAC Trends Anal. Chem. 31 (2012) 129–133, https://doi.org/10.1016/J.TRAC.2011.06.022.

[152] B.K. Saikia, K. Khound, O.P. Sahu, B.P. Baruah, Feasibility studies on cleaning of high sulfur coals by using ionic liquids, Int. J. Coal Sci. Technol. 2 (3) (2015) 202–210, https://doi.org/10.1007/s40789-015-0074-1.

[153] Y. Xu, Y. Liu, H. Xie, M. Chen, L. Wang, Experimental study on organic sulfur removal in bituminous coal by a 1-carboxymethyl-3-methyl imidazolium bisulfate ionic liquid and hydrogen peroxide solution, ACS Omega 5 (33) (2020) 21127–21136, https://doi.org/10.1021/acsomega.0c02795.

[154] T. Ge, B. Zhou, J. Xu, Y. Wei, Study on desulfurization mechanism of ILs-H2O2 system and its influence on coal structures, J. Mol. Liq. 403 (2024) 124847, https://doi.org/10.1016/J.MOLLIQ.2024.124847.

[155] Y. Wang, T. Ge, C. Cai, J. Xu, Screening ionic liquids based on COSMO-SAC model for extracting organic sulfur from coal and mechanism study, Fuel 367 (2024) 131539, https://doi.org/10.1016/J.FUEL.2024.131539.

[156] E. Sahinoglu, Cleaning of high pyritic sulfur fine coal via flotation, Adv. Powder Technol. 29 (2018) 1703–1712, https://doi.org/10.1016/J.APT.2018.04.005.

[157] E.H. Cho, O. Olajide, R.Y.K. Yang, Two-stage coal flotation to remove pyritic sulfur, arsenic, selenium and mercury, Min. Metall. Explor. 30 (2013) 162–168, https://doi.org/10.1007/BF03402263.

[158] W. Xia, A novel and effective method for removing organic sulfur from low rank coal, J. Clean. Prod. 172 (2016) 2708–2710, https://doi.org/10.1016/j.jclepro.2017.11.141.

[159] X. Lin, L. Fu, P. Lu, Q. Zhang, G. Xu, D. Bai, Development of a three-stage process for high coal desulfurization and char yield, J. Energy Inst. 113 (2024) 101536, https://doi.org/10.1016/J.JOEI.2024.101536.

[160] X. Ma, M. Zhang, F. Min, T. Ge, C. Cai, Fundamental study on removal of organic sulfur from coal by microwave irradiation, Int. J. Miner. Process. 139 (2015) 31–35, https://doi.org/10.1016/J.MINPRO.2015.04.009.

[161] B. Ambedkar, R. Nagarajan, S. Jayanti, Ultrasonic coal-wash for de-sulfurization, Ultrason. Sonochem. 18 (2011) 718–726, https://doi.org/10.1016/j.ultsonch.2010.09.006.

[162] F.C. Hawthorne, S. V. Krivovichev, P.C. Burns, The crystal chemistry of sulfate minerals, in: Sulfate Minerals: Crystallography, Geochemistry, and Environmental Significance, Walter de Gruyter GmbH, 2019: pp. 1–112. https://doi.org/10.2138/rmg.2000.40.1.

[163] V.G. Krivovichev, S.V. Krivovichev, G.L. Starova, Structural and Chemical Diversity and Complexity of Sulfur Minerals, Minerals (2023), https://doi.org/10.3390/min13081069.

[164] G. Kullerud, Ore Petrology, Encyclopedia of Physical, Sci. Technol. (2003) 411–433, https://doi.org/10.1016/B0-12-227410-5/00972-8.

[165] W.G. Rice-Jones, Sulfur in Ores, Concentrates, and Other Metallurgical Samples, Anal. Chem. 25 (2002) 1383–1386, https://doi.org/10.1021/ac60081a023.

[166] The World Copper Factbook 2023, 2023. www.icsg.org.

[167] S. Osipov, Assessment Report on Classification of Energy and Mineral Resources and its Management in the Republic of Kazakhstan, 2019.

[168] S.S. Kvon, V.I. Nesterova, A.Y. Omarova, V.Y. Kulikov, Y.P. Chsherbakova, Study of the mineral composition of promising copper ores of the Republic of Kazakhstan, КоМплексное Использование Минерального Сырья 325 (2023) 87–93, https://doi.org/10.31643/2023/6445.22.

[169] Z. Atakhanova, S. Azhibay, Assessing economic sustainability of mining in Kazakhstan, Miner. Econ. 36 (2023) 719–731, https://doi.org/10.1007/s13563-023-00387-x.

[170] B.B. Beisembaev, A.M. Kunaev, B.K. Kenzhaliev, Theory and practice of heap's leaching of copper (Теория и практика кучного выщелачивания Меди), 1st ed., Gylym, Almaty, 1998.

[171] А. Доберсек, А. Аврахов, И. Ферхо, Ю. Фильшин, А. Матинин, С. Штойк, РеализуеМые проекты в области обогащения полиМеталлических руд на МестороЖдениях ЖайреМ и Шалкия в Казахстане, Золото и Технологии 45 (2019) 116–121.

[172] E. Jorjani, A. Ghahreman, Challenges with elemental sulfur removal during the leaching of copper and zinc sulfides, and from the residues; a review, Hydrometall. 171 (2017) 333–343, https://doi.org/10.1016/J.HYDROMET.2017.06.011.

[173] F.K. Crundwell, The dissolution and leaching of minerals: Mechanisms, myths and misunderstandings, Hydrometall. 139 (2013) 132–148, https://doi.org/10.1016/J.HYDROMET.2013.08.003.

[174] H. Rezvanipour, A. Mostafavi, A. Ahmadi, M. Karimimobarakabadi, M. Khezri, Desulfurization of Iron Ores: Processes and Challenges, Steel Res. Int. 89 (2018) 1700568, https://doi.org/10.1002/srin.201700568.

[175] G. Sarapajevaite, Kestutis Baltakys, Purification of Sulfur Waste under Hydrothermal Conditions, Waste Biomass Valoriz. 12 (2021) 3407–3416, https://doi.org/10.1007/s12649-020-01206-y.

[176] S. Yu, R. Liao, B. Yang, C. Fang, Z. Wang, Y. Liu, B. Wu, J. Wang, G. Qiu, Chalcocite (bio)hydrometallurgy—current state, mechanism, and future directions: A review, Chin. J. Chem. Eng. 41 (2022) 109–120, https://doi.org/10.1016/J.CJCHE.2021.12.014.

[177] B. Çavuşoğlu, H. Karaca, Removal of Sulfur From Iron Ore with Physical and Chemical Methods, Çavuşoğlu and Karaca (2017).

[178] J.E. Halfyard, K. Hawboldt, Separation of elemental sulfur from hydrometallurgical residue: A review, Hydrometall. 109 (2011) 80–89, https://doi.org/10.1016/J.HYDROMET.2011.05.012.

[179] Yanshi Baolong Chemical Co Ltd, Simple sulphur purifying method, CN201410423531.1A (2014).

[180] R.C. St Smart, W.M. Skinner, A.R. Gerson, XPS of Sulphide Mineral Surfaces: Metal-deficient, Polysulphides, Defects and Elemental, Sulphur (1999).

[181] A.G.R. Toledo, D. Bevilaqua, S. Panda, A. Akcil, Hydrometallurgical Processing of Sulfide Minerals from the Perspective of Semiconductor Electrochemistry: A Review, Miner. Eng. 204 (2023) 108409, https://doi.org/10.1016/J.MINENG.2023.108409.

[182] K. Osseo-Asare, Semiconductor electrochemistry and hydrometallurgical dissolution processes, Hydrometall. 29 (1992) 61–90, https://doi.org/10.1016/0304-386X(92)90006-L.

[183] G.M. O'Connor, J.J. Eksteen, A critical review of the passivation and semiconductor mechanisms of chalcopyrite leaching, Miner. Eng. 154 (2020) 106401, https://doi.org/10.1016/J.MINENG.2020.106401.

[184] J.E. Dutrizac, The kinetics of dissolution of chalcopyrite in ferric ion media, Metall. Trans. B 9 (1978) 431–439, https://doi.org/10.1007/BF02654418.

[185] F. Barriga Mateos, I. Palencia Pérez, F. Carranza Mora, The passivation of chalcopyrite subjected to ferric sulfate leaching and its reactivation with metal sulfides, Hydrometall. 19 (1987) 159–167, https://doi.org/10.1016/0304-386X(87)90002-8.

[186] I.G. Reilly, D.S. Scott, Recovery of Elemental Sulfur duringthe Oxidative Ammoniacal Leaching of Chalcopyrite, Metall. Trans. B 15 (1984) 726–729.

[187] M.M. McGuire, R.J. Hamers, Extraction and Quantitative Analysis of Elemental Sulfur from Sulfide Mineral Surfaces by High-Performance Liquid Chromatography, Environ. Sci. Tech. 34 (2000) 4651–4655, https://doi.org/10.1021/es0011663.

[188] M.M. Mcguire, J.F. Banfield, R.J. Hamers, Quantitative determination of elemental sulfur at the arsenopyrite surface after oxidation by ferric iron: mechanistic implications, Geochem. Trans. 2 (4) (2001) 25, https://doi.org/10.1039/b104111h.

[189] J.E. Dutrizac, R.J.C. MacDonald, The kinetics of dissolution of enargite in acidified ferric sulphate solutions, Can. Metall. Q. 11 (1972) 469–476, https://doi.org/10.1179/cmq.1972.11.3.469.

[190] P. Lattanzi, S. Da Pelo, E. Musu, D. Atzei, B. Elsener, M. Fantauzzi, A. Rossi, Enargite oxidation: A review, Earth Sci. Rev. 86 (2008) 62–88, https://doi.org/10.1016/J.EARSCIREV.2007.07.006.

[191] B. Escobar, E. Huenupi, J.V. Wiertz, Chemical and biological leaching of enargite, Biotecnhology Letters 19 (1997) 719–722.

[192] C. Kantar, Solution and flotation chemistry of enargite, Colloids Surf. A Physicochem Eng Asp 210 (2002) 23–31, https://doi.org/10.1016/S0927-7757(02)00197-8.

[193] I.C. Hamilton, R. Woods, An investigation of the deposition and reactions of sulphur on gold electrodes, J. Appl. Electrochem. 13 (1983) 783–794, https://doi.org/10.1007/BF00615828.

[194] N.J. Welham, Mechanochemical processing of enargite (Cu3AsS4), Hydrometall. 62 (2001) 165–173, https://doi.org/10.1016/S0304-386X(01)00195-5.
[195] A. Hol, R.D. Van Der Weijden, G. Van Weert, P. Kondos, C.J.N. Buisman, Bio-reduction of elemental sulfur to increase the gold recovery from enargite, Hydrometall. 115–116 (2012) 93–97, https://doi.org/10.1016/J.HYDROMET.2012.01.003.
[196] G. Larrabure, D. Silva-Quiñones, A.V. Teplyakov, J.C.F. Rodriguez-Reyes, Alkaline pretreatment of a polymetallic sulfide (Fe-Pb-Mn) ore containing silver increases the efficiency of cyanidation by decreasing elemental sulfur content and by exposing sulfide surfaces, Miner. Eng. 203 (2023) 108325, https://doi.org/10.1016/J.MINENG.2023.108325.
[197] P. Peng, H. Xie, L. Lu, Leaching of a sphalerite concentrate with H2SO4–HNO3 solutions in the presence of C2Cl4, Hydrometall. 80 (2005) 265–271, https://doi.org/10.1016/J.HYDROMET.2005.08.004.
[198] G. Liu, K. Jiang, B. Zhang, Z. Dong, F. Zhang, F. Wang, T. Jiang, B. Xu, Selective flotation of elemental sulfur from pressure acid leaching residue of zinc sulfide, Minerals 11 (2021) 89–109, https://doi.org/10.3390/min11010089.
[199] Y. Hu, W. Sun, D. Wang, General Review of Electrochemistry of Flotation of Sulphide Minerals, in: Y. Hu, W. Sun, D. Wang (Eds.), Electrochemistry of Flotation of Sulphide Minerals, Springer, Berlin Heidelberg, Berlin, Heidelberg, 2009, pp. 1–19, https://doi.org/10.1007/978-3-540-92179-0_1.
[200] H.P. Hu, Q.Y. Chen, Z.L. Yin, Y.H. He, B.Y. Huang, Mechanism of mechanical activation for sulfide ores, Trans. Nonferrous Met. Soc. China 17 (2007) 205–213, https://doi.org/10.1016/S1003-6326(07)60073-9.
[201] K. Tkáčová, Mechanical activation of minerals, Elsevier, 1989.
[202] D.H. Cowan, F.G. Jahromi, A. Ghahreman, Atmospheric oxidation of pyrite with a novel catalyst and ultra-high elemental sulphur yield, Hydrometall. 173 (2017) 156–169, https://doi.org/10.1016/J.HYDROMET.2017.07.003.
[203] Y. Fan, Y. Liu, L. Niu, T. Jing, T.a. Zhang, Separation and purification of elemental sulfur from sphalerite concentrate direct leaching residue by liquid paraffin, Hydrometall. 186 (2019) 162–169, https://doi.org/10.1016/J.HYDROMET.2019.04.009.
[204] S. Suárez-Gómez, L. Bonavera, J. Carballido-Landeira, P. Blanco, F. Blanco, M. L. Sánchez, F.J. de Cos, Effective extraction of high purity sulfur from industrial residue with low sulfur content, J. Mater. Res. Technol. 9 (2020) 8117–8124, https://doi.org/10.1016/J.JMRT.2020.05.007.
[205] J. Cosmidis, C.W. Nims, D. Diercks, A.S. Templeton, Formation and stabilization of elemental sulfur through organomineralization, Geochim. Cosmochim. Acta 247 (2019) 59–82, https://doi.org/10.1016/J.GCA.2018.12.025.
[206] F. Chen, Q. Gao, J. Zhang, H. Deng, C. Tian, Z. Lin, Enhanced separation of sulfur and metals from polymetallic sulfur slag through recrystallizing regulation of sulfur crystals, Metals (basel) 13 (2023) 603, https://doi.org/10.3390/met13030603.
[207] D.I. Bletskan, Phase equilibrium in the binary systems A IV B VI Part. I. The systems silicon-chalcogen, J. Ovonic Res. 1 (2005) 47–52.
[208] F. Garzon, T. Lopes, T. Rockward, J.-M. Sansiñena, B. Kienitz, R. Mukundan, The impact of impurities on long-term PEMFC performance, ECS Trans. 25 (2009) 1575–1583, https://doi.org/10.1149/1.3210713.
[209] R. Djimasbe, A.F. Kemalov, R.A. Kemalov, Research of the technology for the production of modified sulfur bituminous binders, International Journal of Engineering & Technology 7 (2018) 123–126. www.sciencepubco.com/index.php/IJET.
[210] L.H. Ali, K.A. Al-Ghannam, Bituminous impurity in the elemental sulphur from the Mishraq deposit, Fuel 58 (1979) 883–887.
[211] A.R. Mcneill, S.E. Bodman, A.M. Burney, C.D. Hughes, D.L. Crittenden, Experimental validation of a computational screening approach to predicting redox potentials for a diverse variety of redox-active organic molecules, J. Phys. Chem. C 124 (2020) 24105–24114.
[212] W. Yang, J. Mathews, J.S. Williams, Hyperdoping of Si by ion implantation and pulsed laser melting, Mater. Sci. Semicond. Process. 62 (2017) 103–114, https://doi.org/10.1016/j.mssp.2016.11.005.
[213] J. Lau, R.H. DeBlock, D.M. Butts, D.S. Ashby, C.S. Choi, B.S. Dunn, Sulfide Solid Electrolytes for Lithium Battery Applications, Adv. Energy Mater. 8 (2018), https://doi.org/10.1002/aenm.201800933.
[214] R.L. Birke, S. Venkatesan, Effect of sulfur impurities on Li / TiS 2 cells the polarography of vitamin B 12a in acidic media, Electrochemical Science and Technology (1981) 942–945.
[215] F. Pianezzi, S. Nishiwaki, L. Kranz, C.M. Sutter-Fella, P. Reinhard, B. Bissig, H. Hagendorfer, S. Buecheler, A.N. Tiwari, Influence of Ni and Cr impurities on the electronic properties of Cu(In,Ga)Se2 thin film solar cells, Prog. Photovolt. Res. Appl. 23 (2015) 892–900, https://doi.org/10.1002/pip.2503.
[216] N.I. Dowling, F. Bernard, J. Leung, K.L. Lesage, Analytical procedure for the determination of trace carbon impurity in elemental sulfur, J. Sulfur Chem. 29 (2008) 129–137, https://doi.org/10.1080/17415990701839990.
[217] D. Larcher, J.M. Tarascon, Towards greener and more sustainable batteries for electrical energy storage, Nat. Chem. 7 (2015) 19–29, https://doi.org/10.1038/nchem.2085.
[218] J.B. Hyne, L.L. Lang, Elemental sulfur - a pure product and how to keep it pure, Sulfur 2005 (2005) 1–9.
[219] R.J. Reddy, K. Appa-Rao, K. Ramakrishna, A.N. Kumar, Quantification of residual elemental sulfur present in pharmaceutical ingredients by HPLC and UPLC, Int. J. Adv. Pharm. Biol. Chem. 1 (2012) 121–127.
[220] S.S. Adamchik, A.Y. Malyshev, A.D. Bulanov, E.N. Bab'eva, Fine purification of sulfur from carbon by high-temperature oxidation, Inorg. Mater. 37 (2001) 564–567.
[221] H. Brogdon Jr, W. Edward, Purification of crude sulfur, US2941868A (1960).
[222] A.S. Fedotov, O.A. Kalimeneva, V.A. Fedotov, Tekhnologiya rasplava i ochistki zagryaznennoy sery na Orenburgskom GPZ, Vestnik OGU 2 (2004) 175–176.
[223] G.R. Wessel, Sulfur resources from industrial minerals and rocks, Society for, Min. Metall. Explor. 6 (1994) 1011–1046.
[224] T.J. Murphy, W.S. Clabaugh, R. Gilchrist, Preparation of sulfur of high purity, Journal of Research of the National Bureau of Standards-A, Physics and Chemistry 64 (1960) 355–358.
[225] H. Suzuki, Y. Osumi, M. Nakane, Y. Myake, Studies on preparation of high purity sulfur. II. Removal of trace amounts of selenium and tellurium in sulfur by means of distillation with silver, Bulletin of Chemical Society of Japan 47 (1974) 757–758.
[226] Malyshev A.Yu, Glubokaya Ochistka Sery Ot Ugleroda, Mysh'yaka I Selena Metodom Protivotochnoy Kristallizatsii Iz Rasplava., 2000.
[227] A.I. Sozin, M.F. Churbanov, O.I. Chernova, T.G. Sorochkina, I.V. Skripachev, G. E. Snopatin, Identification of impurities in high-purity sulfur using gas chromatography-mass spectrometry method, Analitika i Kontrol 21 (2017) 225–229, https://doi.org/10.15826/analitika.2017.21.3.005.
[228] C. Scheinert, EU's response to the US Inflation Reduction Act (IRA), Policy Department for Economic, Scientific and Quality of Life Policies (2023) 1–15. https://www.whitehouse.gov/cleanenergy/inflation-reduction-act-.
[229] J. Zhu, J. Zou, H. Cheng, Y. Gu, Z. Lu, High energy batteries based on sulfur cathode, Green Energy Environ. 4 (2019) 345–359, https://doi.org/10.1016/j.gee.2018.07.001.
[230] Y. Gao, Z. Pan, J. Sun, Z. Liu, J. Wang, High-energy batteries: beyond lithium-ion and their long road to commercialisation, Nanomicro Lett 14 (2022) 94, https://doi.org/10.1007/s40820-022-00844-2.
[231] W. Yao, K. Liao, T. Lai, H. Sul, A. Manthiram, Rechargeable Metal-Sulfur Batteries: Key Materials to Mechanisms, Chem. Rev. 124 (2024) 4935–5118, https://doi.org/10.1021/ACS.CHEMREV.3C00919/ASSET/IMAGES/MEDIUM/CR3C00919_0047.GIF.
[232] D. Bresser, S. Passerini, B. Scrosati, Recent progress and remaining challenges in sulfur-based lithium secondary batteries – a review, Chem. Commun. 49 (2013) 10545, https://doi.org/10.1039/c3cc46131a.
[233] A. Eftekhari, D.W. Kim, Cathode materials for lithium-sulfur batteries: A practical perspective, J. Mater. Chem. A Mater 5 (2017) 17734–17776, https://doi.org/10.1039/c7ta00799j.
[234] S. Xia, X. Xu, W. Wu, Y. Chen, L. Liu, G. Wang, L. Fu, Q. Zhang, T. Wang, J. He, Y. Wu, Advancements in functionalized high-performance separators for lithium-sulfur batteries, Mater. Sci. Eng. R. Rep. 163 (2025) 100924, https://doi.org/10.1016/j.mser.2025.100924.
[235] I. Rakhimbek, N. Baikalov, A. Konarov, A. Mentbayeva, Y. Zhang, Z. Bakenov, Nickel and nickel oxide nanoparticle-embedded functional carbon nanofibers for lithium sulfur batteries, Nanoscale Adv. 6 (2023) 578–589, https://doi.org/10.1039/d3na00785e.
[236] Q. Jin, K.X. Zhao, L.L. Wu, L. Li, L. Kong, X.T. Zhang, Enhancing Li cycling coulombic efficiency while mitigating "shuttle effect" of Li-S battery through sustained release of LiNO3, Journal of Energy Chemistry 84 (2023) 22–29, https://doi.org/10.1016/j.jechem.2023.05.020.
[237] Q. Jin, L.R. Zhang, M.L. Zhao, L. Li, X.B. Yu, J.P. Xiao, L. Kong, X.T. Zhang, Nanofiber-Interlocked V2CTx Hosts Enriched with 3D Lithiophilic and Sulfophilic Sites for Long-Life and High-Rate Lithium–Sulfur Batteries, Adv. Funct. Mater. 34 (2024) 1–12, https://doi.org/10.1002/adfm.202309624.
[238] W. Yao, W. Zheng, J. Xu, C. Tian, K. Han, W. Sun, S. Xiao, ZnS-SnS@NC Heterostructure as robust lithiophilicity and sulfiphilicity mediator toward high-rate and long-life lithium-sulfur batteries, ACS Nano 15 (2021) 7114–7130, https://doi.org/10.1021/acsnano.1c00270.
[239] T. Liu, H. Hu, X. Ding, H. Yuan, C. Jin, J. Nai, Y. Liu, Y. Wang, Y. Wan, X. Tao, 12 years roadmap of the sulfur cathode for lithium sulfur batteries (2009–2020), Energy Storage Mater. 30 (2020) 346–366, https://doi.org/10.1016/j.ensm.2020.05.023.
[240] R. Kumar, J. Liu, J.Y. Hwang, Y.K. Sun, Recent research trends in Li-S batteries, J Mater Chem A Mater 6 (2018) 11582–11605, https://doi.org/10.1039/c8ta01483c.
[241] S. Zhang, K. Ueno, K. Dokko, M. Watanabe, Recent advances in electrolytes for lithium-sulfur batteries, Adv. Energy Mater. 5 (2015) 1500117, https://doi.org/10.1002/aenm.201500117.
[242] A. Benítez, J. Amaro-Gahete, Y.C. Chien, Á. Caballero, J. Morales, D. Brandell, Recent advances in lithium-sulfur batteries using biomass-derived carbons as sulfur host, Renew. Sustain. Energy Rev. 154 (2022) 111783, https://doi.org/10.1016/j.rser.2021.111783.
[243] B.B. Gicha, L. Teshome Tufa, N. Nwaji, X. Hu, J. Lee, Advances in All-Solid-State Lithium-Sulfur Batteries for Commercialization, Nanomicro Lett 16 (2024) 172, https://doi.org/10.1007/s40820-024-01385-6.
[244] Z. Yang, Z. Yao, G. Li, G. Fang, H. Nie, Z. Liu, X. Zhou, X. Chen, S. Huang, Sulfur-Doped Graphene as an Efficient Metal-free Cathode Catalyst for Oxygen Reduction, ACS Nano 6 (2012) 205–211, https://doi.org/10.1021/nn203393d.
[245] W. Gao, L.B. Alemany, L. Ci, P.M. Ajayan, New insights into the structure and reduction of graphite oxide, Nat. Chem. 1 (2009) 403–408, https://doi.org/10.1038/nchem.281.
[246] Y. Li, M. Chen, B. Liu, Y. Zhang, X. Liang, X. Xia, Heteroatom Doping: An Effective Way to Boost Sodium Ion Storage, Adv. Energy Mater. 10 (2020) 2000927, https://doi.org/10.1002/aenm.202000927.
[247] X. Chen, X.B. Cheng, Z. Liu, High sulfur-doped hard carbon anode from polystyrene with enhanced capacity and stability for potassium-ion storage, J. Energy Chem. 68 (2022) 688–698, https://doi.org/10.1016/J.JECHEM.2021.12.007.

[248] S. Xia, X. Wu, Z. Zhang, Y. Cui, W. Liu, Practical Challenges and Future Perspectives of All-Solid-State Lithium-Metal Batteries, Chem. 5 (2019) 753–785, https://doi.org/10.1016/j.chempr.2018.11.013.
[249] J. Wang, Z.W. Seh, The Design of Transition Metal Sulfide Cathodes for High-Performance Magnesium-Ion Batteries, Acc. Mater. Res. 5 (2024) 1329–1339, https://doi.org/10.1021/accountsmr.4c00181.
[250] Z. Sun, Y. Hu, F. Qin, N. Lv, B. Li, L. Jiang, Z. Zhang, F. Liu, Sulfurized polyacrylonitrile cathodes with electrochemical and structural tuning for high capacity all-solid-state lithium–sulfur batteries, Sustain, Energy Fuels 5 (2021) 5603–5614, https://doi.org/10.1039/D1SE01187A.
[251] Y. Sun, B. Xing, Y. Zhang, H. Zeng, W. Meng, L. Chen, J. Jia, S. Cheng, B. Xu, C. Zhang, Ice template-induced assembly coupled with carbonization strategy for preparation of sulfur-doped porous carbon nanosheets from lignite as high-capacity anode for lithium-ion batteries, Fuel 372 (2024) 132163, https://doi.org/10.1016/J.FUEL.2024.132163.
[252] X. Xiao, J. Li, X. Meng, J. Qiu, Sulfur-Doped Carbon-Coated Fe0.95S1.05 Nanospheres as Anodes for High-Performance Sodium Storage, Acta Phys. Chim. Sin. 40 (2024) 2307006, https://doi.org/10.3866/PKU.WHXB202307006.
[253] I. Puspitasari, W. Mutmainah, M.P. Nobel, S. Hidayat, Purification of natural sulfur up to the analyst grade to qualify for Li-sulfur battery applications, J. Phys. Conf. Ser. 2780 (1) (2024) 012021, https://doi.org/10.1088/1742-6596/2780/1/012021.
[254] A. Yamano, T. Kubo, F. Chujo, N. Yamashita, T. Mukai, M. Morishita, T. Kojima, M. Yanagida, K. Hochi, S. Furusawa, N. Kikuchi, T. Sakai, Rubber-Derived Sulfur Composite Cathode Material for Li-S/Li-ion Battery, Electrochemistry 90 (2022), https://doi.org/10.5796/ELECTROCHEMISTRY.22-00055.
[255] Method for preparation of battery grade high-purity manganese sulfate from industrial grade manganese sulfate, CN106395910A, 2016.
[256] J.T. Kim, H. Su, Y. Zhong, C. Wang, H. Wu, D. Zhao, C. Wang, X. Sun, Y. Li, All-solid-state lithium–sulfur batteries through a reaction engineering lens, Nature Chemical Engineering 2024 1:6 1 (2024) 400–410. https://doi.org/10.1038/s44286-024-00079-5.
[257] D. Wang, L.J. Jhang, R. Kou, M. Liao, S. Zheng, H. Jiang, P. Shi, G.X. Li, K. Meng, D. Wang, Realizing high-capacity all-solid-state lithium-sulfur batteries using a low-density inorganic solid-state electrolyte, Nat. Commun. 14 (1) (2023) 1–10, https://doi.org/10.1038/s41467-023-37564-z.
[258] B. Tong, Z. Song, H. Wan, W. Feng, M. Armand, J. Liu, H. Zhang, Z. Zhou, Sulfur-containing compounds as electrolyte additives for lithium-ion batteries, InfoMat 3 (2021) 1364–1392, https://doi.org/10.1002/inf2.12235.
[259] Y. Liu, Y. Elias, J. Meng, D. Aurbach, R. Zou, D. Xia, Q. Pang, Electrolyte solutions design for lithium-sulfur batteries, Joule 5 (2021) 2323–2364, https://doi.org/10.1016/j.joule.2021.06.009.
[260] L. Fan, N. Deng, J. Yan, Z. Li, W. Kang, B. Cheng, The recent research status quo and the prospect of electrolytes for lithium sulfur batteries, Chem. Eng. J. 369 (2019) 874–897, https://doi.org/10.1016/j.cej.2019.03.145.
[261] Q. Pang, X. Liang, C.Y. Kwok, L.F. Nazar, Advances in lithium-sulfur batteries based on multifunctional cathodes and electrolytes, Nat. Energy 1 (2016), https://doi.org/10.1038/nenergy.2016.132.
[262] Y. Kato, S. Hori, T. Saito, K. Suzuki, M. Hirayama, A. Mitsui, M. Yonemura, H. Iba, R. Kanno, High-power all-solid-state batteries using sulfide superionic conductors, Nat. Energy 1 (2016), https://doi.org/10.1038/nenergy.2016.30.
[263] S. Li, Z. Yang, S.B. Wang, M. Ye, H. He, X. Zhang, C.W. Nan, S. Wang, Sulfide-based composite solid electrolyte films for all-solid-state batteries, Commun Mater 5 (2024), https://doi.org/10.1038/s43246-024-00482-8.
[264] D. Wang, L.J. Jhang, R. Kou, M. Liao, S. Zheng, H. Jiang, P. Shi, G.X. Li, K. Meng, D. Wang, Realizing high-capacity all-solid-state lithium-sulfur batteries using a low-density inorganic solid-state electrolyte, Nat. Commun. 14 (2023), https://doi.org/10.1038/s41467-023-37564-z.
[265] J.B. Robinson, K. Xi, R.V. Kumar, A.C. Ferrari, H. Au, M.M. Titirici, A.P. Puerto, A. Kucernak, S.D.S. Fitch, N.G. Araez, Z.L. Brown, M. Pasta, L. Furness, A. J. Kibler, D.A. Walsh, L.R. Johnson, C. Holc, G.N. Newton, N.R. Champness, F. Markoulidis, C. Crean, R.C.T. Slade, E.I. Andritsos, Q. Cai, S. Babar, T. Zhang, C. Lekakou, N. Kulkarni, A.J.E. Rettie, R. Jervis, M. Cornish, M. Marinescu, G. Offer, Z. Li, L. Bird, C.P. Grey, M. Chhowalla, D. Di Lecce, R.E. Owen, T. S. Miller, D.J.L. Brett, S. Liatard, D. Ainsworth, P.R. Shearing, 2021 roadmap on lithium sulfur batteries, JPhys Energy 3 (2021) 031501, https://doi.org/10.1088/2515-7655/abdb9a.
[266] Lithium sulfur battery market size & share analysis - industry research report - growth trends, Https://Www.Marketsandmarkets.ComLithium-Sulfur Lithium-SUlfur Battery Market. /Market-Reports/Lithium-Sulfur-Battery-Market-231442524.Html. (2024).
[267] Ganguli B, Mikolajczak C, Favors Z, Performance and safety behavior of lyten's li-s pouch and cylindrical 18650 cells., NASA Aerospace Battery Workshop (2023).
[268] Li-S in the media Li-S energy celebrates 45% increase in volumetric energy density, Li-S Energy May 2023 Newsletter. Retrieved from Https://Www.Lis.Energy/. (2023).
[269] A. Barde, K. Jin, M. Shinn, K. Nithyanandam, R.E. Wirz, Demonstration of a low cost, high temperature elemental sulfur thermal battery, Appl. Therm. Eng. 137 (2018) 259–267, https://doi.org/10.1016/j.applthermaleng.2018.02.094.
[270] K. Jin, A. Barde, K. Nithyanandam, R.E. Wirz, Sulfur heat transfer behavior in vertically-oriented isochoric thermal energy storage systems, Appl. Energy 240 (2019) 870–881, https://doi.org/10.1016/j.apenergy.2019.02.077.
[271] H.M. Ali, T.u. Rehman, M. Arıcı, Z. Said, B. Duraković, H.I. Mohammed, R. Kumar, M.K. Rathod, O. Buyukdagli, M. Teggar, Advances in thermal energy storage: fundamentals and applications, Prog. Energy Combust. Sci. 100 (2024) 101109, https://doi.org/10.1016/J.PECS.2023.101109.
[272] H. Jouhara, A. Żabnieńska-Góra, N. Khordehgah, D. Ahmad, T. Lipinski, Latent thermal energy storage technologies and applications: A review, Int. J. Thermofl. 5–6 (2020) 100039, https://doi.org/10.1016/J.IJFT.2020.100039.
[273] H.M. Ali, T. ur Rehman, M. Arıcı, Z. Said, B. Duraković, H.I. Mohammed, R. Kumar, M.K. Rathod, O. Buyukdagli, M. Teggar, Advances in thermal energy storage: Fundamentals and applications, Prog Energy Combust Sci 100 (2024) 101109. https://doi.org/10.1016/J.PECS.2023.101109.
[274] J. Sunku Prasad, P. Muthukumar, F. Desai, D.N. Basu, M.M. Rahman, A critical review of high-temperature reversible thermochemical energy storage systems, Appl Energy 254 (2019) 113733, https://doi.org/10.1016/J.APENERGY.2019.113733.
[275] K. Jin, S. Pan, T. Wang, Z. Zhang, Non-negligible corrosion process in a novel sulfur-based energy storage system, J. Power Sources 490 (2021) 229529, https://doi.org/10.1016/j.jpowsour.2021.229529.
[276] X. Huang, K. Jin, R. Yang, The corrosion mechanism of elemental sulfur on iron–chromium alloys in thermal energy storage systems, J Energy Storage 111 (2025), https://doi.org/10.1016/j.est.2025.115471.
[277] M.C. Oliver, M. Shah, J. Martinek, K. Nithyanandam, Z. Ma, M.J. Martin, Exploring the Limits of Empirical Correlations for the Design of Energy Systems With Complex Fluids: Liquid Sulfur Thermal Energy Storage as a Case Study, J. Energy Res. Technol. 145 (2023), https://doi.org/10.1115/1.4063256/1166474.